TP 13243E

PROPELLER DESIGN LOAD MODEL

PREPARED UNDER SUB-CONTRACT TO

THE INSTITUTE FOR MARINE DYNAMICS
NATIONAL RESEARCH COUNCIL CANADA
ST. JOHN'S, NEWFOUNDLAND

FOR

TRANSPORTATION DEVELOPMENT CENTRE
SAFETY and SECURITY
TRANSPORT CANADA

BY

R.P. BROWNE MARINE CONSULTANTS LIMITED
CALGARY, ALBERTA

APRIL 1998

TP 13243E

PROPELLER DESIGN LOAD MODEL

BY

R.P. BROWNE	R.P. BROWNE MARINE CONSULTANTS LIMITED
C.R. REVILL	C.R. REVILL MARINE CONSULTANTS LIMITED
A.R. RITCH	AVRON RITCH CONSULTING LIMITED
A.J. KEINONEN	AKAC INC.

APRIL 1998

This report reflects the views of the authors and not necessarily those of the Transportation Development Centre.

Un sommaire français se trouve avant la table des matières.

Transport Canada / Transports Canada

PUBLICATION DATA FORM

1. Transport Canada Publication No. TP 13243E	2. Project No. 9021	3. Recipient's Catalogue No.
4. Title and Subtitle Propeller Design Load Model		5. Publication Date April 1998
		6. Performing Organization Document No.
7. Author(s) R.P. Browne, C.R. Revill, A.R. Ritch, and A.J. Keinonen		8. Transport Canada File No. ZCD1460-320-6
9. Performing Organization Name and Address Institute for Marine Dynamics, Marine Systems Research Kerwin Place, Memorial University Campus P.O. Box 12093, Station A St. John's, Newfoundland A1B 3T5		10. PWGSC File No.
		11. PWGSC or Transport Canada Contract No.
12. Sponsoring Agency Name and Address Transportation Development Centre (TDC) 800 René Lévesque Blvd. West Suite 600 Montreal, Quebec H3B 1X9		13. Type of Publication and Period Covered Final
		14. Project Officer Ernst Radloff

15. Supplementary Notes (Funding programs, titles of related publications, etc.)

Co-sponsored by TC Prairie and Northern Region

16. Abstract

This project's objective was to obtain information on propeller and ice interaction loads from seven sets of Canadian full-scale trials data. Propeller-ice thrust and torque loads were calculated from the measured shaft thrust and torque data. The impulse response functions were based on shafting response characteristics determined from a knowledge of the system masses, inertias, stiffnesses, and damping.

Parametric analysis on the resulting propeller-ice loads data indicated that positive ice thrust loads were larger than negative loads for the ducted propellers, and vice versa for the open propellers. For both the ducted and open propellers, propeller-ice torque generally increased with increasing pitch angle. Investigation into the influence of rpm and ship speed on all loads, and pitch angle on thrust loads, was inconclusive. Ice loads varied significantly less than linearly with ice strength.

Long-term predictions of propeller-ice loads were made for 10,000 hours of operation. The data revealed that, in thick ice, ice thrust varied approximately with the square of propeller diameter for the ducted propellers, and ice torque varied approximately with the cube of propeller diameter.

The Canadian data, with a bias towards larger propellers and ducted propellers, appear to support the Unified Load Model, which is based on numerical modelling and a separate set of Finnish full-scale data.

17. Key Words Propeller-ice interaction	18. Distribution Statement Limited number of copies available from the Transportation Development Centre

19. Security Classification (of this publication) Unclassified	20. Security Classification (of this page) Unclassified	21. Declassification (date) —	22. No. of Pages xvi, 102, apps	23. Price Shipping/ Handling

Transports Canada / Transport Canada

FORMULE DE DONNÉES POUR PUBLICATION

1. N° de la publication de Transports Canada TP 13243E	2. N° de l'étude 9021	3. N° de catalogue du destinataire
4. Titre et sous-titre Propeller Design Load Model		5. Date de la publication Avril 1998 6. N° de document de l'organisme exécutant
7. Auteur(s) R.P. Browne, C.R. Revill, A.R. Ritch et A.J. Keinonen		8. N° de dossier - Transports Canada ZCD1460-320-6
9. Nom et adresse de l'organisme exécutant Institute for Marine Dynamics, Marine Systems Research Kerwin Place, Memorial University Campus P.O. Box 12093, Station A St. John's, Newfoundland A1B 3T5		10. N° de dossier - TPSGC 11. N° de contrat - TPSGC ou Transports Canada
12. Nom et adresse de l'organisme parrain Centre de développement des transports (CDT) 800, boul. René-Lévesque Ouest Bureau 600 Montréal (Québec) H3B 1X9		13. Genre de publication et période visée Final 14. Agent de projet Ernst Radloff

15. Remarques additionnelles (programmes de financement, titres de publications connexes, etc.)

Projet coparrainé par la Région des Prairies et du Nord

16. Résumé

Ce projet consistait à dépouiller sept séries de données canadiennes concernant des essais en vraie grandeur, afin d'approfondir la question des charges dues aux interactions glaces-hélice. Les charges de poussée et de couple de torsion dues aux interactions glaces-hélice ont été calculées d'après les valeurs de poussée et de couple mesurées sur l'arbre. Les fonctions de réponse impulsionnelle ont été établies d'après les caractéristiques de comportement de l'arbre, compte tenu des valeurs connues de masse, d'inertie, de rigidité et d'amortissement des systèmes.

Les charges dues aux interactions glaces-hélice ainsi obtenues ont été soumises à une analyse paramétrique qui a révélé que les charges de poussée positives exercées par les glaces étaient supérieures aux charges négatives, dans le cas des hélices sous tuyère, tandis que l'on constatait l'inverse dans le cas des hélices non carénées. Quant au couple dû aux interactions glaces-hélice, il augmentait généralement en raison directe de l'angle de pas, peu importe si l'hélice était carénée ou non. L'examen de l'effet du régime de rotation de l'hélice et de la vitesse du navire sur toutes les charges, et de l'angle de pas sur les charges de poussée, n'a pas abouti à des résultats concluants. Il n'a pas non plus été possible d'établir une relation linéaire significative entre les charges glacielles et la résistance de la glace.

Des prévisions à long terme des charges dues aux interactions glaces-hélice ont été établies pour 10 000 heures de navigation. Les données ont révélé que, dans le cas d'hélices sous tuyère évoluant dans des glaces de forte épaisseur, la poussée due à la glace variait à peu près en fonction du carré du diamètre de l'hélice, tandis que le couple dû à la glace variait à peu près en fonction du cube du diamètre de l'hélice.

Les données canadiennes, dans lesquelles les hélices de grand diamètre et les hélices sous tuyère sont surreprésentées, semblent concorder avec le modèle de charges unifié, fondé sur la modélisation numérique et sur une série distincte de données finnoises issues d'essais en vraie grandeur.

17. Mots clés Interactions glaces-hélice	18. Diffusion Le Centre de développement des transports dispose d'un nombre limité d'exemplaires.

19. Classification de sécurité (de cette publication)	20. Classification de sécurité (de cette page)	21. Déclassification (date)	22. Nombre de pages	23. Prix
Non classifiée	Non classifiée	—	xvi, 102, ann.	Port et manutention

CDT/TDC 79-005
Rev. 96

Canada

ACKNOWLEDGMENTS

This Design Load Model project was carried out by R.P. Browne of R.P. Browne Marine Consultants Limited, C.R. Revill of C.R. Revill Marine Consultants Limited, A.R. Ritch of Avron Ritch Consulting Limited, and A.J. Keinonen of AKAC Inc., who wish to make the following acknowledgments.

To the staff of the Institute for Marine Dynamics, St. John's, Newfoundland, for their technical assistance and contractual support. In particular, to Mr. David Molyneux, IMD, contract manager for the project, and Dr. Brian Veitch, IMD, project manager.

To the Transport Canada personnel who supported the project as part of Canada's contribution to the development of unified international regulations for Arctic vessel machinery protection, especially Mr. Victor Santos-Pedro, Regional Director Marine, Transport Canada, Ship Safety, Prairie and Northern Region, and Mr. Ernst Radloff, Senior Development Officer, Transportation Development Centre.

EXECUTIVE SUMMARY

The objective of this project was to derive information on propeller and ice interaction loads from seven sets of Canadian full-scale trials data, measured on the shaft, for the vessels *Louis S. St. Laurent*, *Oden*, *Robert Lemeur*, *Terry Fox*, *Kalvik*, and *Ikaluk* (two trials).

Propeller-ice thrust and torque loads were calculated from the measured shaft thrust and torque data, using an inverse application of Duhamel's convolution theorem. The impulse response functions for this procedure were based on shafting response characteristics determined from a knowledge of the system masses, inertias, stiffnesses, and damping, which was measured from free decay portions of the shaft response time histories.

Parametric analysis on the resulting propeller-ice loads data indicated that positive ice thrust loads were larger than negative loads for ducted propellers and vice versa for the open propellers. For both the ducted and open propellers, propeller-ice torque generally increased with increasing pitch angle. Investigation into the influence of rpm and ship speed on all loads, and for pitch angle upon thrust loads, was inconclusive. Ice loads varied significantly less than linearly with ice strength.

Long-term predictions of propeller-ice loads for 10,000 hours of operation were made from Weibull Type 3 distributions of the propeller-ice load data. These data showed that, for the ducted propellers in thick ice, ice thrust varied approximately with the square of propeller diameter and ice torque varied approximately with the cube of propeller diameter. The diameter range for the open propellers was too small to investigate diameter influence. Maximum negative ice thrust for the open propellers was up to four times that of a ducted propeller of similar diameter and over twice the maximum positive thrust for the ducted propeller. Open propellers generated higher ice torques than ducted propellers, but this difference was much less than that between open and ducted propellers for ice thrust. The degree of exposure to ice interaction due to hull form and propeller arrangement significantly influenced ice loads.

The long-term propeller-ice load predictions from trials data were compared with predictions using the Unified Load Model for the specific propeller design and operational and environmental conditions on the trials. The comparisons indicated generally good agreement, particularly for the largest, most reliable trials data sets.

The Canadian data, with a bias towards larger propellers and ducted propellers, appear to support the Unified Load Model, which is based on numerical modelling and a separate set of Finnish full-scale data.

SOMMAIRE

Ce projet visait à recueillir des informations sur les charges dues aux interactions glaces-hélice à partir de sept séries de données canadiennes concernant des essais en vraie grandeur mettant en jeu les navires *Louis S. St-Laurent*, *Oden*, *Robert Lemeur*, *Terry Fox*, *Kalvik* et *Ikaluk* (deux essais).

Les charges de poussée et de couple associées aux interactions glaces-hélice ont été calculées à l'aide d'une application inverse du théorème de convolution de Duhamel aux valeurs de poussée et de couple mesurées sur l'arbre. Les fonctions de réponse impulsionnelle pour cette procédure ont été établies d'après les caractéristiques de comportement de l'arbre, mesurées à partir des segments décroissants des séries chronologiques d'enregistrements, compte tenu des valeurs connues de masse, d'inertie, de rigidité et d'amortissement des systèmes.

Les charges dues aux interactions glaces-hélice ainsi obtenues ont été soumises à une analyse paramétrique qui a révélé que les charges de poussée positives exercées par les glaces étaient supérieures aux charges négatives, dans le cas des hélices sous tuyère, tandis que l'on constatait l'inverse dans le cas des hélices non carénées. Quant au couple dû aux interactions glaces-hélice, il augmentait généralement en raison directe de l'angle de pas, peu importe si l'hélice était carénée ou non. L'examen de l'effet du régime de rotation de l'hélice et de la vitesse du navire sur toutes les charges, et de l'angle de pas sur les charges de poussée, n'a pas abouti à des résultats concluants. Il n'a pas non plus été possible d'établir une relation linéaire significative entre les charges glacielles et la résistance de la glace.

Des prévisions à long terme des charges dues aux interactions glaces-hélice ont été établies pour 10 000 heures de navigation, à partir de distributions Weibull de type 3 des charges dues aux interactions glaces-hélice. Les données ont révélé que, dans le cas d'hélices sous tuyère évoluant dans des glaces de forte épaisseur, la poussée due à la glace variait à peu près en fonction du carré du diamètre de l'hélice, tandis que le couple dû à la glace variait à peu près en fonction du cube du diamètre de l'hélice. La plage des diamètres d'hélice, dans le cas des hélices non carénées, était trop étroite pour que l'on puisse se prononcer sur l'effet de la dimension de l'hélice. La charge de poussée négative maximale exercée par la glace sur les hélices non carénées pouvait atteindre jusqu'à quatre fois celle exercée sur une hélice sous tuyère de diamètre équivalent, et plus de deux fois la poussée positive maximale exercée sur l'hélice sous tuyère. Les hélices non carénées ont produit des couples dus à la glace plus grands que les hélices sous tuyère, mais cette différence était beaucoup moins importante que celle entre les deux types d'hélices pour ce qui est de la poussée due à la glace. Le degré d'exposition aux interactions glaces-hélice dû à la forme de la coque et à la configuration de l'hélice avait une influence significative sur les sollicitations exercées par les glaces.

Un examen comparatif a été fait des prévisions à long terme des charges dues aux interactions glaces-hélice, découlant d'une part des données d'essai et d'autre part du modèle de charges unifié, pour le même type d'hélice essayé dans des conditions

opérationnelles et environnementales semblables. Il en est ressorti une assez bonne concordance, en particulier pour les ensembles de données les plus volumineux et les plus fiables.

Les données canadiennes, dans lesquelles les hélices de grand diamètre et les hélices sous tuyère sont surreprésentées, semblent appuyer le modèle de charges unifié, fondé sur la modélisation numérique et sur une série distincte de données finnoises issues d'essais en vraie grandeur.

TABLE OF CONTENTS

Figures

Tables

1. INTRODUCTION

1.1. The Unified Load Model

Under the Joint Research Project Arrangement #6, Propeller Ice Interaction, (JRPA#6), made between the Canadian Coast Guard and Finnish Board of Navigation in 1991, studies were carried out in order to define the loads on propellers during propeller and ice interaction. This work included full-scale data, model test data and a numerical simulation model. In late 1995/early 1996, the JRPA#6 project culminated in the development of a set of simple formulae, denoted the Unified Load Model (1). These formulae describe the loads on propellers, alone and separate from the ship (i.e. in the open water condition), due to propeller and ice interaction.

1.2. The Design Load Model

The Unified Load Model must be modified into a Design Load Model for use in proposed revised Machinery Design Standards. The modifications should take into account the impact upon ice loads of factors other than those addressed in the unified load model. These factors include:

- Ship hull design and propulsion arrangement
- Propulsion system type
- Vessel Ice Class
- Method of operation
- Long-term exposure

The model should also be calibrated with all available full-scale propeller ice load data.

The resulting Design Load Model will be used in the Machinery Design Standards to determine the ice loads applied at the propeller, and will define the minimum standards for which the propeller and complete propulsion system must be designed.

1.3. The IMD Development Program

The Institute for Marine Dynamics developed an applied research program for development of the Design Load Model, on behalf of the Transportation Development Centre. This program fulfills the requirements of Transport Canada, Ship Safety, the regulatory authority. The program uses all available propeller and ice interaction information to investigate the impact of design, environmental and operational factors upon design loads.

This report and project, carried out by R.P. Browne Marine Consultants Limited and sub-contractors, covers those items of the IMD design load model research program related to the analysis of full-scale propeller and ice interaction load data.

1.4. Project Objective

The project objective was to derive as much information as possible on propeller and ice interaction loads, from seven sets of Canadian full-scale trials data, measured on the shaft, for the vessels Louis S. St. Laurent, Kalvik, Ikaluk (two trials), Terry Fox, Robert Lemeur, and Oden. The trials are:

a) CCGS Louis S. St. Laurent, Trans Polar Voyage 1994.
b) M.V. Kalvik - NW Passage 1986
c) M.V. Ikaluk and Terry Fox - Herschel Basin 1990
d) M.V. Ikaluk - Herschel Basin 1989
e) M.V. Robert Lemeur - Beaufort Sea 1984
f) Oden - North Pole Voyage 1991

The steps followed were as follows:

1. Correct the shaft measured ice thrust and torque measurements for the influence of shaft dynamics, thereby obtaining propeller ice thrust and torque data, which can be compared with the unified load model.
2. Carry out a parametric analysis of the calculated propeller ice loads. Compare the parameter trends with those of the unified load model.
4. Carry out a statistical analysis of the calculated propeller ice loads and determine the influence of long-term exposure on load magnitude. Compare long-term predictions of propeller ice loads with those provided by the unified load model.
5. Identify any other parameter trends associated with ship and propeller design and operation.

Shaft measured data from the 1994 Trans Polar Voyage of CCGS Louis S. St. Laurent, were analyzed to obtain propeller ice loads and subsequent parametric influences in a previous project (2), the results of which are incorporated into this project and report.

The shaft measured data from the remaining six vessel trials, without correction for shaft dynamics, were analyzed for parametric influences and are reported in Reference 3. The complete analysis listed above was therefore required for these data sets.

2. DERIVATION OF PROPELLER ICE LOADS FROM SHAFT ICE LOADS

2.1. The Process

The response of a vibrating system (shaft load time history) to an input function (propeller load time history) can be determined by the Convolution method, and alternatively, the input function (propeller load time history) can be determined from the response (shaft load time history) by the de-convolution method, as shown in Figure 1.

This approach can therefore be used to determine propeller thrust and torque loads from shaft measured loads (and vice-versa), thereby allowing more full-scale data to supplement the available directly measured blade load data, for the validation and calibration of load models.

In the convolution approach, the response to an arbitrary load input time history is obtained as the super-position of consecutive load impulse responses. Figure 2 shows the response to an impulse part way through a load input. Responses to all impulses are summed to obtain the response history.

If the impulse time were longer, say doubled, the response amplitude would be approximately doubled, but its relative shape would be the same. The accuracy of the method increases as impulse time is reduced, since this provides the better definition of the input time history. However, this increases the size of the matrices to be handled in the convolution process, including inversion in the de-convolution process. In practice, a practical lower limit on impulse time is therefore determined on the basis of the scan rate of the input signal (rate at which the original shaft signal was sampled, digitized, and recorded, determining the shortest possible impulse time), the duration of the input signal (giving the total number of impulses), and the capability of available computing.

The shaft data used in this analysis were recorded at a rate of 200 scans/sec, and an impulse rate of 100/sec (impulse time of 0.01 seconds) was used in the convolution analysis, in order to keep matrix size to the order of 500^2.

The de-convolution process makes no assumptions regarding the shape of the input propeller load (amplitude, duration and timing of individual blade loads). The shape is obtained by determining the succession of impulses which result in the shaft load.

2.2. Worked Example using Robert Lemeur Data

The frequency response of the Robert Lemeur shaftline in thrust is shown in Figure 3. The response is calculated in a similar manner to that used in "The Shaft Modeling Tool Kit", Reference 4. Blade excitation frequency is 13.8 Hz and the first natural response is at 25 Hz. Shaft thrust loads due to sinusoidal excitation are 40% higher than propeller loads.

The thrust impulse response function in Figure 4 is determined by a numerical technique that uses the same information regarding the vibrating system, as required to calculate the thrust frequency response characteristics in Figure 3. That is:

- Propeller and shafting masses, from engineering drawings, including propeller added mass $\rho D^3/3$.
- Shafting axial stiffness and thrust block stiffness, from manufacturer's specifications.
- System damping, measured from free decay portions found in some of the shaft thrust records.

Torque impulse response functions are determined using corresponding rotational inertias, torsional stiffnesses, and damping.

Measured system damping factors, used in the analysis, are given in Table 1.

Table 1 Measured Ship Propulsion System Damping Factors

	Measured Ship Propulsion System Damping Factors as Percentage of Critical Damping	
Vessel	Thrust	Torque
Louis S. St. Laurent	6.9	2.7
Kalvik/Terry Fox	6.3	6.0
Ikaluk	6.4	4.0
Robert Lemeur	6.3	8.0
Oden	No thrust records	11.0

In Figure 4, the thrust impulse has a duration of 0.01 seconds and an amplitude of 100 units. It is seen that initial response amplitude is greater than the input amplitude. With a smaller impulse duration (less input energy), individual impulse response amplitude would be proportionally smaller, and vice-versa. Decay response is at the first natural frequency of 25Hz (0.04 second period).

A test for the stability of the response function is shown in Figure 5, where an instantaneous ramp input of 100 units is applied and held. The system responds transiently, and steadies down correctly to the new load offset of 100 units.

Figure 6 shows the torque impulse response function to an impulse of 100 units and duration 0.01 seconds. The initial response amplitude is less than input amplitude, and decay is at the first natural frequency of 4.2 Hz (0.24 seconds period). Figure 7 is the corresponding stability check for an instantaneous load of 100 units.

The irregular nature of the initial impulse response in Figure 6 shows a transition from input blade frequency to the lower shaft natural frequency, at which the system tends to respond. In the case of the ramp (infinite frequency) input, Figure 7, initial response irregularities are barely present.

The impulse response functions in Figure 4 and 6 have been used, in the de-convolution approach, to calculate propeller loads for Robert Lemeur from measured shaft loads.

Trials Event 132

Figures 8 and 9 show the measured shaft ice thrust and predicted propeller ice thrust. It is evident that propeller thrust is lower than shaft thrust, as one would expect from the frequency response function in Figure 3. Otherwise, the two records show a high degree of similarity, as might be expected in a system where the excitation is at a significantly lower frequency than the first natural response. Thrust is predominantly at blade rate, and blade bending is predominantly in the forward direction, as shown directly from the corresponding blade bending stress record in Figure 10. For ducted propellers, such as those on Robert Lemeur, large forward blade bending loads are common.

Figures 11 and 12 are for measured shaft and calculated propeller ice torque. Mean torque is the same in both cases, except for very small shaft inertia influences resulting from rpm changes. However, the dynamic nature of the records is significantly different. The propeller torque is predominantly at blade rate, as shown by the fast Fourier transform in Figure 13. However blade rate excitation is suppressed by the shaft dynamics, and shaft response at the first natural frequency of 4.2 Hz becomes evident in the shaft record, as shown by the FFT in Figure 14. Maximum propeller ice torque is greater than maximum shaft ice torque.

2.3. Other Examples

Several other examples of measured shaft and calculated propeller load histories are also provided. These load histories show the same general characteristics for thrust and torque, and similar comparisons between shaft and propeller ice loads, as the detailed example given above.

Robert Lemeur - Trials Event 73

Thrust	Figures 15 (shaft), 16 (propeller), 17 (blade bending stress)
Torque	Figure 18 (shaft), 19 (propeller)

M.V. Kalvik - Trials Event 24

Thrust	Figures 20 (shaft), 21 (propeller) Thrust is predominantly backward blade bending, as expected for an open propeller
Torque	Figures 22 (shaft), 23 (propeller)

M.V. Kalvik - Trials Event 8

Thrust	Figures 24 (shaft), 25 (propeller)

M.V. Ikaluk - Trials Event 46

Thrust	Figures 26 (shaft), 27 (propeller)
Torque	Figures 28 (shaft), 29 (propeller)

Oden - Trials Event M2331834

Torque	Figures 30 (shaft), 31 (propeller)

Oden - Trials Event M2331103

Torque	Figures 32 (shaft), 33 (propeller)

2.4. Tabulated Results

The propeller and ice interaction loads, calculated from the seven sets of Canadian full-scale trials data, measured on the shaft, for the vessels Louis S. St. Laurent, Kalvik, Ikaluk (two trials), Terry Fox, Robert Lemeur, and Oden, are given in Appendix A.

For each identified trials event, maximum positive propeller ice thrust, maximum negative propeller ice thrust, maximum propeller ice torque, and maximum average propeller ice torque are listed, as well as corresponding ship speed, rpm, pitch angle, and ice interaction information.

Subsequent investigation of parametric influences and long-term load predictions were carried out using these data.

A few of the events presented in the shaft loads report, Reference 3, are not included in the tables in Appendix A. Upon re-examination, these few event time traces were suspected of being influenced by minor interference "spikes". Where the time trace included an alternative acceptable interaction, it was analyzed and included.

Moreover, the exact timing of the event maxima for shaft and propeller loads are not necessarily the same. Shaft dynamics introduces a small phase lag in response and, commonly, in the case of torque, a transfer of energy from blade rate excitation to shaft natural frequency response.

2.5. Ratios of Propeller/Shaft Ice Loads

The relationships between propeller and shaft ice loads, resulting from shaft dynamics, are shown in Table 2. For each vessel trial analyzed in this project by the de-convolution method the average ratios of propeller/shaft loads, for all events, are listed.

Table 2 Ratios of Propeller/Shaft Ice Loads

Vessel	Max Prop Torque / Max Shaft Torque	Positive Prop Thrust / Positive Shaft Thrust	Negative Prop Thrust / Negative Shaft Thrust
Ikaluk '89	1.07	0.47	0.49
Ikaluk '90	0.99	0.65	0.61
Robert Lemeur	1.46	0.60	0.51
Oden	1.08	No measurements	No measurements
Kalvik	1.35	0.40	0.54
Terry Fox	1.74	0.58	0.63

It is noted that for these typical geared diesel drive vessels, maximum propeller ice thrust loads, positive for ducted and negative for open propellers, are approximately 60% of the measured shaft loads. Maximum propeller torque, on the other hand, is in the range of 100-175% of shaft torque.

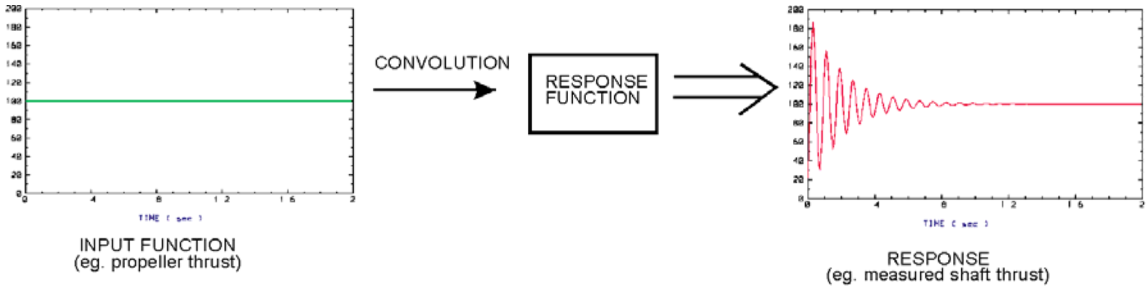

(a) Convolution Process of Calculating Response from the Input Function

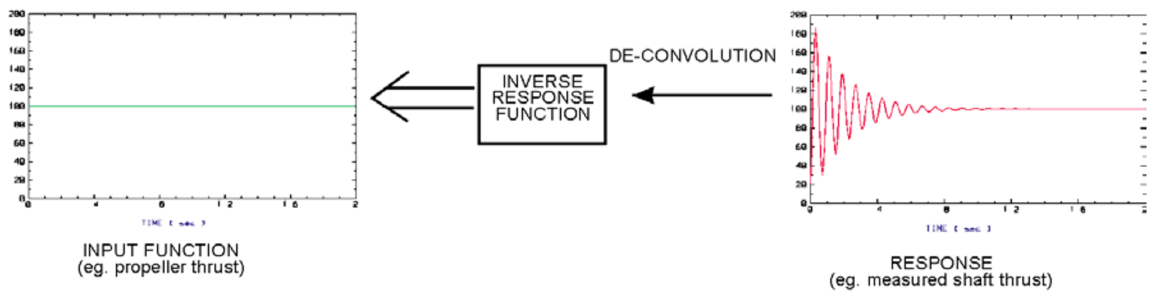

(b) De-convolution Process of Calculating Input Function from the Response

Figure 1 Diagrammatic Representation of the Convolution Method

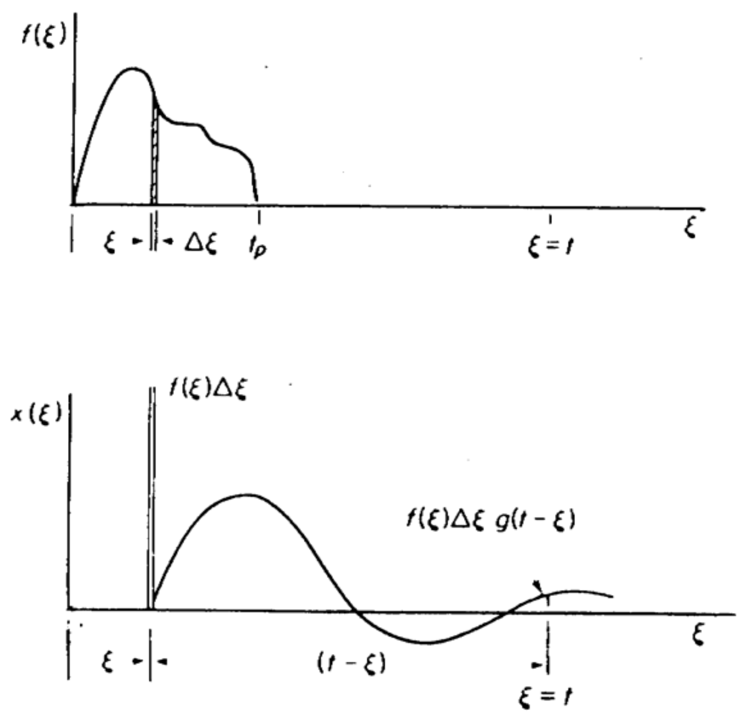

Figure 2 Response to an Impulse

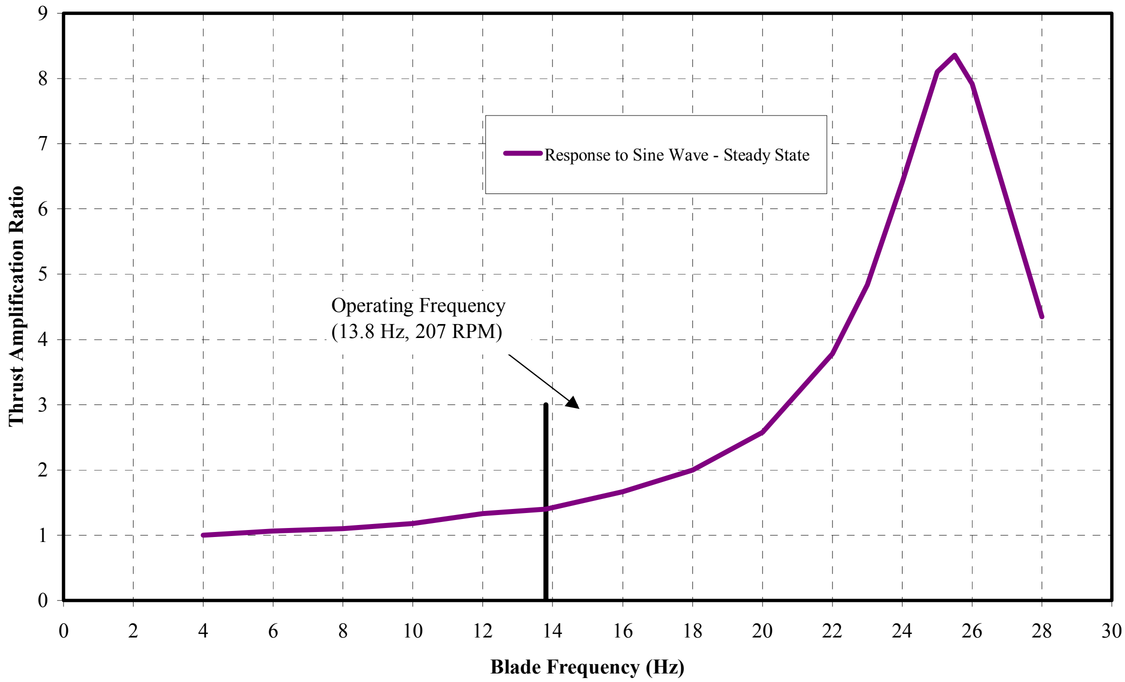

Figure 3 Robert Lemeur - Thrust Response

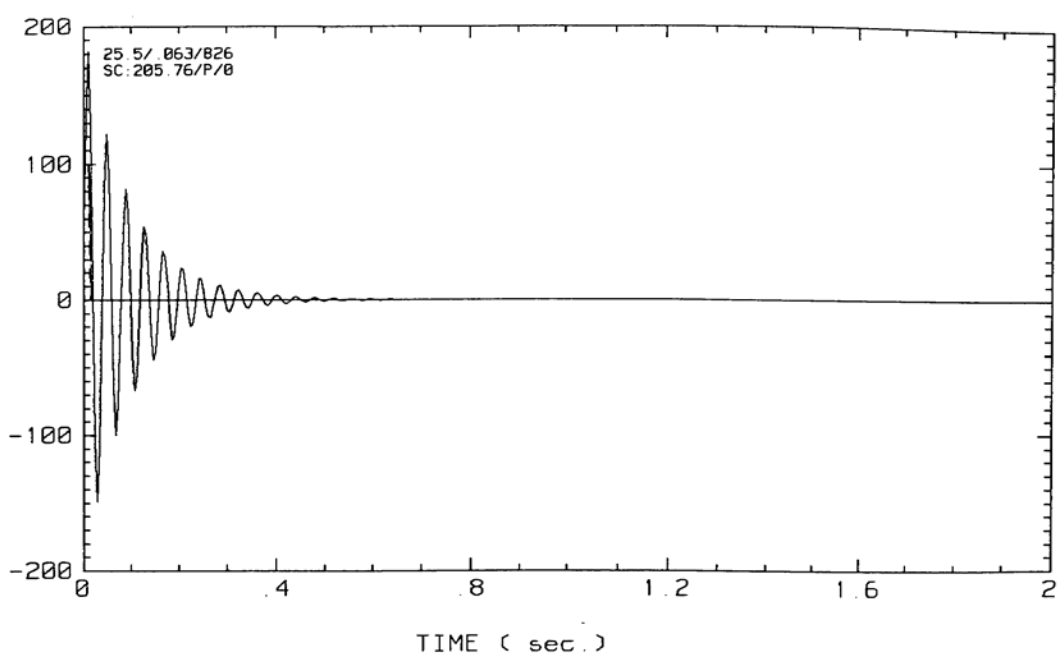

Figure 4 Robert Lemeur Thrust Impulse Response Function

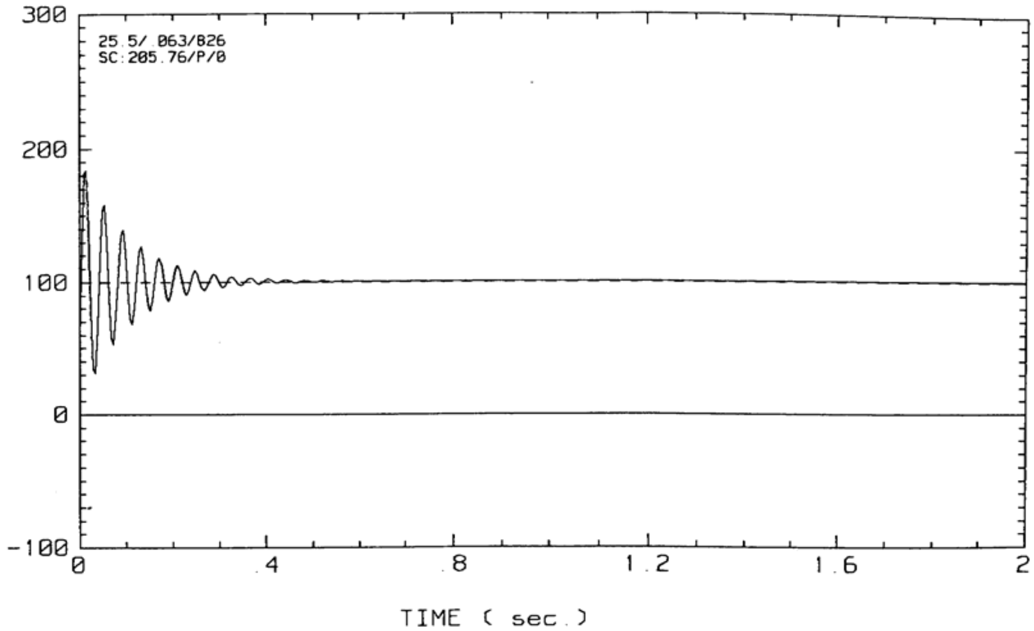

Figure 5 Robert Lemeur Thrust Impulse Stability Check

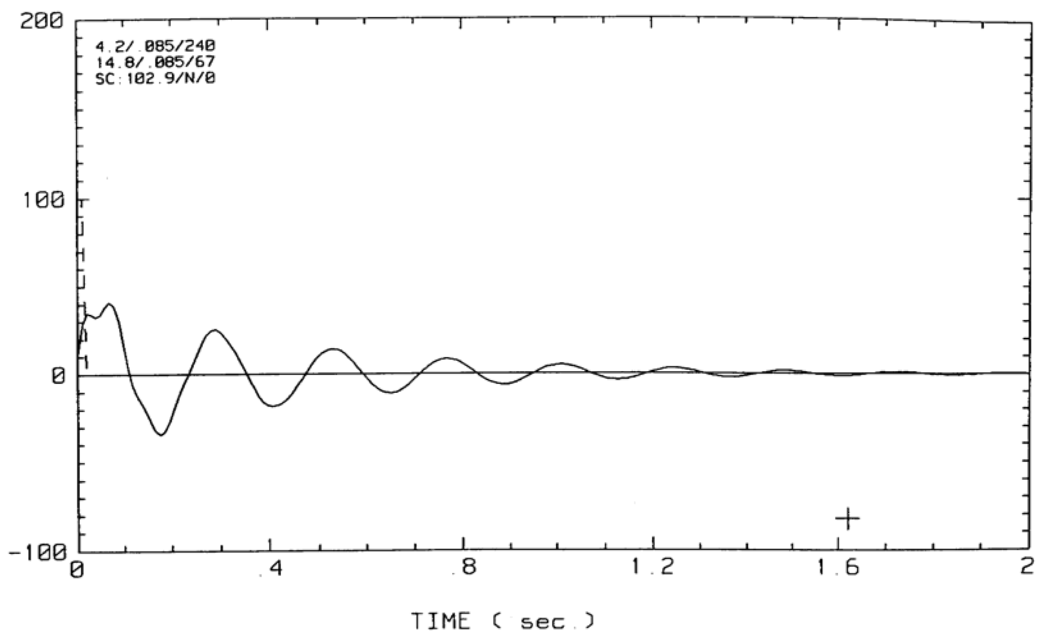

Figure 6 Robert Lemeur Torque Impulse Response Function

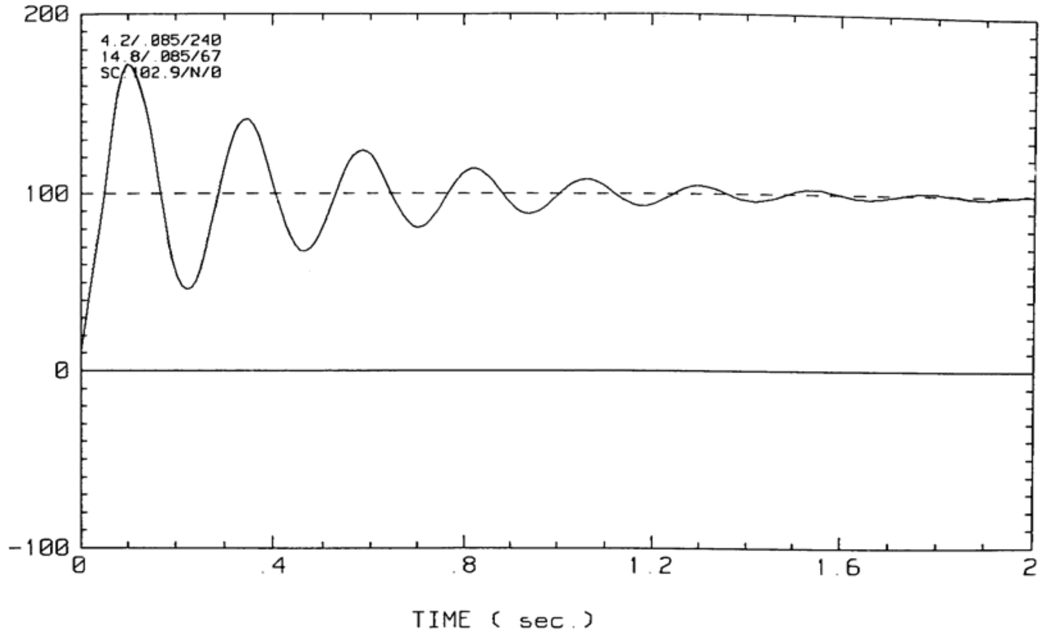

Figure 7 Robert Lemeur Torque Impulse Stability Check

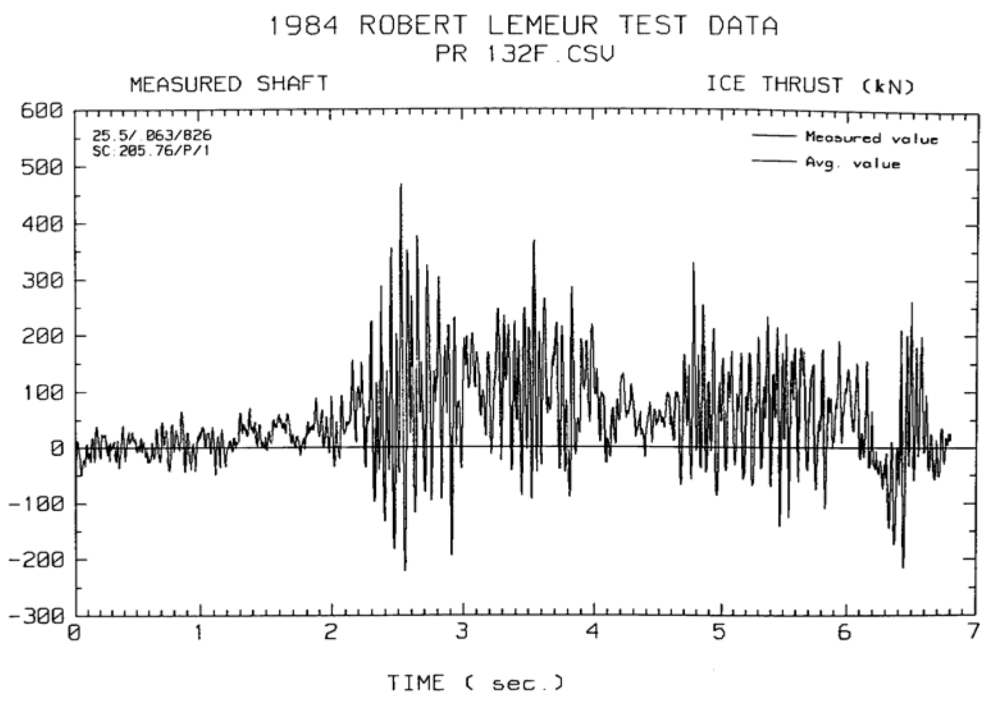

Figure 8 Robert Lemeur measured Shaft Ice Thrust - Event 132

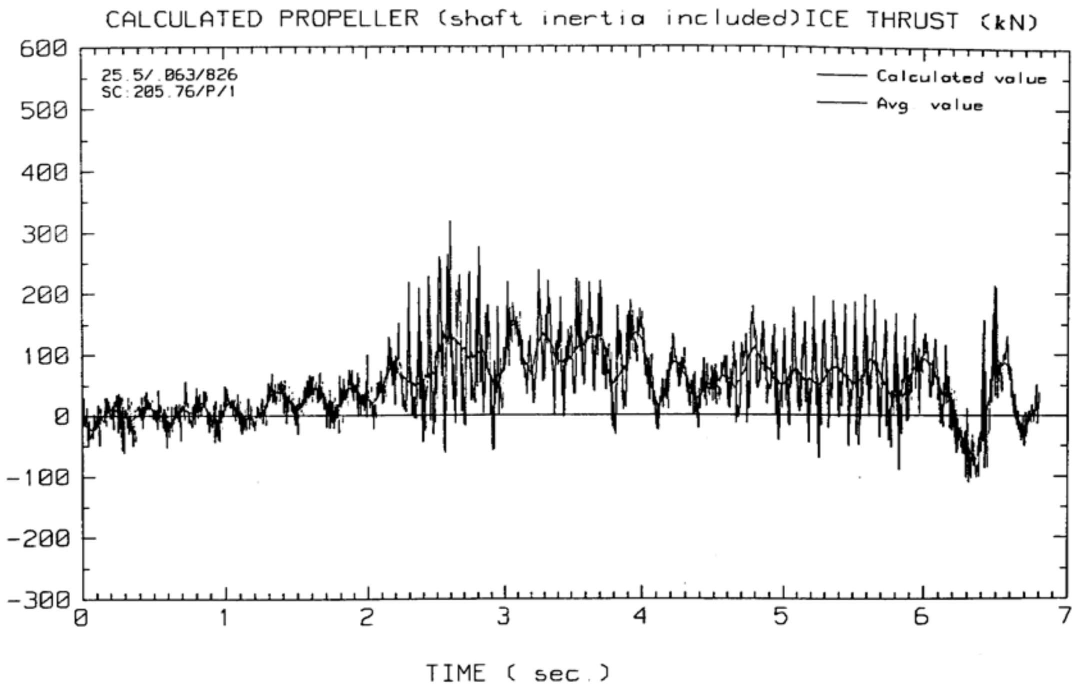

Figure 9 Robert Lemeur calculated Propeller Ice Thrust - Event 132

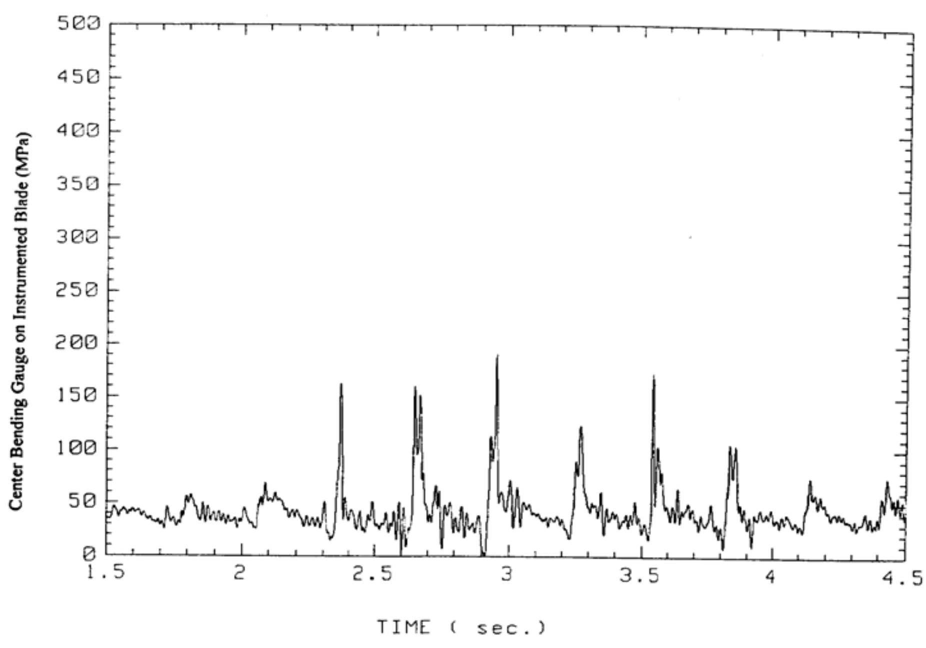

Figure 10 Robert Lemeur Blade Bending Stress - Event 132

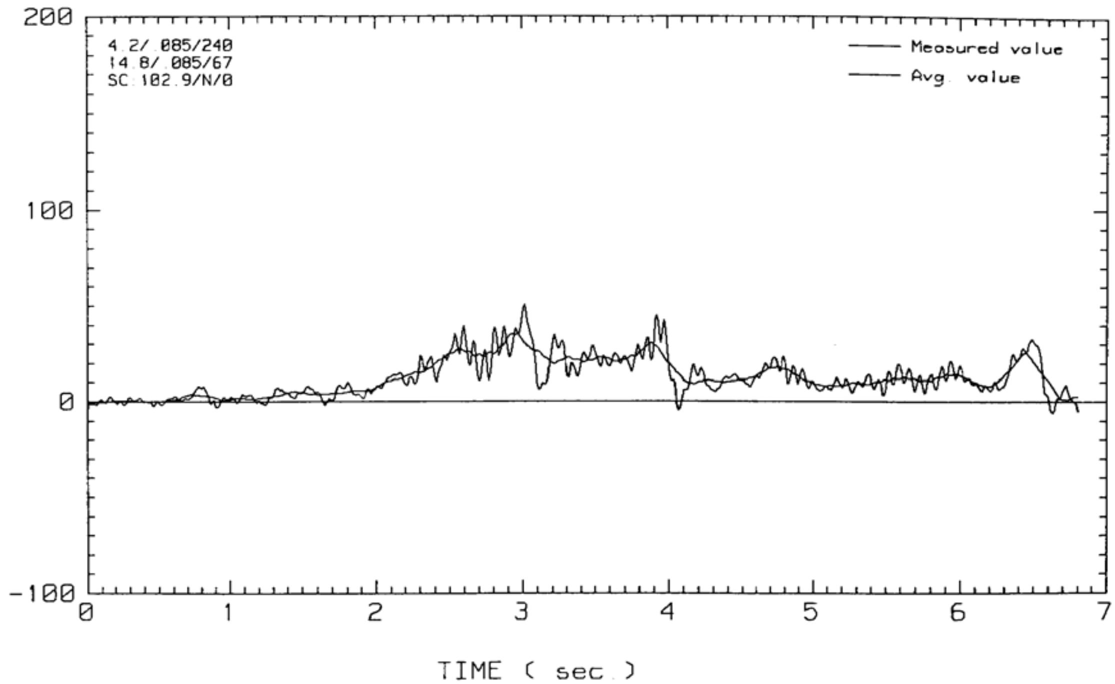

Figure 11 Robert Lemeur measured Shaft Ice Torque - Event 132

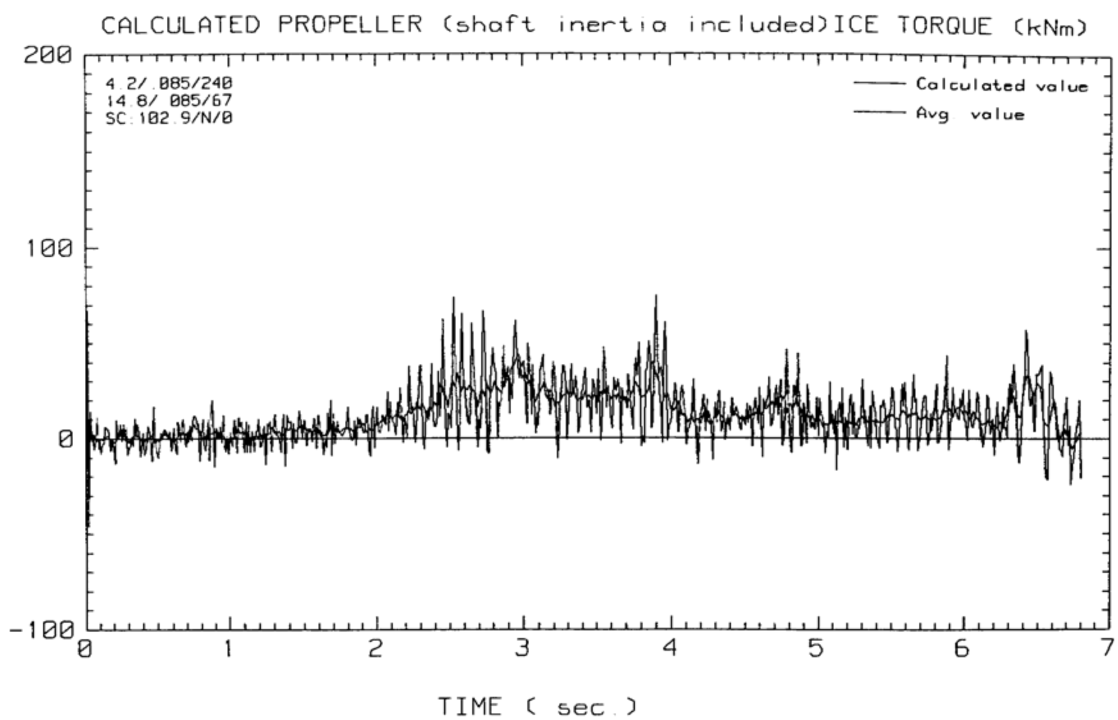

Figure 12 Robert Lemeur calculated Propeller Ice Torque - Event 132

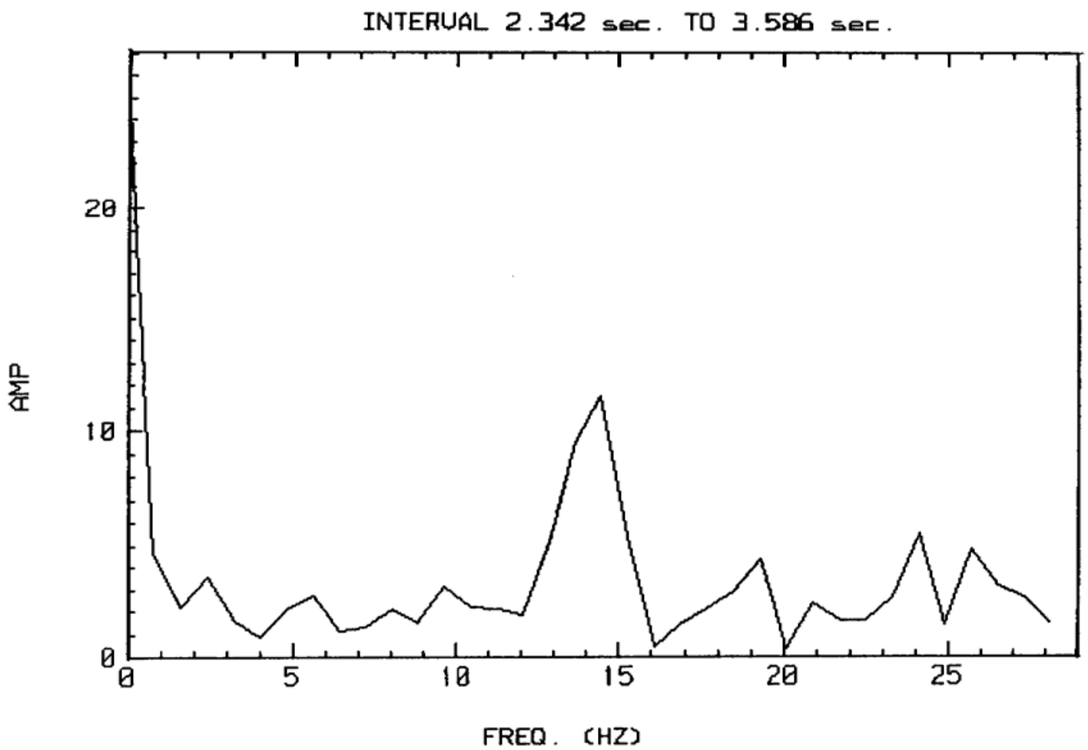

Figure 13 FFT for Propeller Ice Torque - Event 132

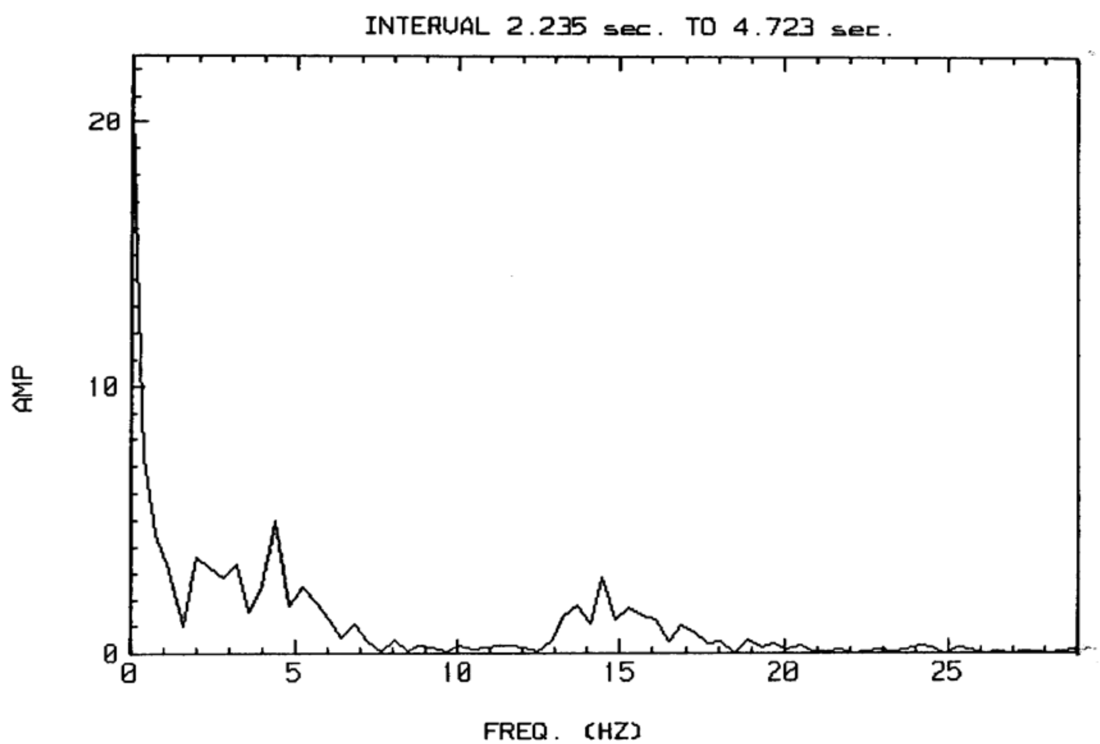

Figure 14 FFT for Shaft Ice Torque - Event 132

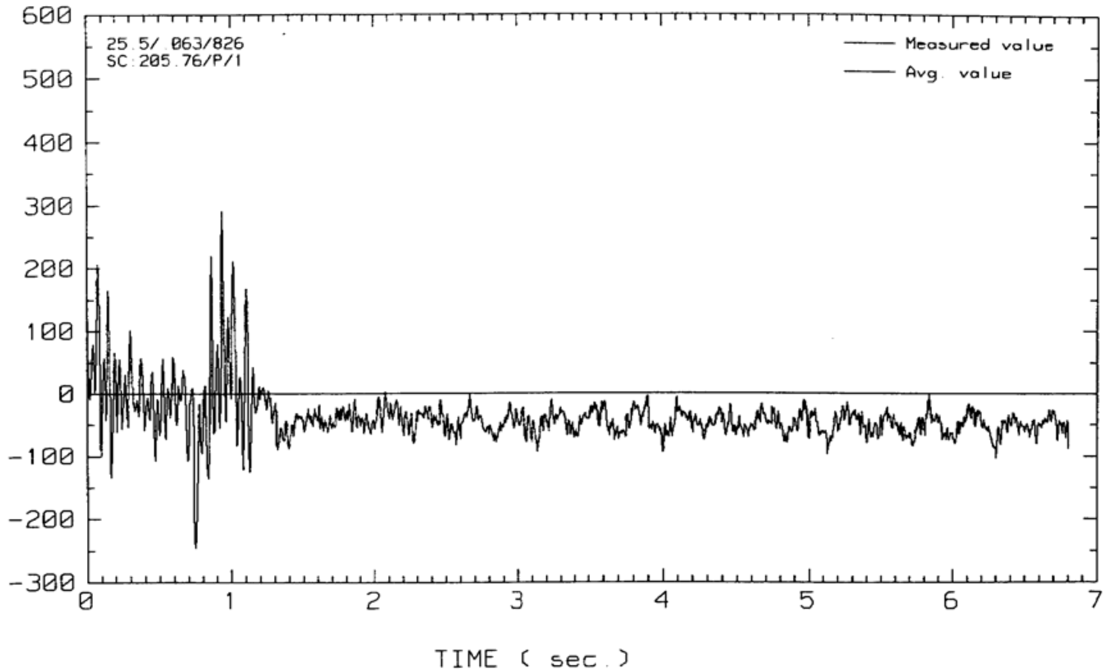

Figure 15 Robert Lemeur measured Shaft Ice Thrust - Event 073

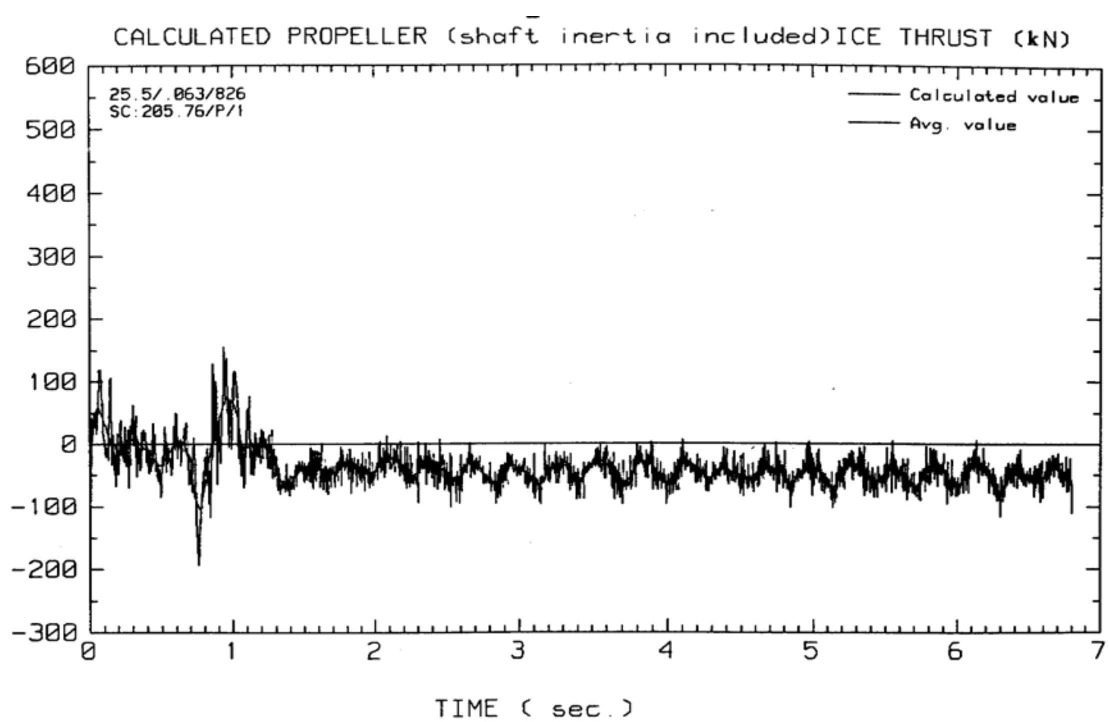

Figure 16 Robert Lemeur calculated Propeller Ice Thrust - Event 073

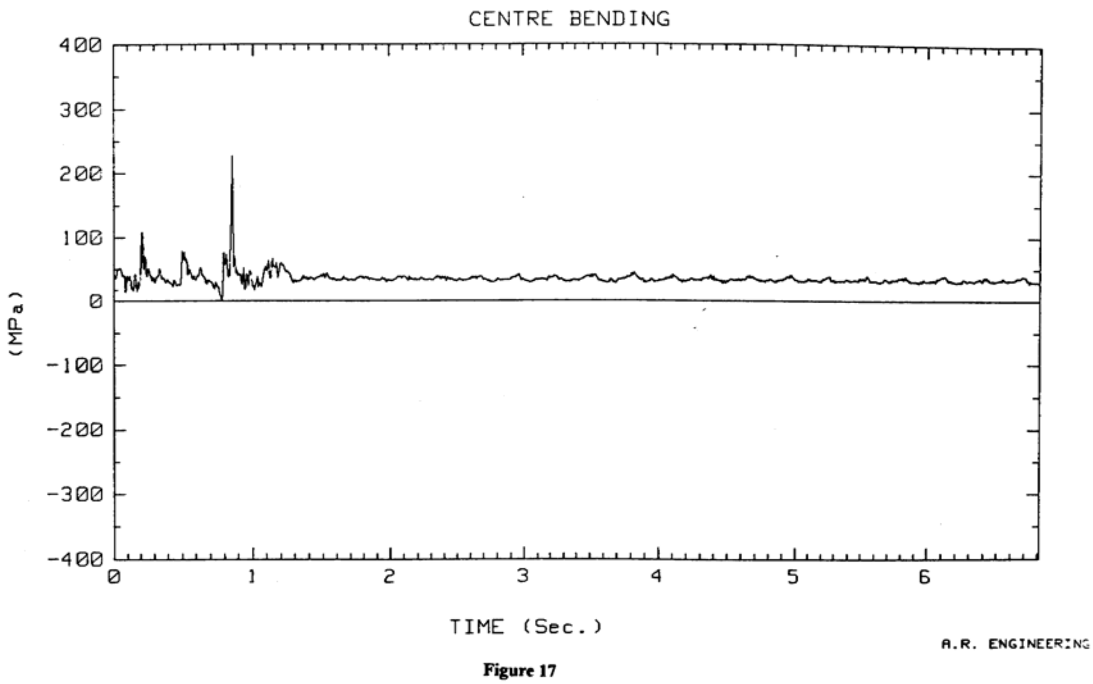

Figure 17 Robert Lemeur Blade Bending Stress - Event 073

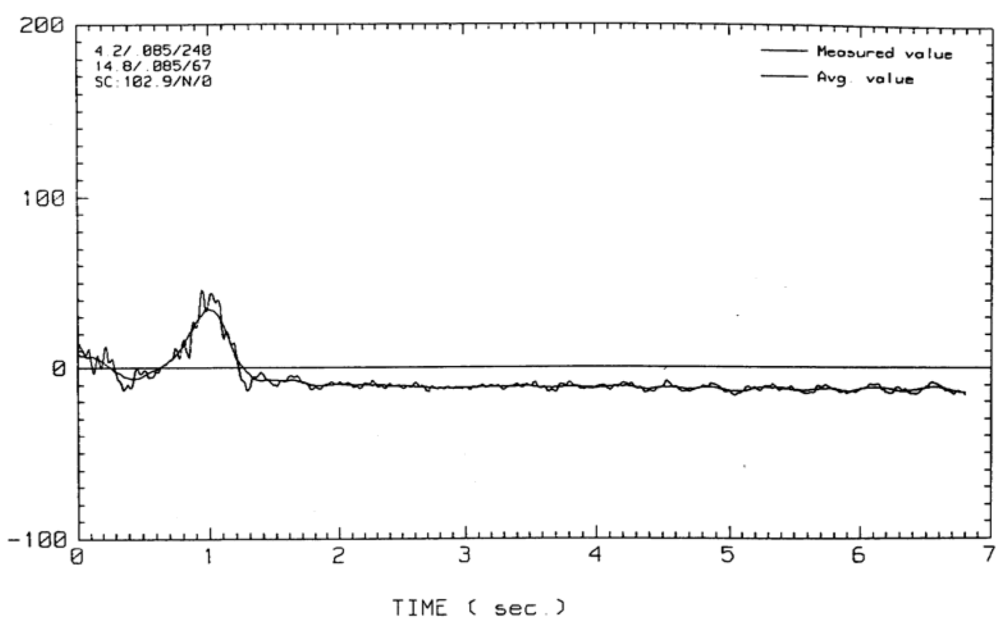

Figure 18 Robert Lemeur measured Shaft Ice Torque - Event 073

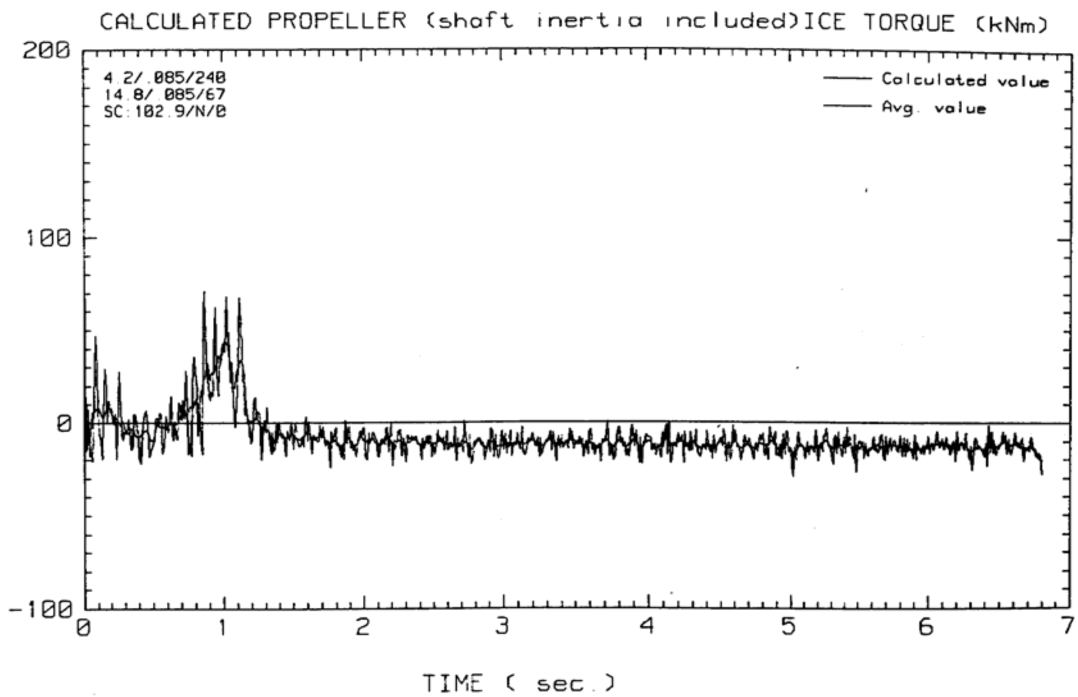

Figure 19 Robert Lemeur calculated Propeller Ice Torque - Event 073

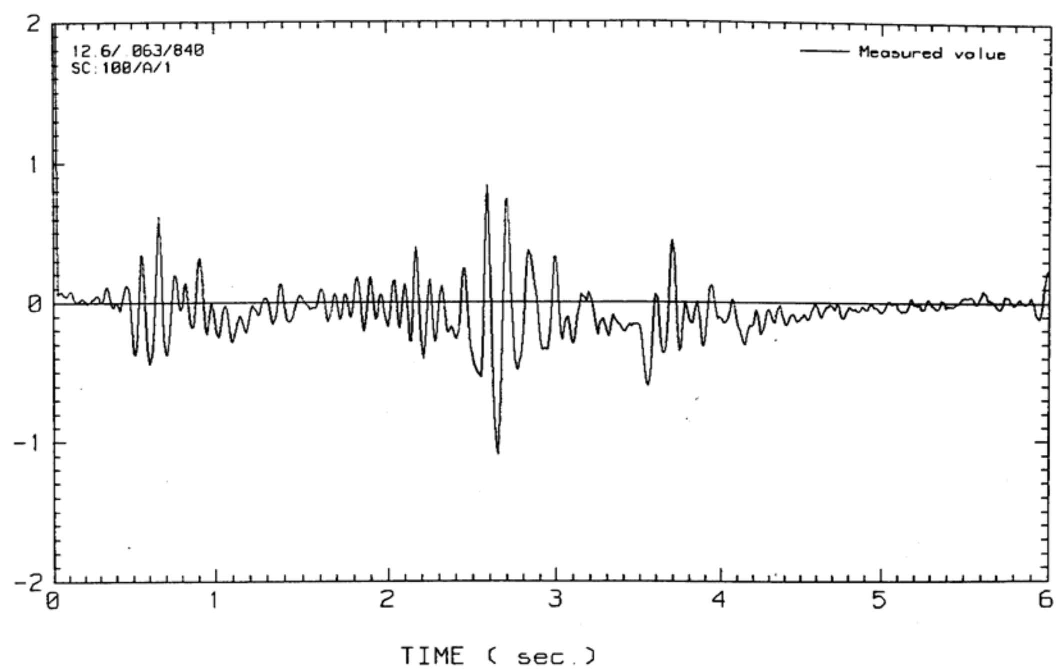

Figure 20 Kalvik measured Shaft Ice Thrust - Event 24

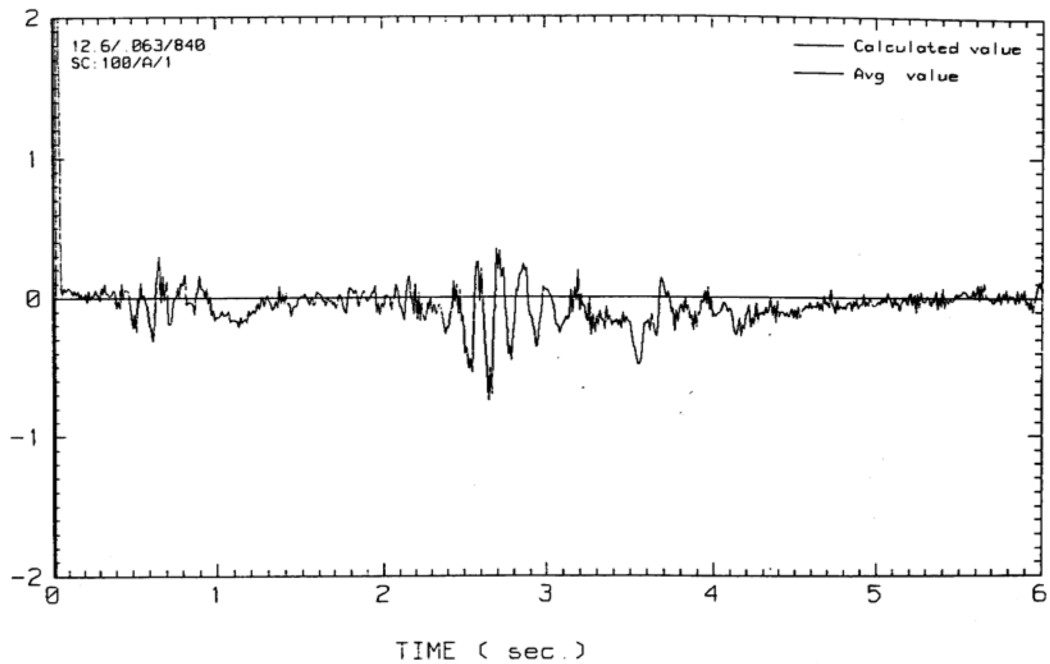

Figure 21 Kalvik calculated Propeller Ice Thrust - Event 24

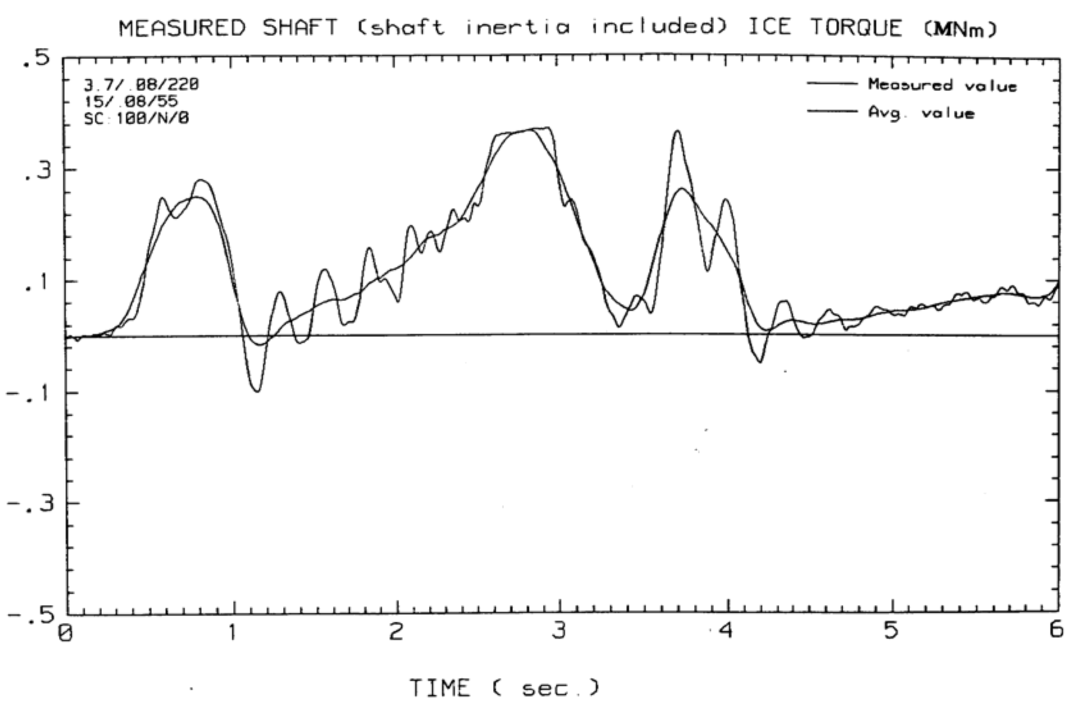

Figure 22 Kalvik measured Shaft Ice Torque - Event 2

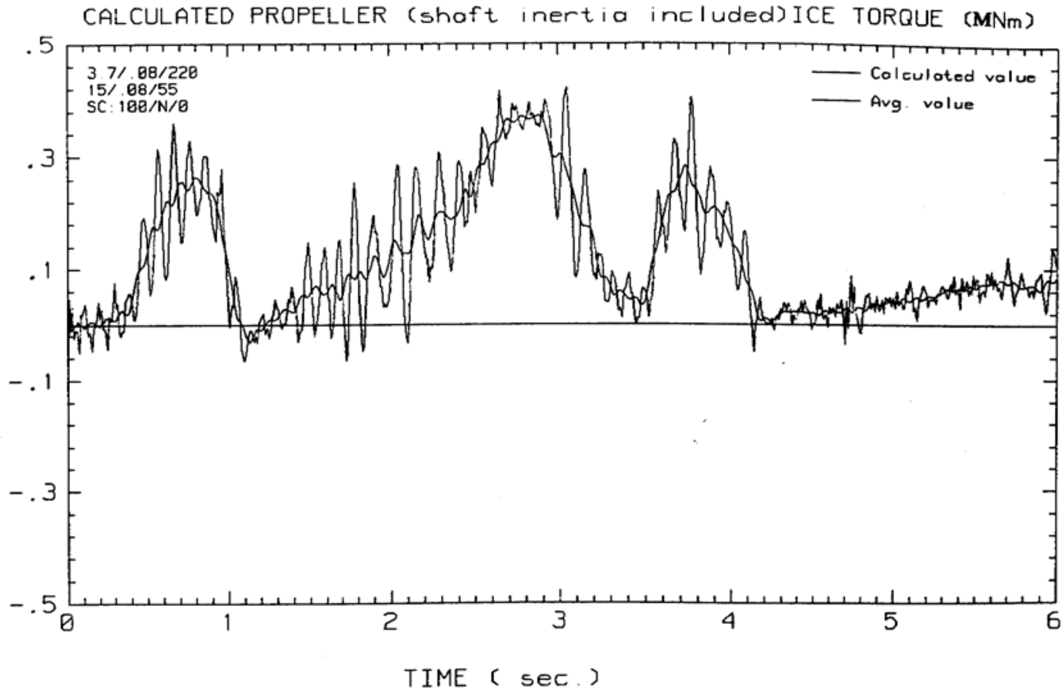

Figure 23 Kalvik calculated Propeller Ice Torque - Event 24

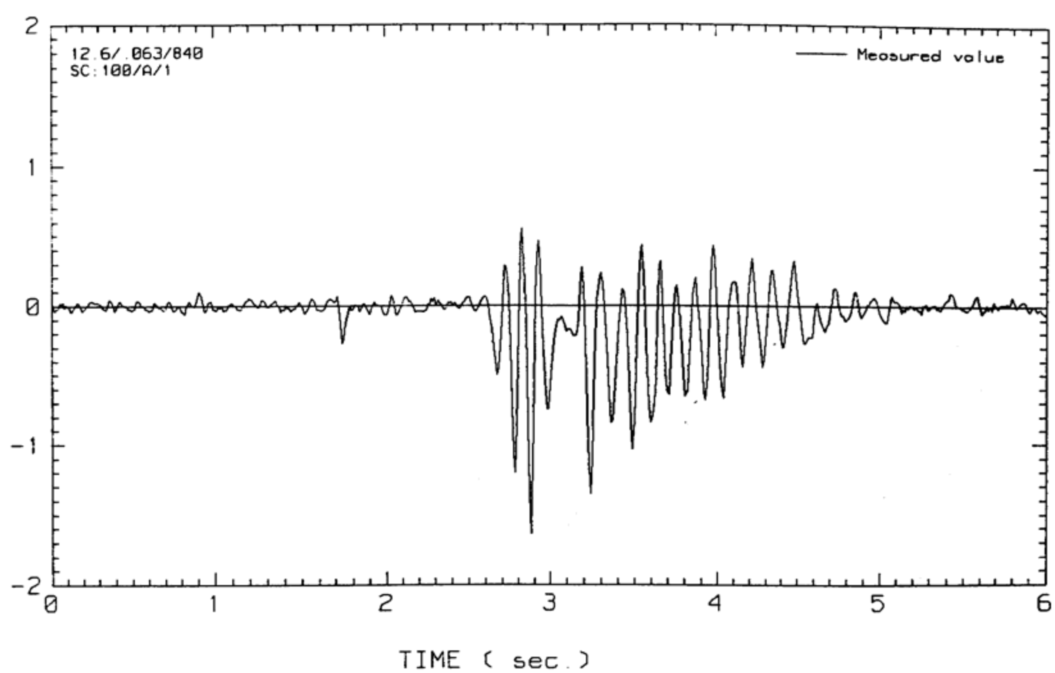

Figure 24 Kalvik measured Shaft Ice Thrust - Event 08

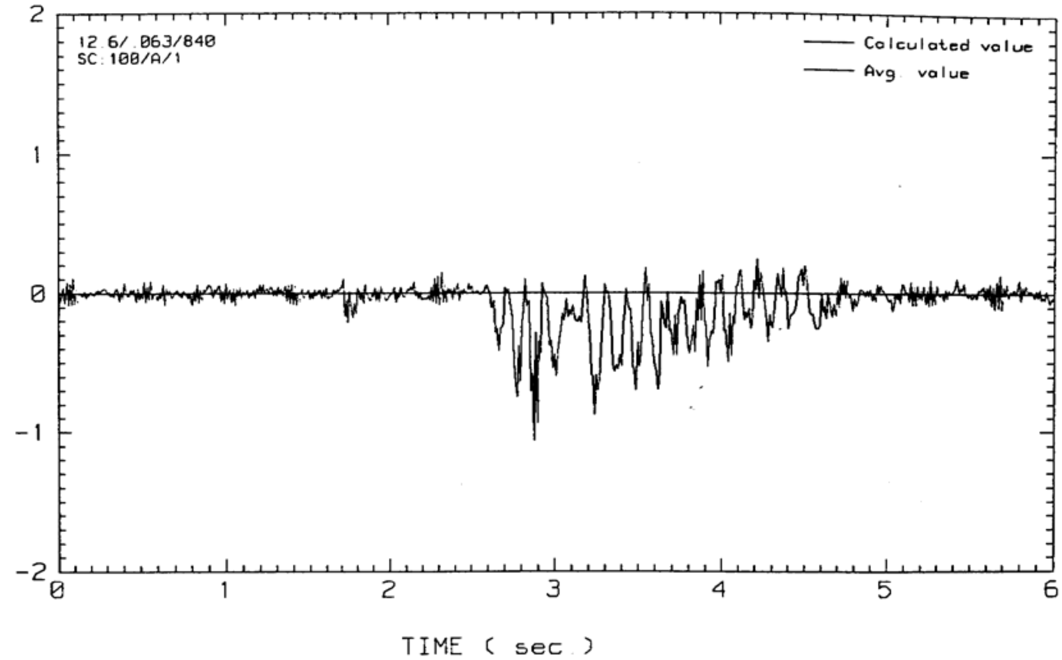

Figure 25 Kalvik calculated Propeller Ice Thrust - Event 08

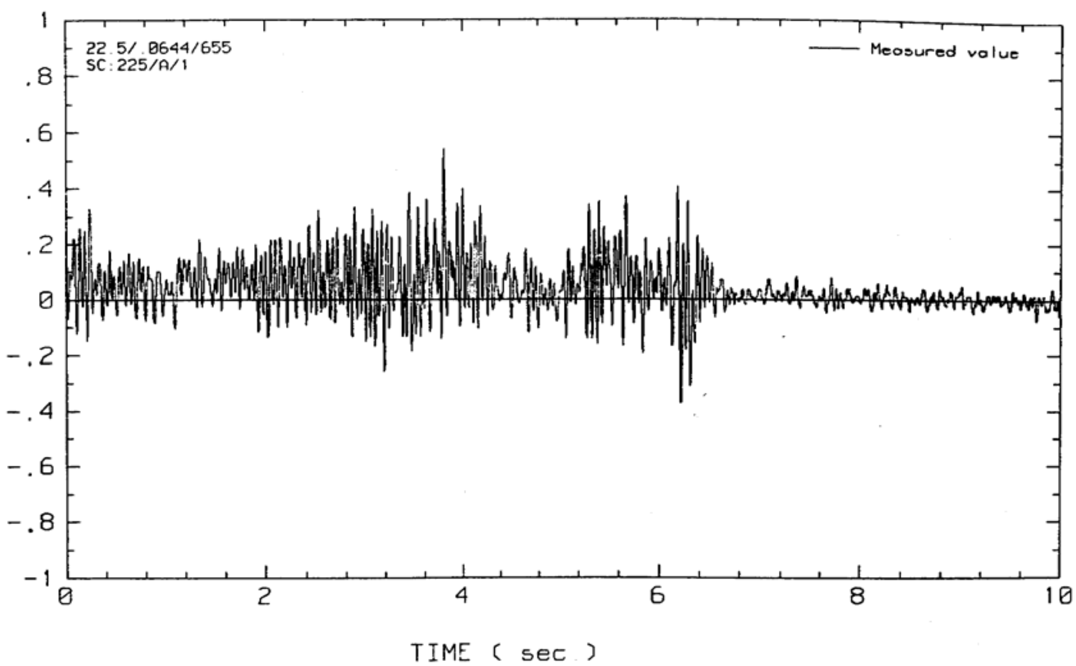

Figure 26 Ikaluk measured Shaft Ice Thrust - Event 46

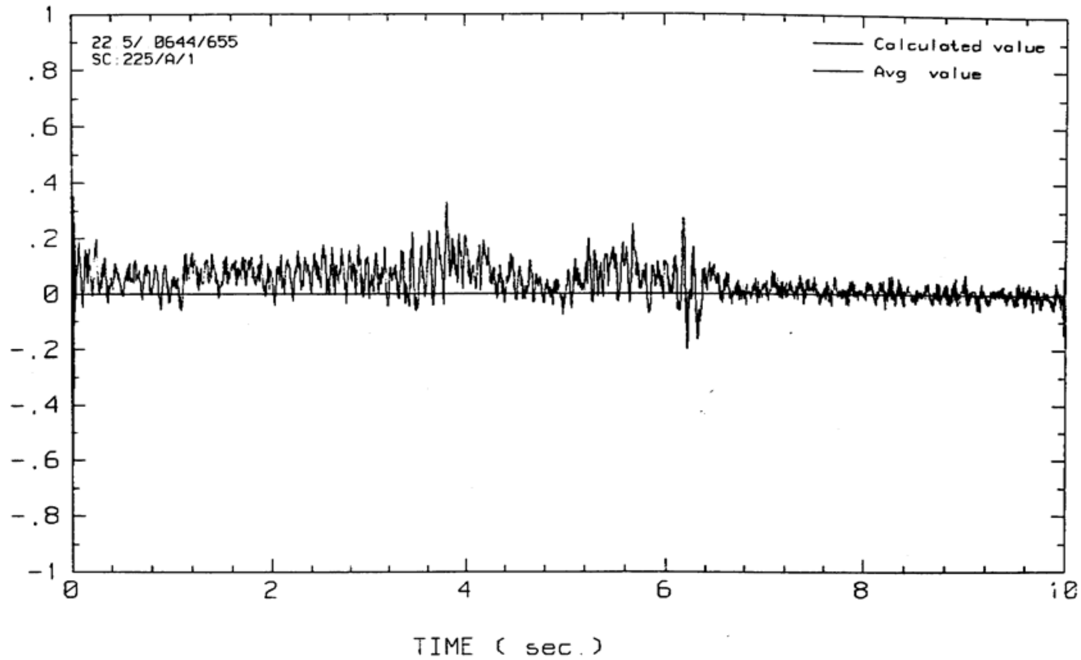

Figure 27 Ikaluk calculated Propeller Ice Thrust - Event 46

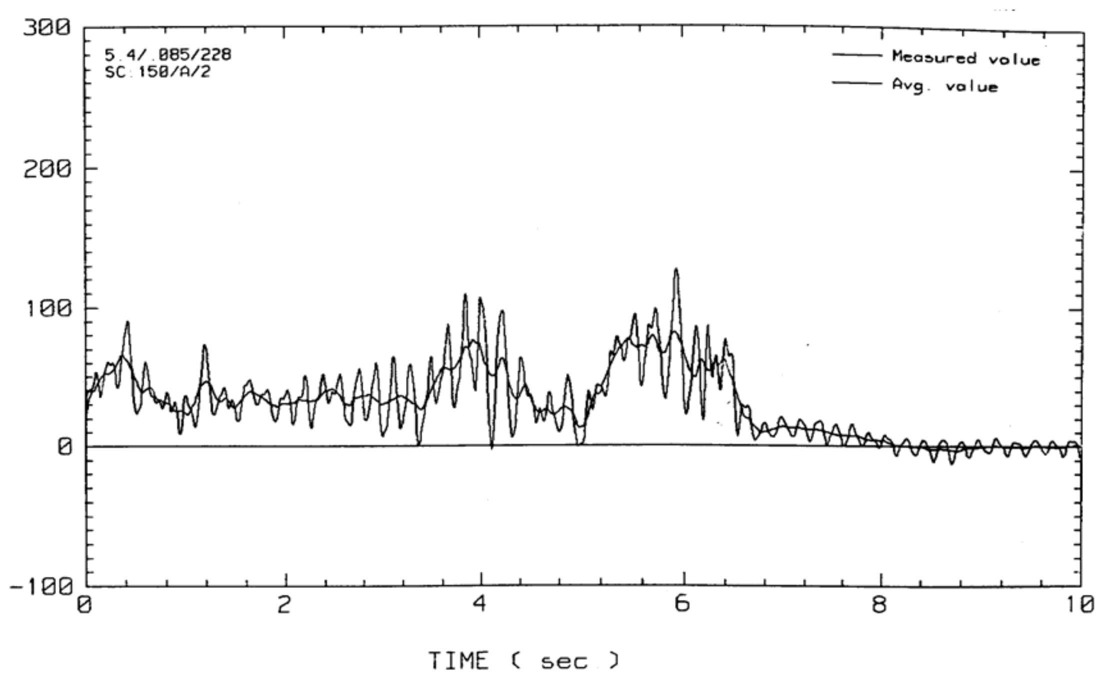

Figure 28 Ikaluk measured Shaft Ice Torque - Event 46

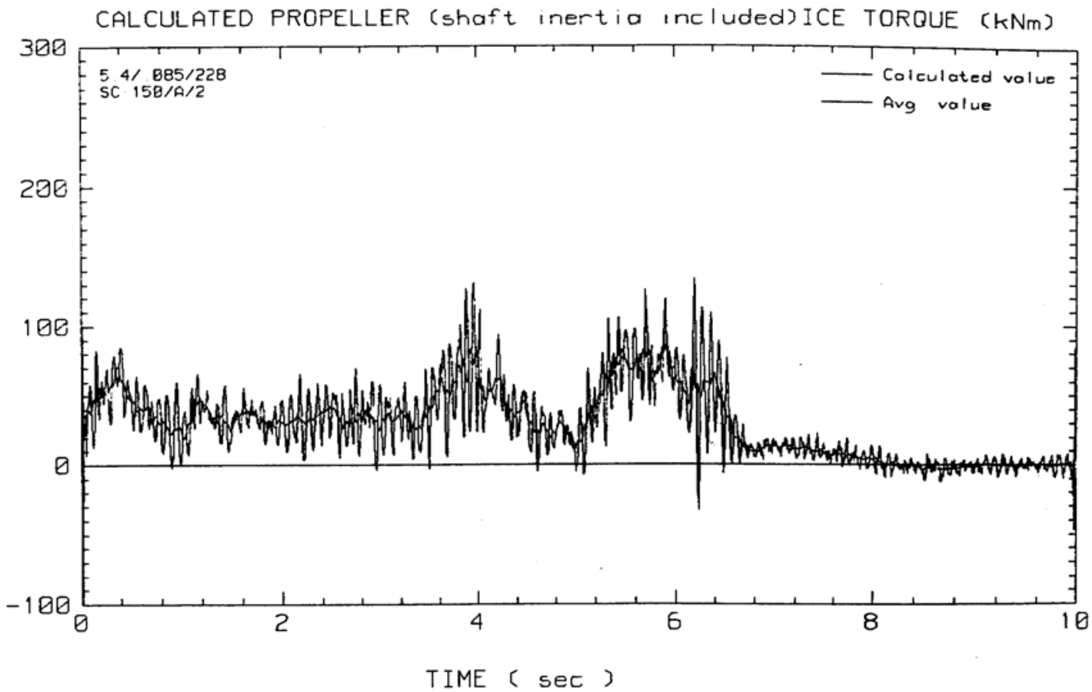

Figure 29 Ikaluk calculated Propeller Ice Torque - Event 46

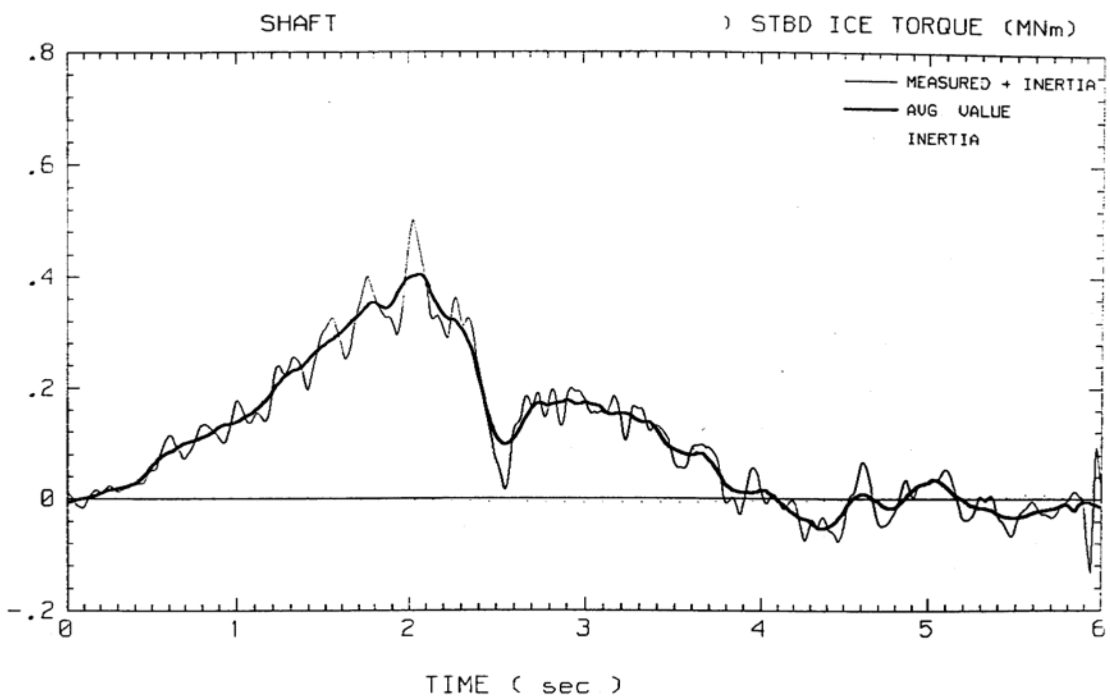

Figure 30 Oden measured Shaft Ice Torque - Event M2331834

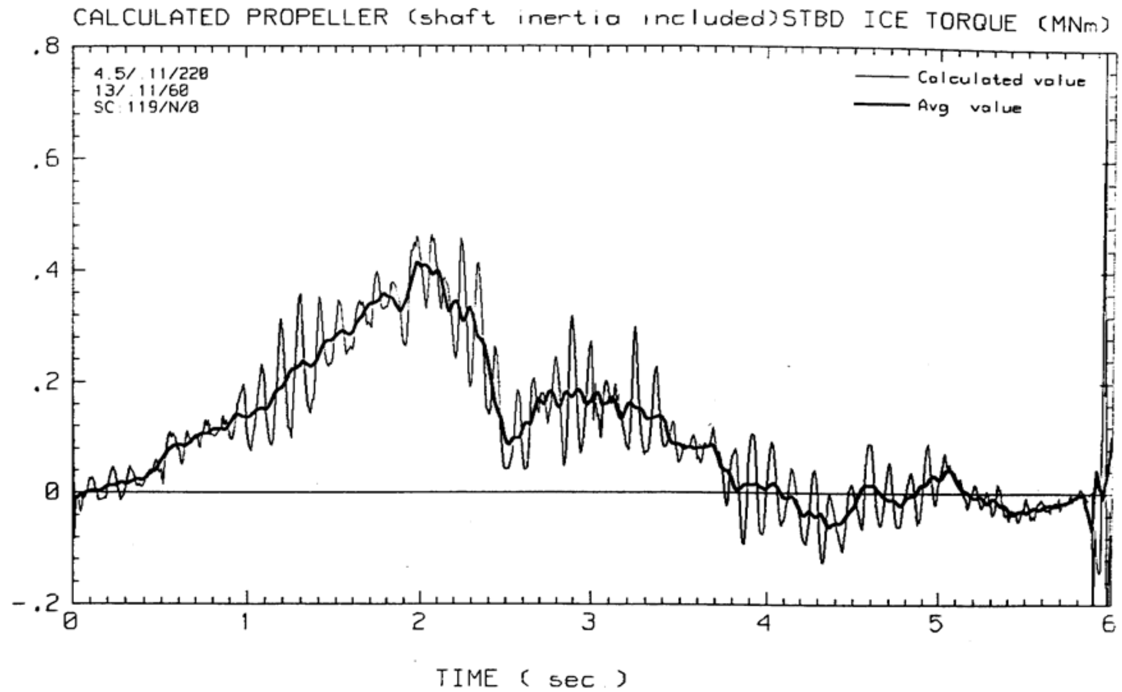

Figure 31 Oden calculated Propeller Ice Torque - Event M2331834

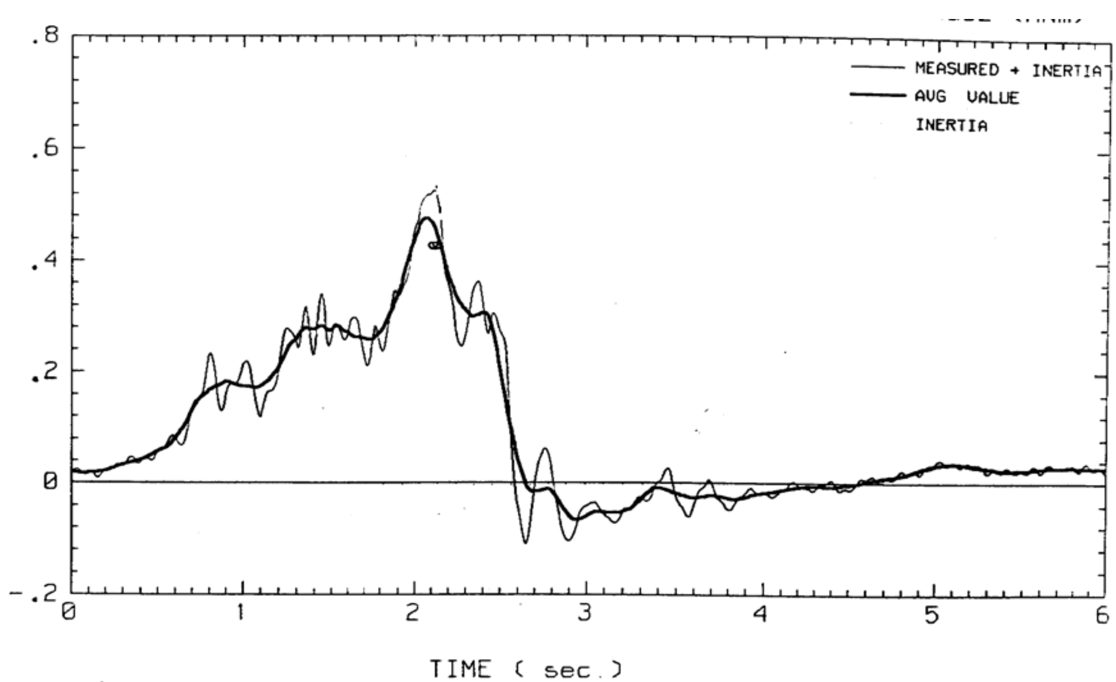

Figure 32 Oden measured Shaft Ice Torque - Event M2331103

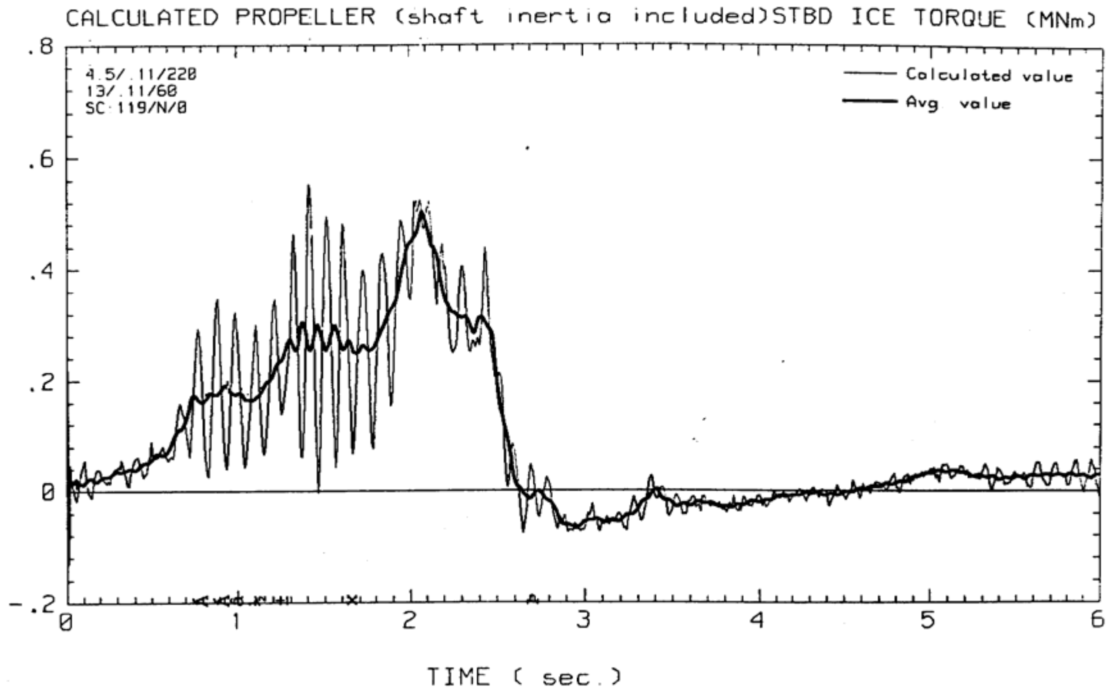

Figure 33 Oden calculated Propeller Ice Torque - Event M2331103

3. PARAMETRIC INFLUENCES

3.1. Introduction

The data used to calculate the parametric dependencies for each ship are given in the tables found in Appendix A. These tables also show the environmental conditions associated with each event. Where environmental conditions are not shown, they were either unavailable or similar for all events. The environmental data are more fully described for each ship in the earlier project report, Reference 3, on shaft loads.

Parametric dependencies for Louis S. St. Laurent are taken from Reference 2.

3.2. Kalvik (1986)

Kalvik has twin, open, controllable pitch propellers, with geared diesel drive.

The data consist of the calculated propeller ice torque (maximum and mean), propeller ice thrust (maximum positive and maximum negative), the ship operating condition (pitch angle, rpm and ship speed), and the environmental conditions (maximum ice thickness and crushing strength) associated with each event. In addition, each event was classed as either a single impact or milling event. Although the maximum ice thickness and representative strength at the location at which each event occurred was known, the characteristics of the ice piece causing the event are not known.

Figure 34 Maximum Propeller Ice Torque versus Pitch Angle
When one considers data points in any narrow pitch range, stronger ice tends to generate higher ice torque values. Although the data, taken as a whole, might suggest an increase in ice torque with increasing pitch, no consistent trend can be determined when one considers events grouped by event type, rpm, and ice strength. The few events with negative pitch are similar in magnitude to those with comparable positive pitch.

Figure 35 Mean Propeller Ice Torque versus Pitch Angle
The mean ice torque shows similar trends to the maximum ice torque in the previous figure.

Figure 36 Comparison of Maximum and Mean Propeller Ice Torque
The ratio of maximum ice torque to mean ice torque reduces with increase in ice torque, from approximately 2.0 at low ice torque to 1.2 at the highest ice torque.

Figure 37 Positive Propeller Ice Thrust versus Pitch Angle
The largest data set, for milling events with ice strength of 600 kPa and rpm > 125, suggests a positive ice thrust increase with increasing pitch. No other data set is large enough, or has sufficient pitch variation, to indicate a trend.

The highest positive ice thrust value occurs at low pitch (7.7 degrees) in the strongest ice. However, no overall ice strength influence can be determined from the data. The few events with negative pitch have comparable magnitudes to those with positive pitch.

Figure 38 Negative Propeller Ice Thrust versus Pitch Angle
As in the previous figure, the highest values occur at low pitch. However, in this case, the weakest ice produces the highest load. The events at negative pitch are much lower than those at positive pitch. The largest negative ice thrust value is 39% larger than the largest positive ice thrust in the previous figure.

Figures 39 and 40 Positive and Negative Propeller Ice Thrust versus Ship Speed
There are too few data in any set to determine trends.

3.3. Terry Fox (1990)

Terry Fox has twin, open, controllable pitch propellers, with geared diesel drive.

The data consist of the calculated propeller ice torque (maximum and mean), propeller ice thrust (maximum positive and maximum negative), and the ship operating condition (pitch angle and rpm). Ice torque data are available for both shafts, but ice thrust data are only available for the port propeller. The rpm for all events were in a narrow range (127-130 rpm), close to the nominal operating speed of 129 rpm. Ice torque events outnumber ice thrust events, due to problems with some of the thrust signals. The environmental conditions were similar for all events. Each event was classed as either a single impact or milling event.

Figure 41 Maximum Propeller Ice Torque versus Pitch Angle
The results with positive pitch indicate an increasing value of ice torque with increasing pitch. Milling events are higher than single impact events. The few events at negative pitch are significantly higher than events at similar positive pitch.

Figure 42 Mean Propeller Ice Torque versus Pitch Angle
The mean ice torque data show similar trends as the maximum ice torque data in the previous figure.

Figure 43 Comparison of Maximum and Mean Propeller Ice Torque
An approximately linear trend is noted, with maximum ice torque being, on average, 1.82 times the mean ice torque.

Figure 44 Positive Propeller Ice Thrust versus Pitch Angle
For positive pitch angles, the pitch range is too small to determine any trends. Milling and single impact events have similar magnitudes. The two events at negative pitch are significantly higher than the largest event at positive pitch.

Figure 45 Negative Propeller Ice Thrust versus Pitch Angle
For positive pitch angles, the range of pitch is too small to determine any trends. Milling events are larger than single events. The two negative pitch events are a little higher than the largest positive pitch event. For positive pitch, the largest negative ice thrust is 18% larger than the largest positive ice thrust. For negative pitch, the largest positive ice thrust is 49% larger than the largest negative ice thrust.

3.4. Ikaluk (1990)

Ikaluk has twin, ducted, controllable pitch propellers, with geared diesel drive.

This ship was tested at the same time and in the same ice conditions as the Terry Fox. The data consist of the calculated propeller ice torque (maximum and mean), propeller ice thrust (positive and negative), and the ship operating condition (pitch angle and rpm). Torque and thrust data are available for both shafts. The rpm for all events were in a narrow range (163-167 rpm) close to the nominal operating speed of 166 rpm. The environmental conditions were similar for all events. Each event was classed as either a single impact or milling event.

Figure 46 Maximum Propeller Ice Torque versus Pitch Angle
The range of pitch angle is too small to determine any trends. Milling events are higher than single impact events, with the port milling events being considerably higher than the starboard milling events (in excess of 40% higher).

Figure 47 Mean Propeller Ice Torque versus Pitch Angle
The range of pitch angle is too small to determine any trends. Milling events are higher than single impact events, with the port milling events being considerably higher than the starboard milling events (about 80% higher).

Figure 48 Comparison of Maximum and Mean Propeller Ice Torque
An approximately linear trend is noted, with maximum ice torque being, on average, 1.19 times the mean ice torque.

Figure 49 Positive and Negative Propeller Ice Thrust versus Pitch Angle
The range of pitch angle is too small to determine any trends. Positive ice thrust events are larger than negative ice thrust events, the largest positive ice thrust event being 60% larger than the largest negative ice thrust event.

3.5. Ikaluk (1989)

The data consist of the calculated propeller ice torque (maximum and mean), propeller ice thrust (maximum positive and maximum negative), and the ship operating condition (pitch angle, rpm, and ship speed). Ice torque and thrust data are available for the starboard shaft only. For the majority of events, rpm was in a narrow range (159-164 rpm), close to the nominal operating speed of 166 rpm. Two events had the recorded incident occurring at approximately 140 rpm. Three types of ice conditions were encountered: level ice, old ridges, and hummocked ice, each with an associated thickness and strength. Events were classed as blockage/milling, blockage, and milling. As there were few pure blockage events, they were plotted together with the blockage/milling events.

Figure 50 Maximum Propeller Ice Torque versus Pitch Angle
The range of pitch angle is too small and the results too few to determine any trends. Milling events and blockage/milling events have similar magnitudes, as do the positive and negative pitch events. Ice loads in the thinner, weaker ice are as high as in the stronger, thicker ice.

Figure 51 Mean Propeller Ice Torque versus Pitch Angle
As in the case of maximum ice torque, the range of pitch angle is too small and the results too few to determine any trends. Milling events and blockage/milling events have similar magnitudes, and the highest positive pitch event is approximately 27% higher than the highest negative pitch event. Ice loads in the thinner, weaker ice are as high as in the stronger, thicker ice.

Figure 52 Comparison of Maximum and Mean Propeller Ice Torque
An approximately linear trend is noted, with maximum ice torque being, on average, 1.45 times the mean ice torque.

Figure 53 Positive Propeller Ice Thrust versus Pitch Angle
The range of pitch angle is too small to determine any trends. Positive pitch thrust events are larger than negative pitch events, the largest positive pitch event being 60% larger than the largest negative pitch event. Although the highest event is in the thickest ice, the next highest event is in the thinnest ice.

Figure 54 Negative Propeller Ice Thrust versus Pitch Angle
The range of pitch angle is too small to determine any trends. Positive and negative pitch events are comparable in magnitude.

Positive ice thrust events (Figure 53) are larger than negative ice thrust events, the largest positive ice thrust event being 65% larger than the largest negative ice thrust.

3.6. Robert Lemeur (1984)

Robert Lemeur has twin, ducted, controllable pitch propellers, with geared diesel drive.

The data consist of the calculated propeller ice torque (maximum and mean), propeller ice thrust (maximum positive and maximum negative), and the ship operating condition (pitch angle, rpm, and ship speed). Ice torque and thrust data are available for the starboard shaft only. The nominal operating speed is 208 rpm. The majority of events are at greater than 200 rpm, although a number of events are below 200 (lowest 167). In general, events were not linked to ice conditions, although a few events were noted as occurring in weak ice. Events were classed as single impact, blockage/milling, blockage and milling. Events were also classified as to speed forward or astern, giving rise to some events with astern pitch and forward speed, and others with ahead pitch and astern speed.

Figure 55 Maximum Propeller Ice Torque versus Pitch Angle
For data groups with a large pitch range and many events (e.g. mill fwd, single fwd), ice torque increases with increasing ahead pitch. Milling and blockage/ milling events are larger than single events (approximately 20% larger). Negative pitch events are not significant. Loads in the rotten ice were much lower than the largest events in stronger ice.

Figure 56 Mean Propeller Ice Torque versus Pitch Angle
As for maximum ice torque above.

Figure 57 Comparison of Maximum and Mean Propeller Ice Torque
An approximately linear trend is noted, with maximum ice torque being, on average, 1.74 times the mean ice torque.

Figure 58 Mean Propeller Ice Torque versus RPM – Milling Events
The data groups for pitch>25, pitch 24-25 and pitch 22-23, cover an rpm range of 25 to 40 rpm, and suggest an increase in mean ice torque with increasing rpm. However, the data groups are small, and a more statistically significant sample would be required to check this possible trend.

Figure 59 Mean Propeller Ice Torque versus Ship Speed – Single Events
There is no discernible trend with ship speed. Although the highest events are at low speed, this might be indicative of more onerous ice conditions.

Figure 60 Positive Propeller Ice Thrust versus Pitch Angle
For some event groups with a large pitch range and many events (milling, single), maximum positive ice thrust increases with increasing ahead pitch. However, for the blockage/milling group, the opposite trend is noted. Milling, blockage/milling, and single impact events are all approximately equal in magnitude. Negative pitch events are as high as positive pitch events. Loads in rotten ice are much lower than the largest events in stronger ice.

Figure 61 Negative Propeller Ice Thrust versus Pitch Angle
Single impact and milling events provide the highest loads. The highest blockage event is approximately 80% of the maximum load. Negative pitch events are approximately 60% of the largest positive pitch event, and comparable to the ahead loads in rotten ice.

The maxima in the data groups, single and milling suggest an increase in negative thrust with decrease in pitch angle. However, weaker and sometimes contrary trends are seen in other data groups (e.g. blockage/milling).

Figure 62 Positive Propeller Ice Thrust versus RPM – Milling Events
A general trend is noted within the three data groups of positive ice thrust increasing with rpm increase. However, the data groups are small, and the magnitudes of the trends are different. Larger data samples would be required to be sure of these trends.

Figure 63 Negative Propeller Ice Thrust versus RPM – Milling Events
No clear trends with rpm are noted.

Figure 64 Positive Propeller Ice Thrust versus Ship Speed – Single Events
Figure 65 Negative Propeller Ice Thrust versus Ship Speed – Single Events
In general, high loads occur at all speeds.

3.7. Oden (1991)

Oden has twin, ducted, controllable pitch propellers, with geared diesel drive.

The data were collected on a voyage to the North Pole, and consist of the calculated propeller ice torque (maximum and mean), and the ship operating condition (pitch angle, rpm, and ship speed). Ice torque data are available for the starboard and port shafts. The nominal operating speed is 144 rpm, with very few events falling significantly below this value. Ice measurements were taken along the route, but due to the mixed ice regime, the characteristics of the ice causing a particular event are not known. Events were classed as impact (less than 2 seconds), blockage/milling, and milling.

Figure 66 Maximum Port Propeller Ice Torque versus Voyage Date and Ice Strength
Figure 67 Mean Port Propeller Ice Torque versus Voyage Date and Ice Strength
The ice strength decreases slightly with time. Both maximum and mean values of ice torque also show this decrease. Milling events are larger than impact loads, but only marginally. Milling/blockage loads are significantly lower.

Figure 68 Maximum Port Propeller Ice Torque versus Pitch Angle
Figure 69 Mean Port Propeller Ice Torque versus Pitch Angle
Both the maximum and mean plots show increasing ice torque with increasing pitch, for the milling and impact loads. Milling and impact loads are comparable at the same pitch angles. The milling/blockage loads do not seem to increase after about 20 degrees of

pitch. Negative pitch loads are less than positive pitch loads (50% less for maximum and 40% less for mean loads).

Figure 70 Comparison of Maximum and Mean Port Propeller Ice Torque
An approximately linear trend is noted, with maximum ice torque being, on average, 1.30 times the mean ice torque.

Figure 71 Maximum Starboard Propeller Ice Torque versus Voyage Date and Ice Strength
Figure 72 Mean Starboard Propeller Ice Torque versus Voyage Date and Ice Strength
The starboard torque values are consistent with the results for the port propeller, i.e. decreasing load with decreasing ice strength. The highest milling event for maximum ice torque is significantly higher (35% higher) than the other results for both port and starboard maximum ice torque.

Figure 73 Maximum Starboard Propeller Ice Torque versus Pitch Angle
Figure 74 Mean Starboard Propeller Ice Torque versus Pitch Angle
The results are comparable to those noted for the port propeller. The loads for negative pitch are an even smaller percentage of the positive pitch loads, when compared to the port propeller results.

Figure 75 Comparison of Maximum and Mean Starboard Propeller Ice Torque
An approximately linear trend is noted, with maximum ice torque being, on average, 1.38 times the mean ice torque.

Figure 76 Maximum Starboard Propeller Ice Torque versus Ship Speed – Impact Events
Figure 77 Mean Starboard Propeller Ice Torque versus Ship Speed – Impact Events
There is no discernible trend with speed. Although the highest events are at low speed, this might be indicative of more onerous ice conditions, causing lower speeds and higher loads.

3.8. Louis S. St. Laurent (1994)

Parametric dependencies for Louis S. St. Laurent are taken from Reference 2.

Louis S. St. Laurent has triple, open, fixed pitch propellers, with diesel-electric drive. No information regarding pitch angle influence can therefore be determined.

Propeller ice thrust and ice torque were found to be independent of both ship speed and apparent angle of attack. Investigation for the separate influence of ice strength and rpm was inconclusive. The largest ice thrust events had negative (backward blade bending) values at positive rpms, and the largest ice torque events were at positive rpms.

3.9. The Influence of Ice Strength on Propeller Loads

The influence of ice strength on propeller loads is investigated for the following cases, where the same vessel or identical vessels were tested in both weak and strong ice.

3.9.1. Identical Sister Ships, Kalvik (1986) and Terry Fox (1990).

Reference Figures:
Figure 78 Comparison of Kalvik and Terry Fox Maximum Propeller Ice Torque
Figure 79 Comparison of Kalvik and Terry Fox Mean Propeller Ice Torque
Figure 80 Comparison of Kalvik and Terry Fox Positive Propeller Ice Thrust
Figure 81 Comparison of Kalvik and Terry Fox Negative Propeller Ice Thrust

The comparison is carried out on the basis of single impacts, to avoid the complication of a large ice piece interacting with multiple blades, or several ice pieces acting simultaneously. The comparison of loads and ice flexural strength is shown in Table 3. The ice flexural strengths are 582 kPa for the strong ice and 150 kPa for the weak ice.

Table 3 Ice Strength Influence - Kalvik and Terry Fox

Item	Load in Weak Ice	Load in Strong Ice	Ratio of Loads	Ratio of Ice Strengths
Max Q kNm	132	414	0.32	0.26
Mean Q kNm	61	191	0.32	0.26
+ T kN	234	320	0.73	0.26
- T kN	-190	-328	0.58	0.26

Ikaluk (1989) and Ikaluk (1990)

Reference Figures:
Figure 82 Comparison of Ikaluk '89 and Ikaluk '90 Maximum Propeller Ice Torque
Figure 83 Comparison of Ikaluk '89 and Ikaluk '90 Mean Propeller Ice Torque
Figure 84 Comparison of Ikaluk '89 and Ikaluk '90 Positive Propeller Ice Thrust
Figure 85 Comparison of Ikaluk '89 and Ikaluk '90 Negative Propeller Ice Thrust

The comparison is carried out on the basis of the Ikaluk, 1989, tests in level ice, as this is the closest condition to the Ikaluk, 1990, ice conditions. The comparison of loads and ice flexural strength is shown in Table 4. The ice flexural strengths are 460 kPa for the strong ice and 150 kPa for the weak.

Table 4 Ice Strength Influence - Ikaluk

Item	Load in Weak Ice	Load in Strong Ice	Ratio of Loads	Ratio of Ice Strengths
Max Q kNm	93	140	0.66	0.33
Mean Q kNm	72	91	0.79	0.33
+ T kN	329	162	2.03	0.33
- T kN	-353	-222	1.59	0.33

3.9.2. Robert Lemeur (1984)

Reference Figures:
Figure 55 Maximum Propeller Ice Torque versus Pitch Angle
Figure 56 Mean Propeller Ice Torque versus Pitch Angle
Figure 60 Positive Propeller Ice Thrust versus Pitch Angle
Figure 61 Negative Propeller Ice Thrust versus Pitch Angle

The comparison of loads and ice flexural strength is shown in Table 5. The ice flexural strengths are 631 kPa for the strong ice and 150 kPa for the weak ice.

Table 5 Ice Strength Influence - Robert Lemeur

Item	Load in Weak Ice	Load in Strong Ice	Ratio of Loads	Ratio of Ice Strengths
Max Q kNm	61	163	0.37	0.24
Mean Q kNm	40	92	0.43	0.24
+ T kN	152	416	0.37	0.24
- T kN	-147	-232	0.63	0.24

3.9.3. Discussion

From Table 3 and Table 5, for Kalvik/Terry Fox and Robert Lemeur, it is noted that propeller thrust and torque ice loads increase with increase in ice flexural strength. From Table 4 for Ikaluk, ice torque varies in the same manner. Although the ratios of loads to ratios of ice strengths vary considerably, the tendency is for loads to vary less than linearly (ratio between 0.35 and 0.80) with ice flexural strength. The results for the comparison of Ikaluk 1989 and 1990 thrust data, Table 4, are completely counter to this trend, with the ice loads in the weaker ice being larger than those in the stronger ice. It was noted during the trials of the Ikaluk in 1990 that the nozzle clogged often, due to the large volume of ice going under the ship. This was not the case in the 1989 tests.

3.9.4. Canmar Kigoriak Gearbox Data Analysis

A search for additional full-scale data with which to investigate the ice strength influence on propeller ice loads identified a Canmar report, Reference 5, which had recently been released from confidential status.

In 1980, the gearbox of Canmar Kigoriak was fitted with a Renk Checker, in order to measure gear tooth contact pressures, corresponding to a measure of shaft torque due to propeller and ice interaction, over periods of ship operation. Detailed measurements of ice conditions were made. The most important data were for two trials in the Canadian Beaufort Sea in 1980, both in level ice conditions, one in strong mid-winter ice and the other in weak Spring ice. An analysis of these data is given in the Appendix B. The analysis shows that shaft ice torque increases with increase in confined ice crushing strength, as measured by borehole jack, but at a rate much less than linear. In fact, doubling ice crushing strength, increased the ice loads by 15%, which is very similar to the influence incorporated in the Design Load Model, Reference 1, through a propeller and ice contact extrusion model.

The Kigoriak gearbox data analysis therefore confirms the general trend of the ice strength influence upon propeller ice loads, determined from the Kalvik/Terry Fox, Ikaluk, and Robert Lemeur trials. However, the exact degree to which ice loads increase with increasing ice strength is not clear. One difficulty here is quantifying the influence of the different reference ice strengths, which is confined crushing strength for the Kigoriak trials and flexural strength for the remainder.

3.10. Summary of Results

In general, for both the ducted (Robert Lemeur and Oden) and open propellers (Terry Fox 1990), propeller ice torque increases with increasing pitch angle.

Investigation for the influence of pitch angle upon ducted propeller ice thrust is inconclusive. For the open propeller (Kalvik), in heavy ice conditions, the highest ice thrust loads occur at low pitch angles.

For the ducted propellers, positive ice thrust loads are larger than negative ice thrust loads.

For the open propellers, negative ice thrust loads are larger than positive ice thrust loads.

In general, the magnitudes of ice thrust and torque at negative pitch angles are less than those at positive pitch values. In a small number of cases, however, comparable or higher loads occurred at negative pitch.

Investigation for the separate influence of rpm upon ice loads was inconclusive.

It was not possible determine trends in ice loads with ship speed, although high load values occur at all speeds.

Single impact events generate ice loads as high as during milling, for both ducted and open propellers. Although blockage loads for ducted propellers are lower than the contact loads, they are still significant.

The propeller ice load analysis has indicated that ice loads vary less than linearly (ratio between 0.35 and 0.80) with ice flexural strength. An additional analysis, using previously confidential Canmar data for gear tooth loads, suggests a weaker dependency, but in this case relative to confined crushing strength, which is very similar to the influence incorporated in the Design Load Model, Reference 1.

The ratio of maximum to mean ice torque varied considerably from ship to ship, as summarized in Table 6.

Table 6 Ratios of Maximum/Mean Propeller Ice Torque

Ship	Open/Duct	Prop Dia. m	Ice Strength	Qmax/Qmn
Kalvik	Open	4.80	Strong	1.2 - 2.0
Terry Fox	Open	4.80	Weak	1.82
Ikaluk 90	Duct	3.73	Weak	1.19
Ikaluk 89	Duct	3.73	Strong	1.45
Robert Lemeur	Duct	3.00	Strong	1.74
Oden Port	Duct	4.50	Strong	1.30
Oden Stbd	Duct	4.50	Strong	1.38

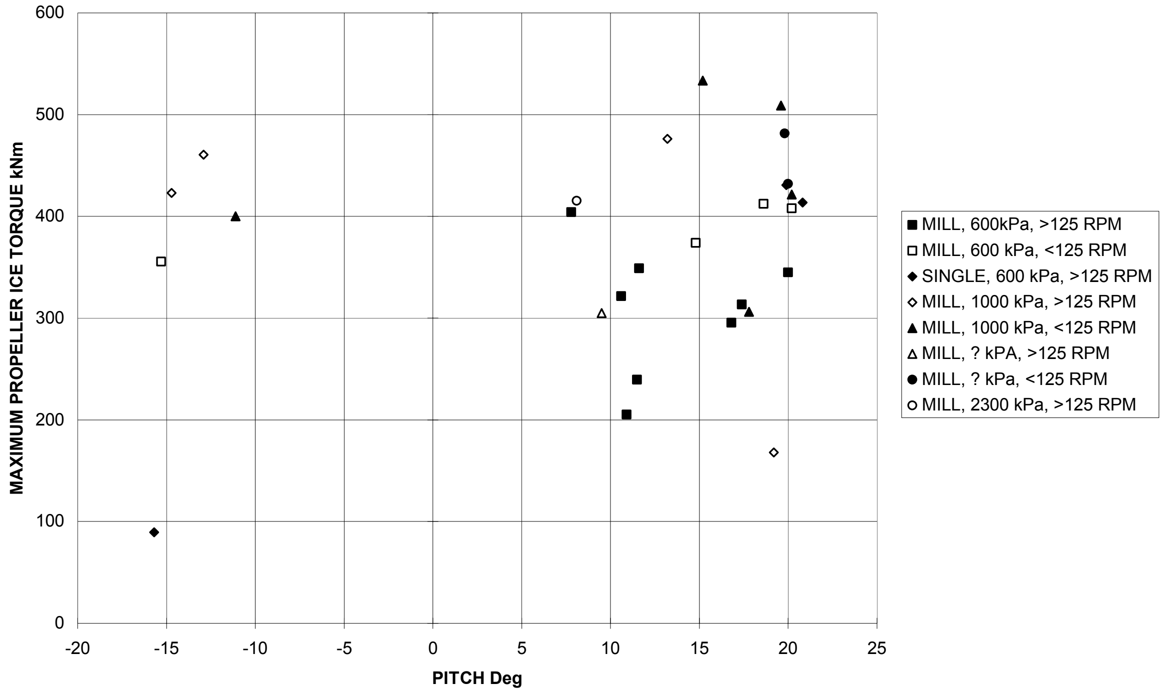

Figure 34 Kalvik - Maximum Propeller Ice Torque versus Pitch Angle

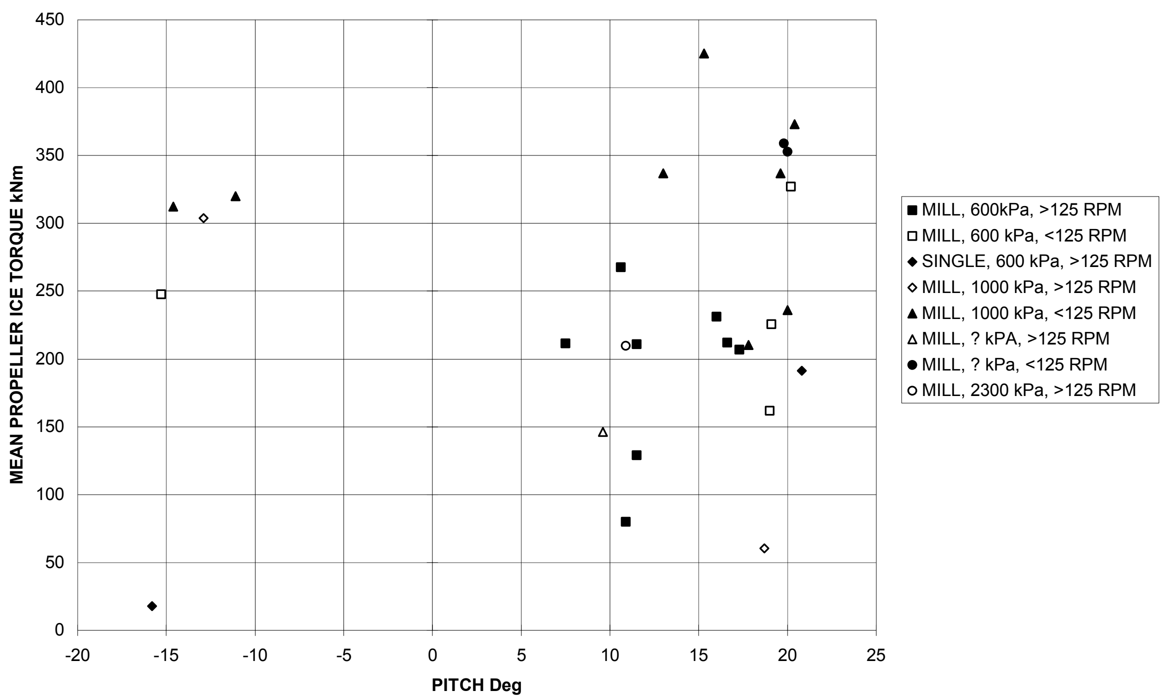

Figure 35 Kalvik - Mean Propeller Ice Torque versus Pitch Angle

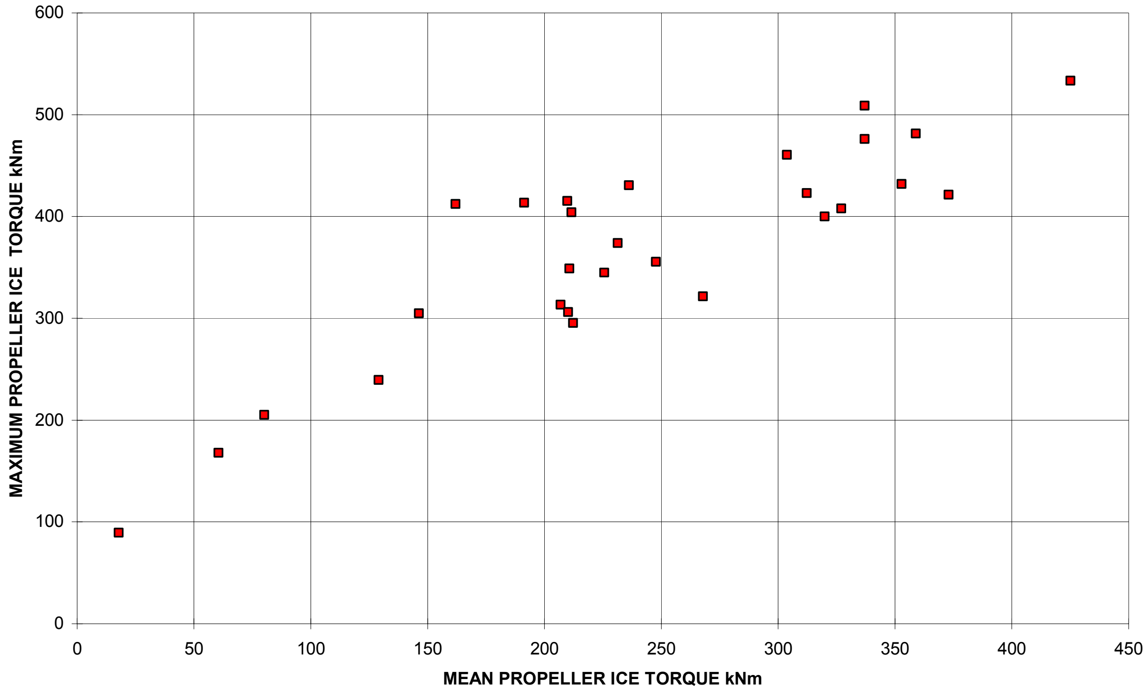

Figure 36 Kalvik - Comparison of Maximum and Mean Propeller Ice Torque

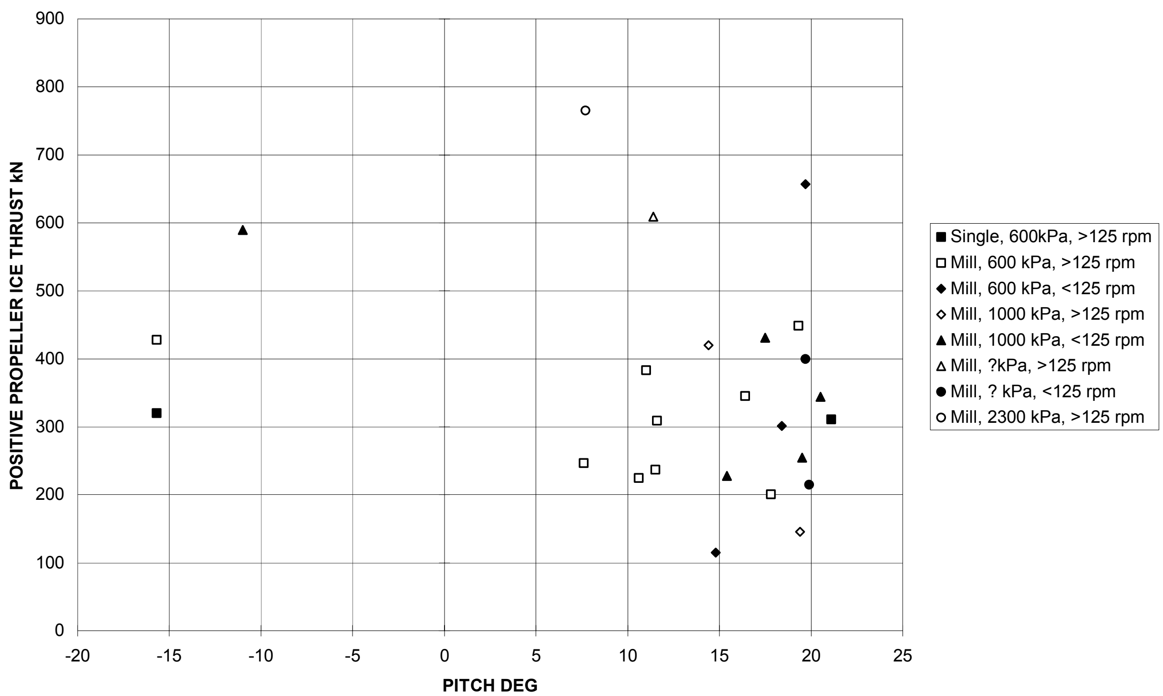

Figure 37 Kalvik - Positive Propeller Ice Thrust versus Pitch Angle

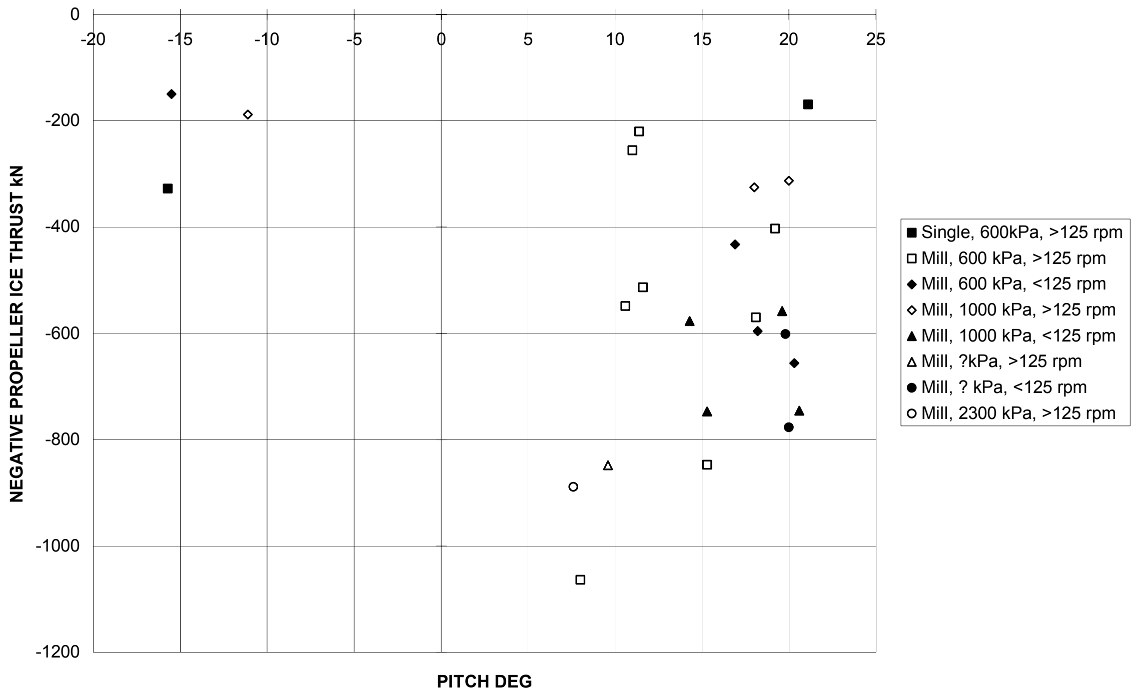

Figure 38 Kalvik - Negative Propeller Ice Thrust versus Pitch Angle

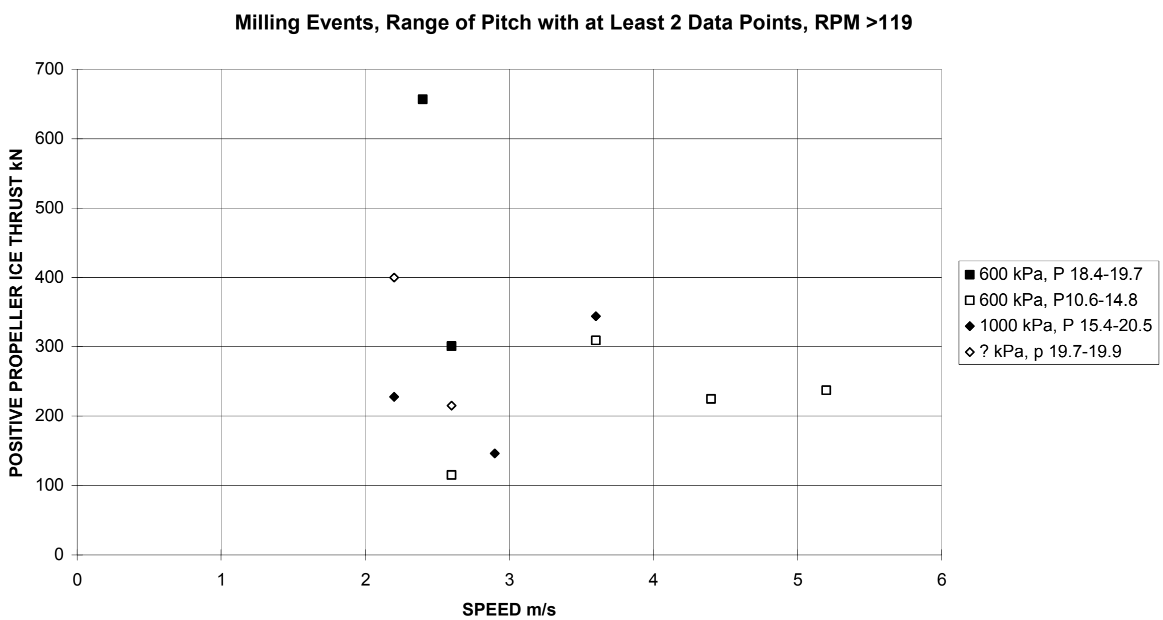

Figure 39 Kalvik - Positive Propeller Ice Thrust versus Ship Speed

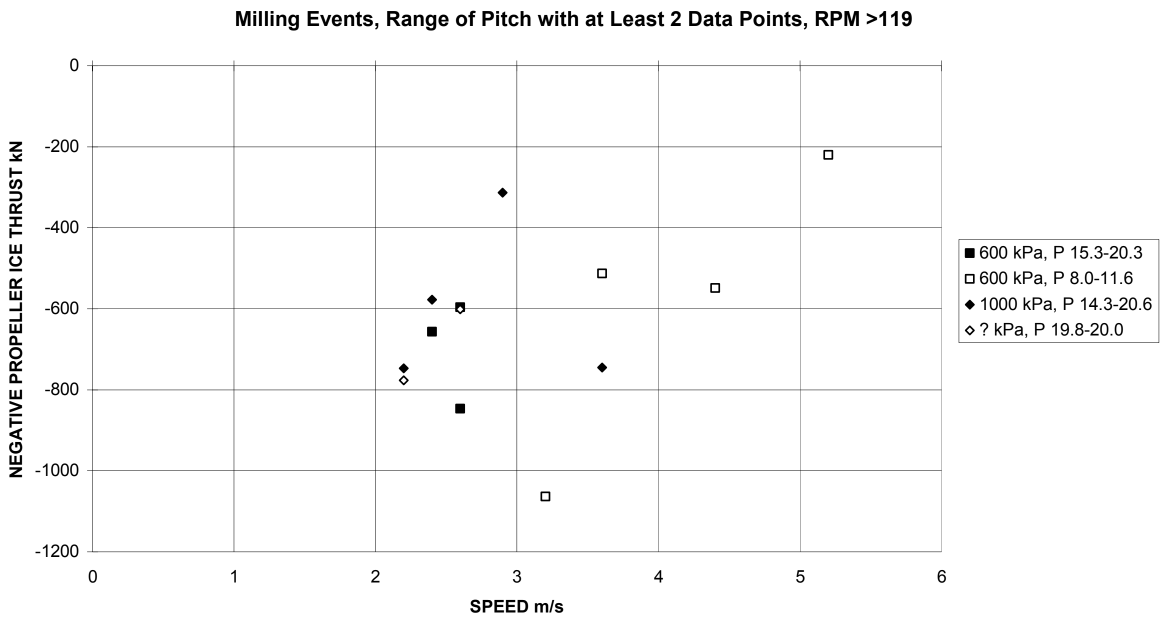

Figure 40 Kalvik - Negative Propeller Ice Thrust versus Ship Speed

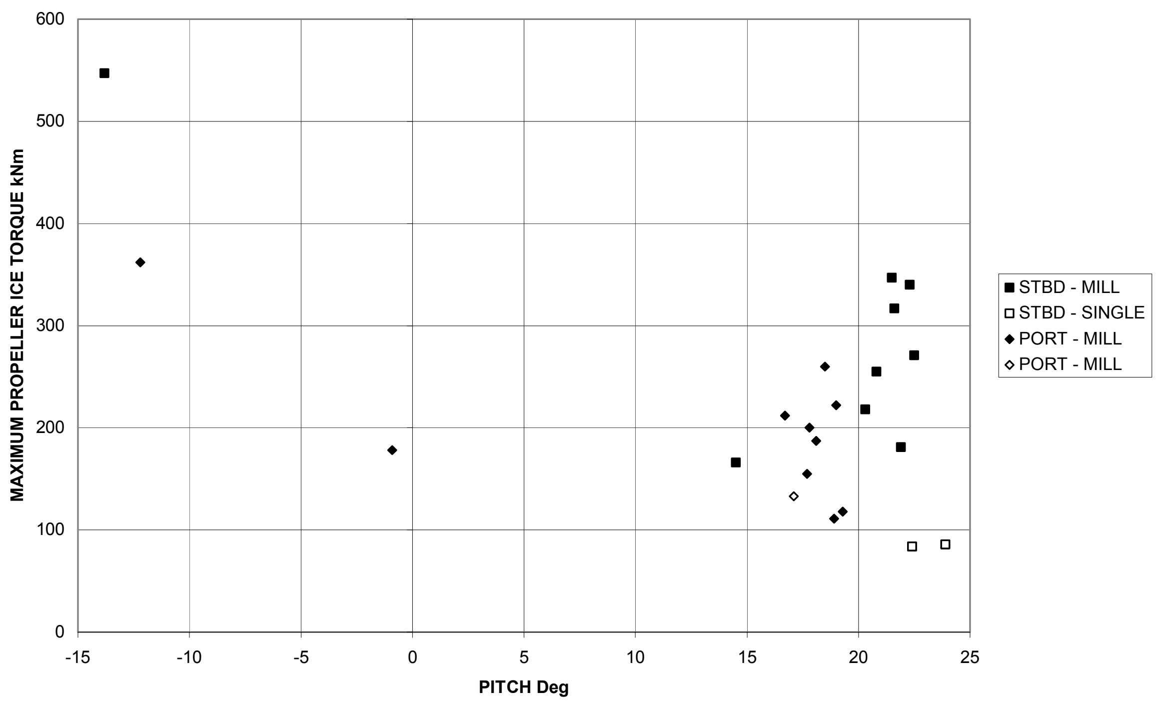

Figure 41 Terry Fox - Maximum Propeller Ice Torque versus Pitch Angle

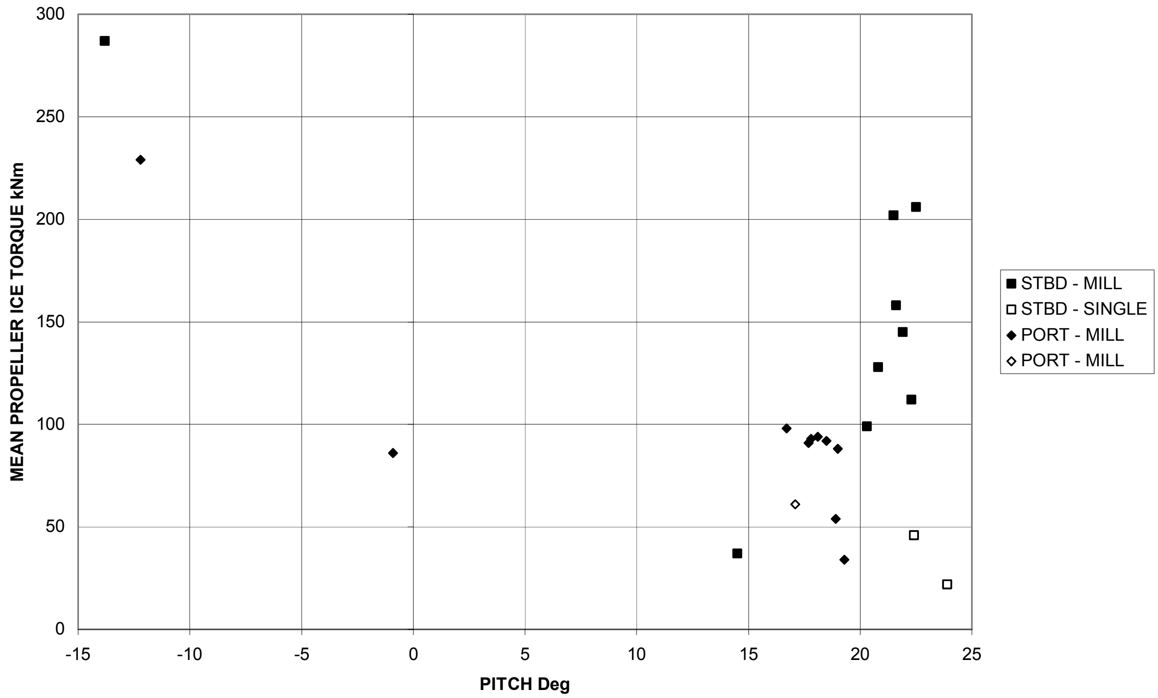

Figure 42 Terry Fox - Mean Propeller Ice Torque versus Pitch Angle

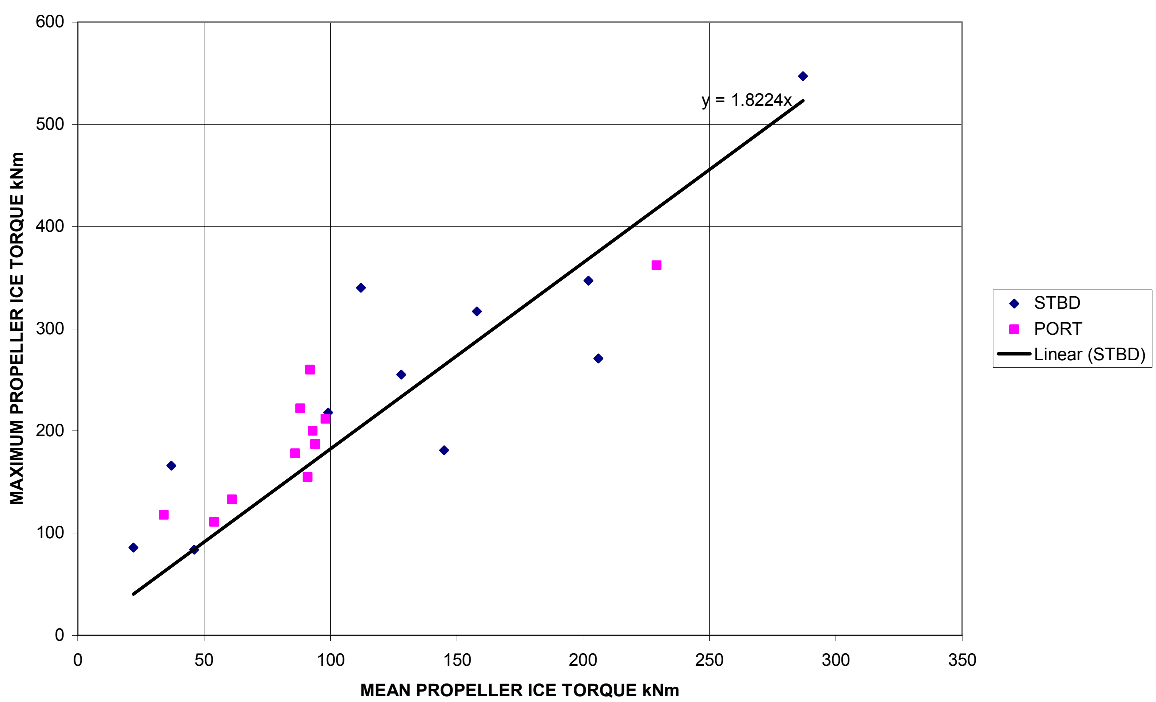

Figure 43 Terry Fox - Comparison of Maximum and Mean Propeller Ice Torque

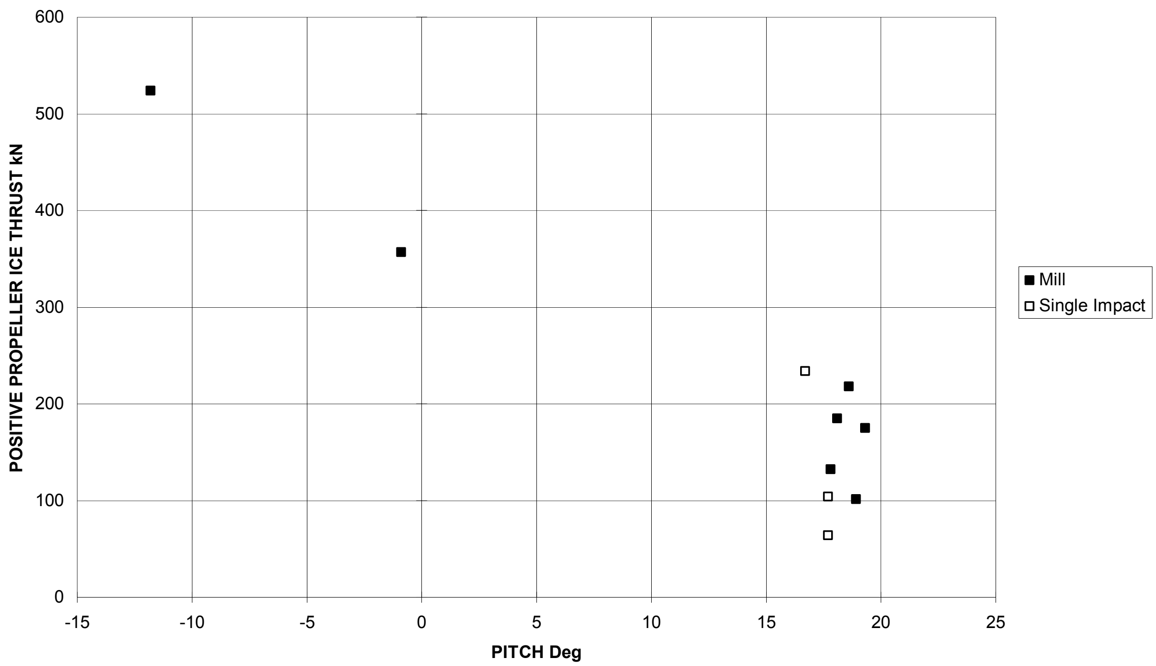

Figure 44 Terry Fox - Positive Propeller Ice Thrust versus Pitch Angle

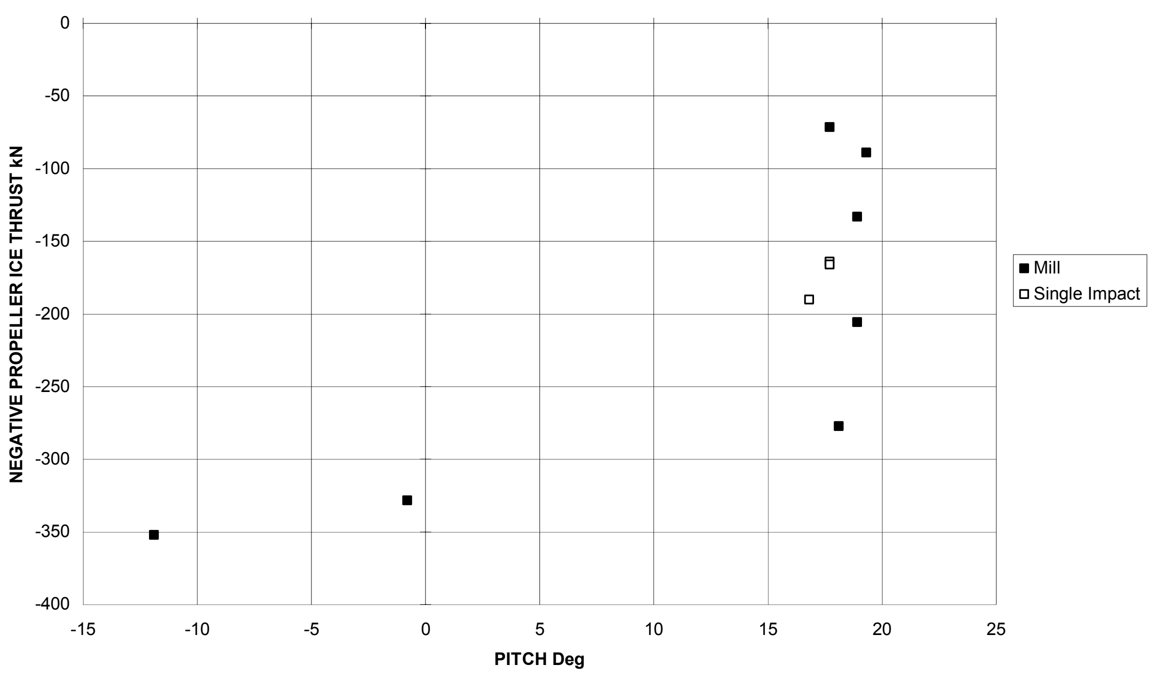

Figure 45 Terry Fox - Negative Propeller Ice Thrust versus Pitch Angle

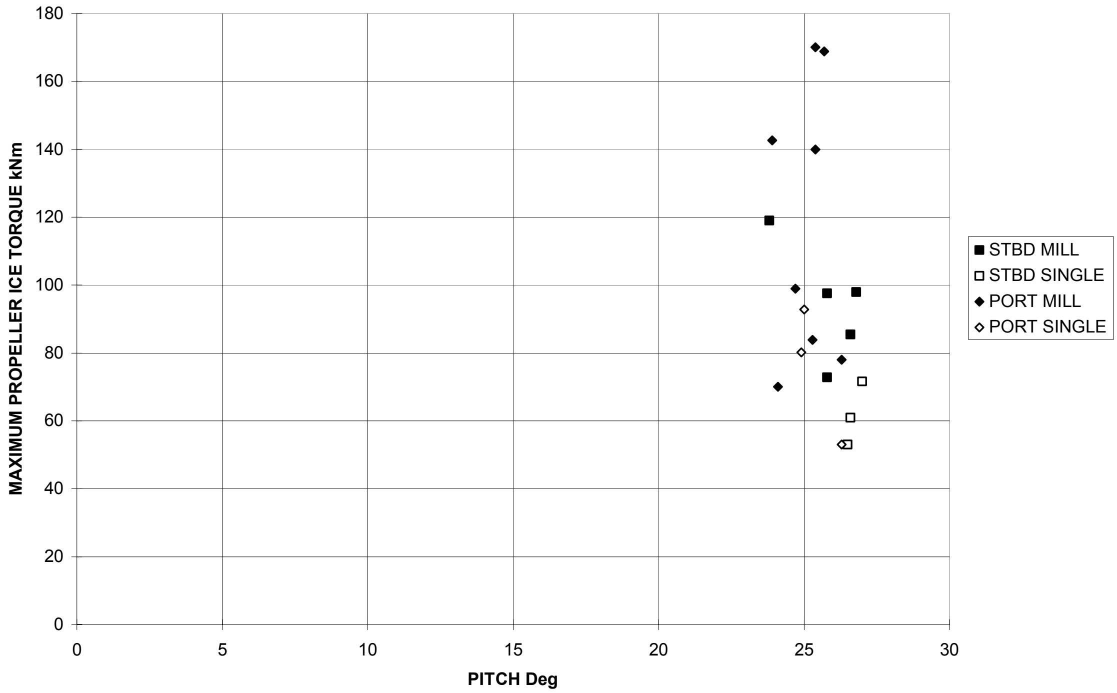

Figure 46 Ikaluk '90 - Maximum Propeller Ice Torque versus Pitch Angle

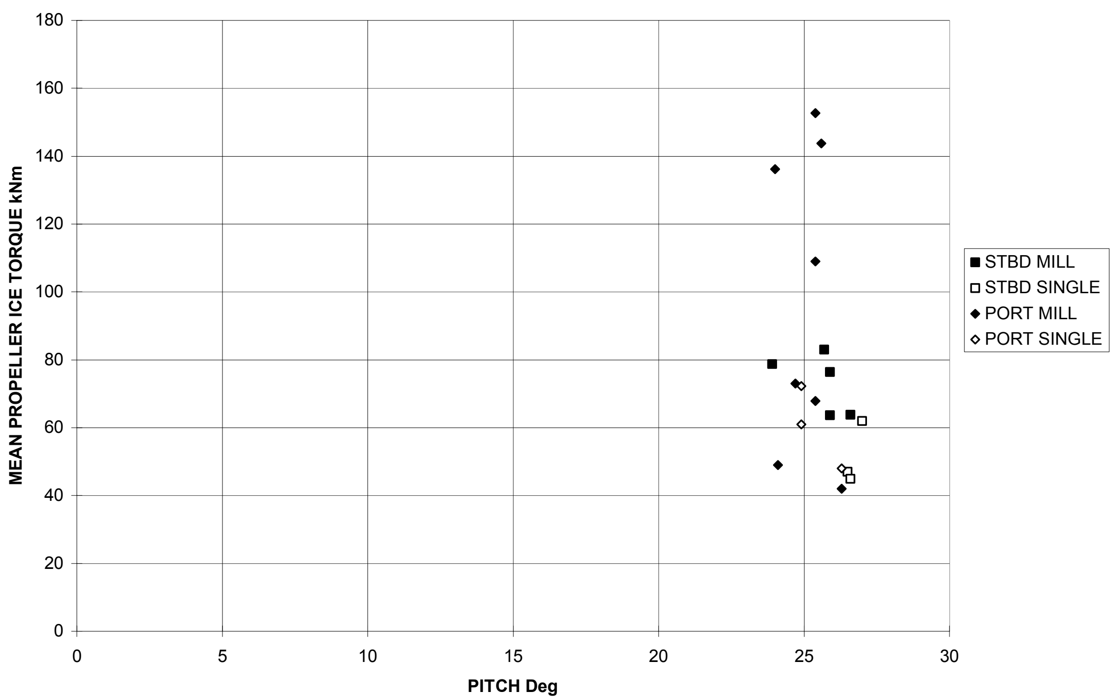

Figure 47 Ikaluk '90 - Mean Propeller Ice Torque versus Pitch Angle

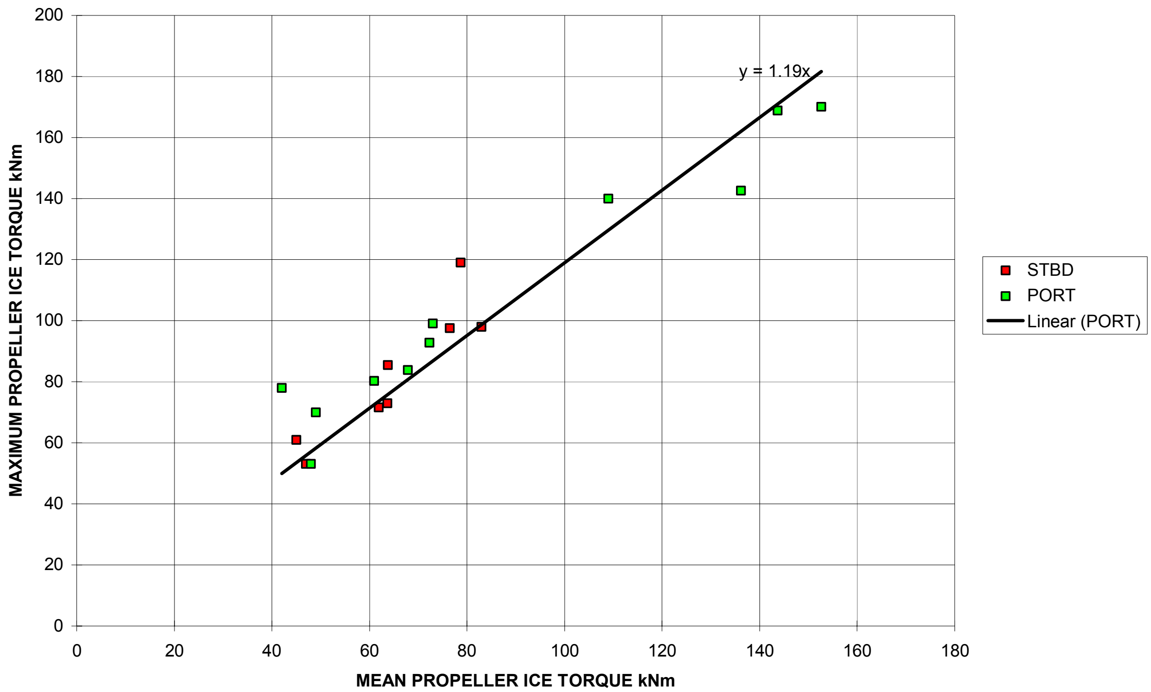

Figure 48 Ikaluk '90 - Comparison of Maximum and Mean Propeller Ice Torque

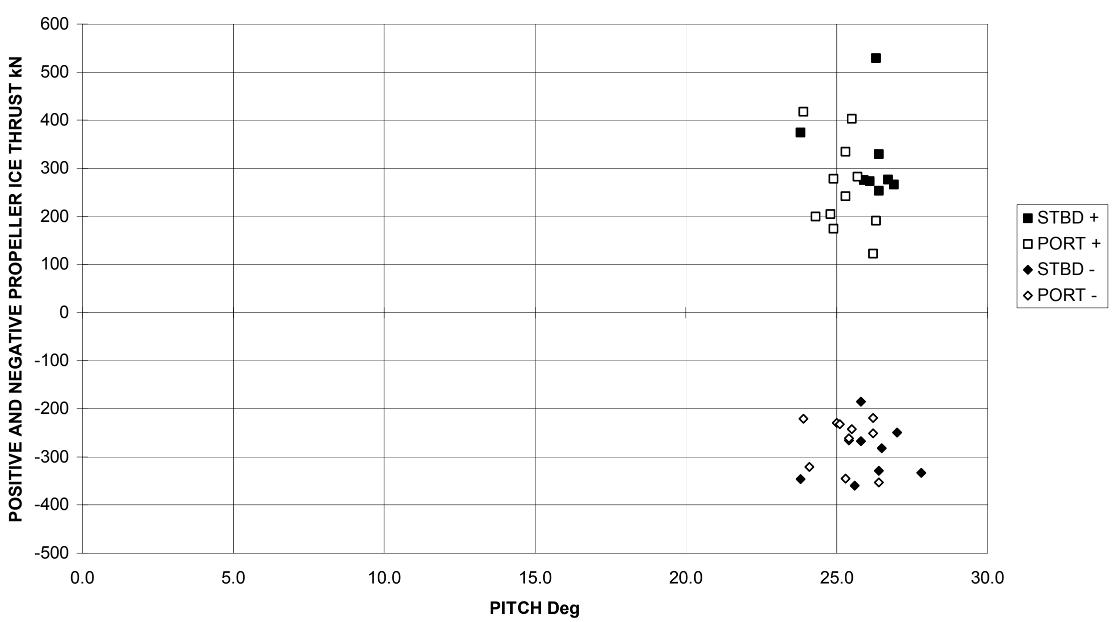

Figure 49 Ikaluk '90 - Positive and Negative Propeller Ice Thrust versus Pitch Angle

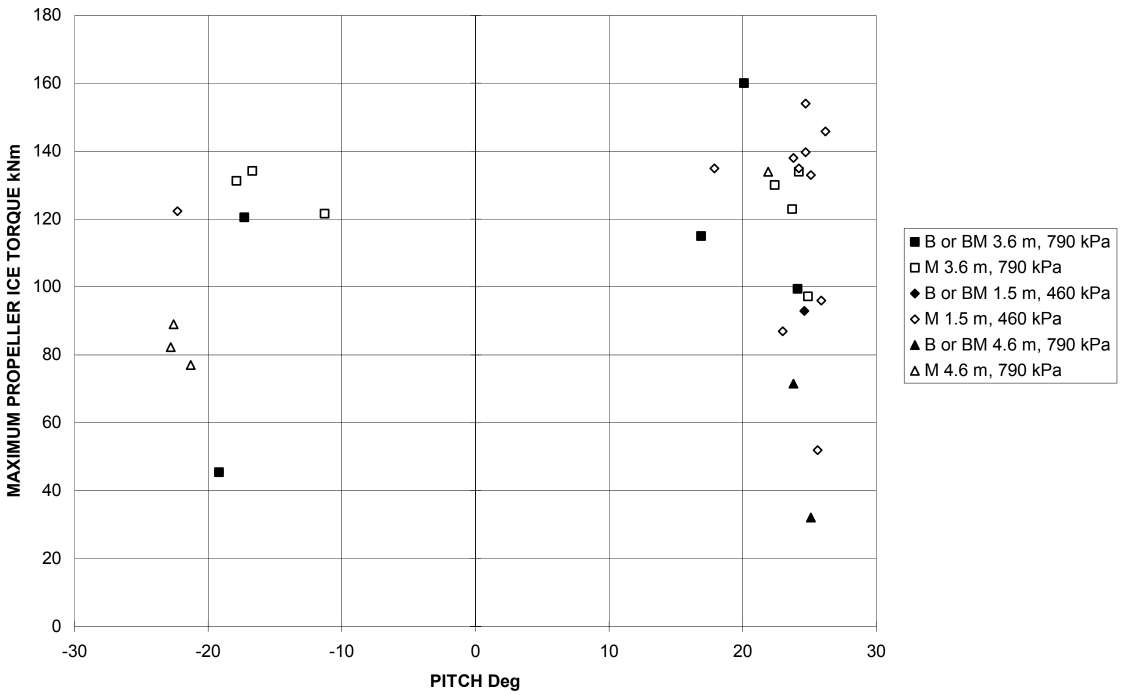

Figure 50 Ikaluk '89 - Maximum Propeller Ice Torque versus Pitch Angle

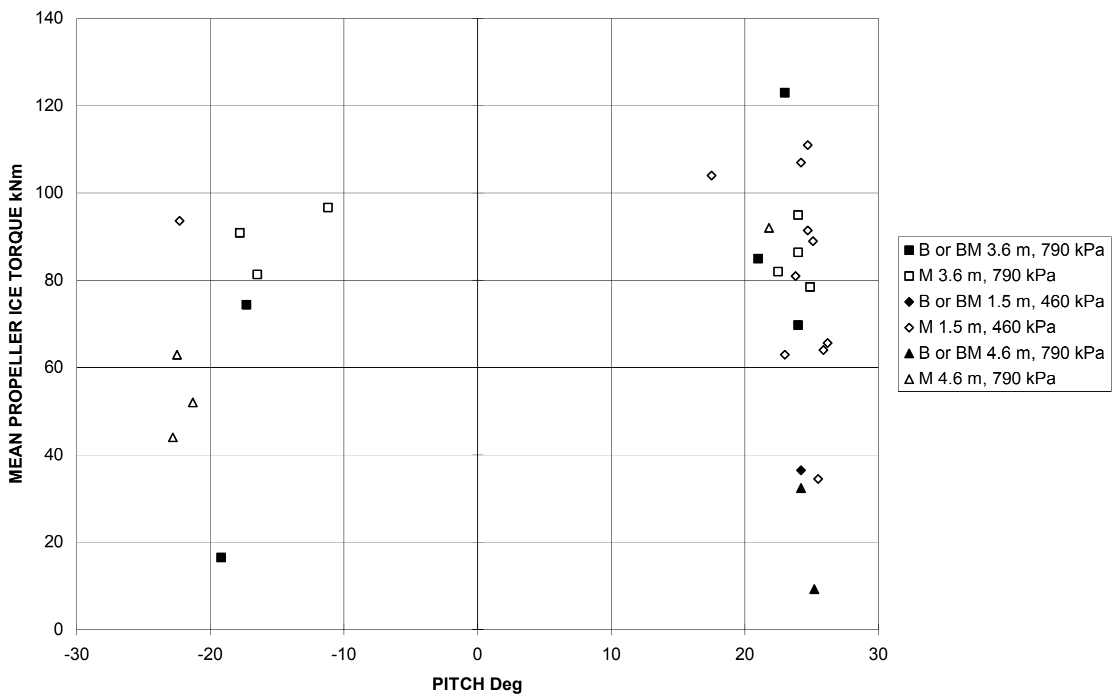

Figure 51 Ikaluk '89 - Mean Propeller Ice Torque versus Pitch Angle

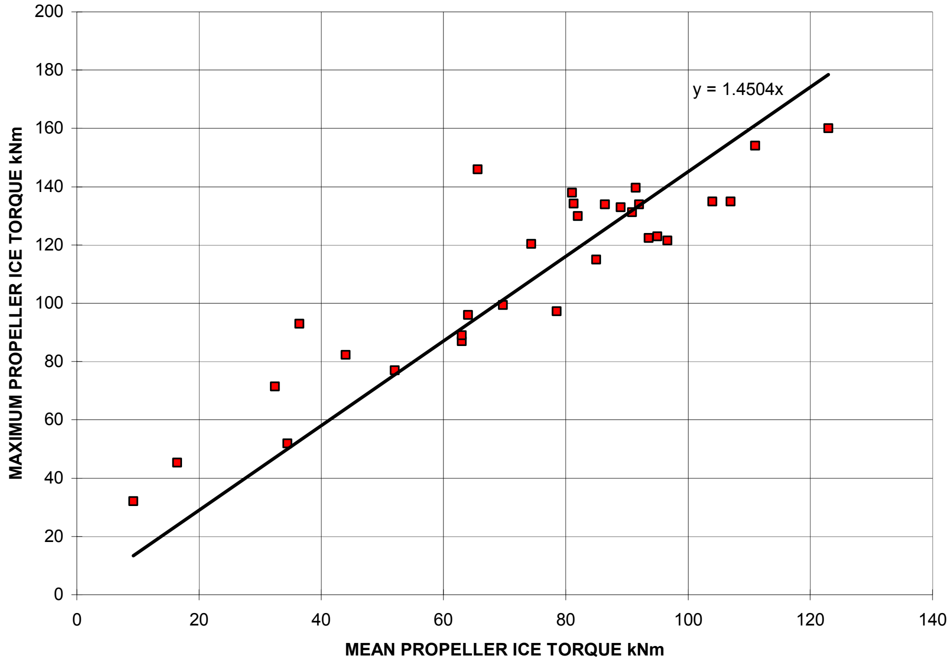

Figure 52 Ikaluk '89 – Comparison of Maximum and Mean Propeller Ice Torque

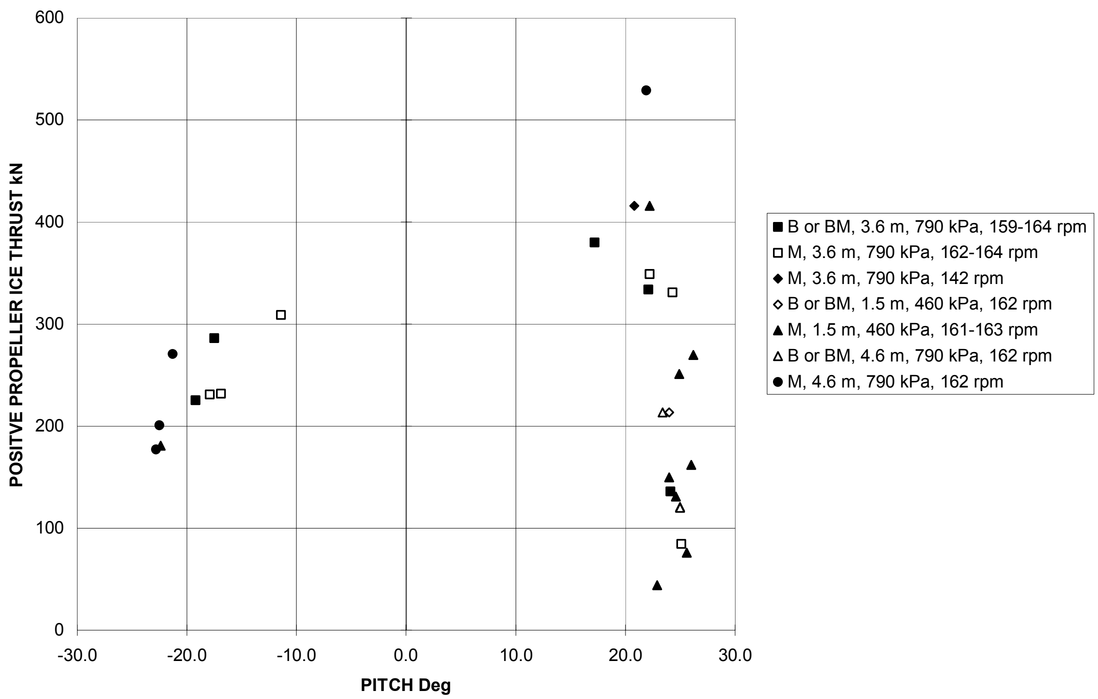

Figure 53 Ikaluk '89 - Positive Propeller Ice Thrust versus Pitch Angle

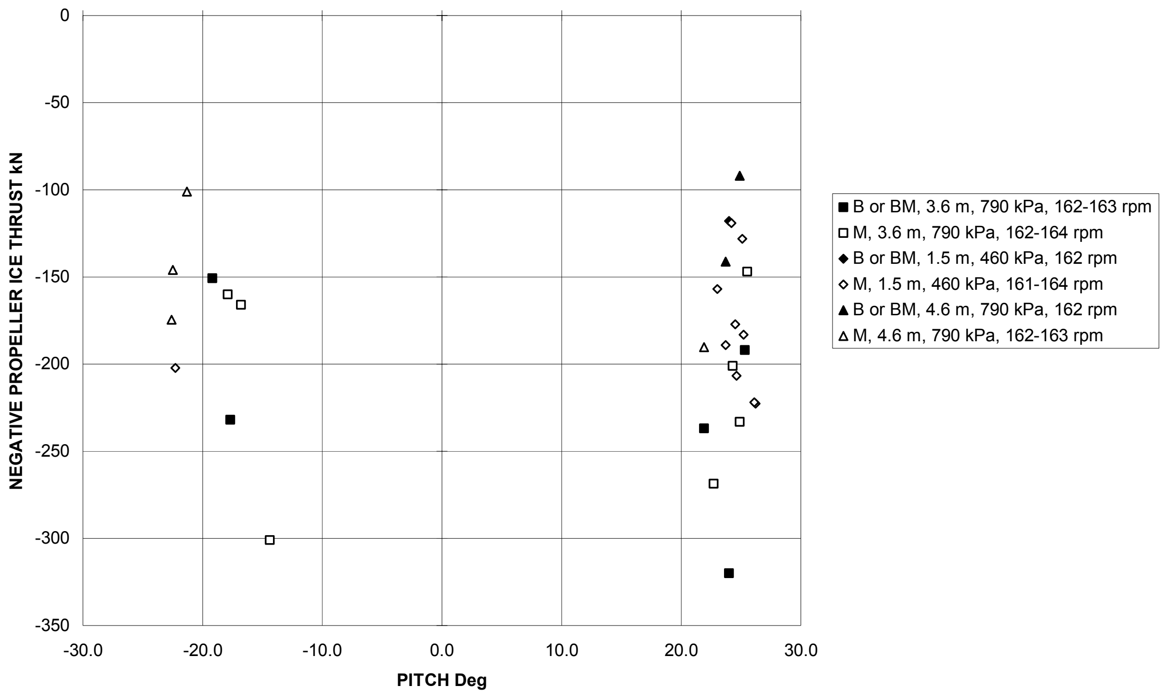

Figure 54 Ikaluk '89 - Negative Propeller Ice Thrust versus Pitch Angle

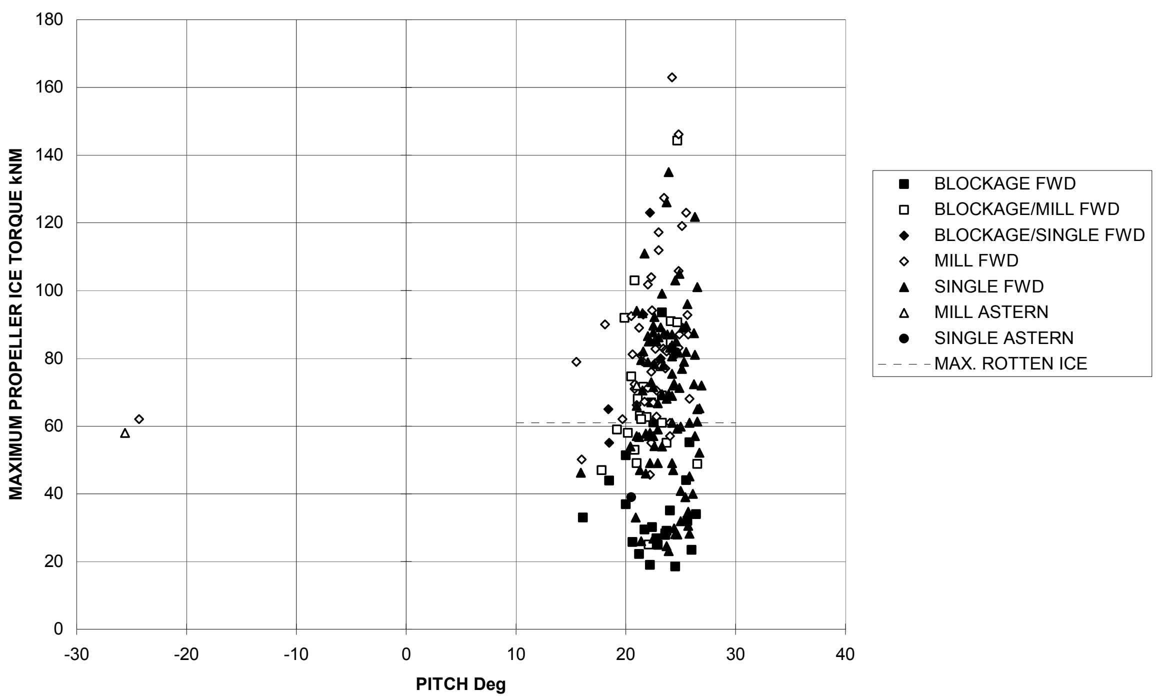

Figure 55 Robert Lemeur - Maximum Propeller Ice Torque versus Pitch Angle

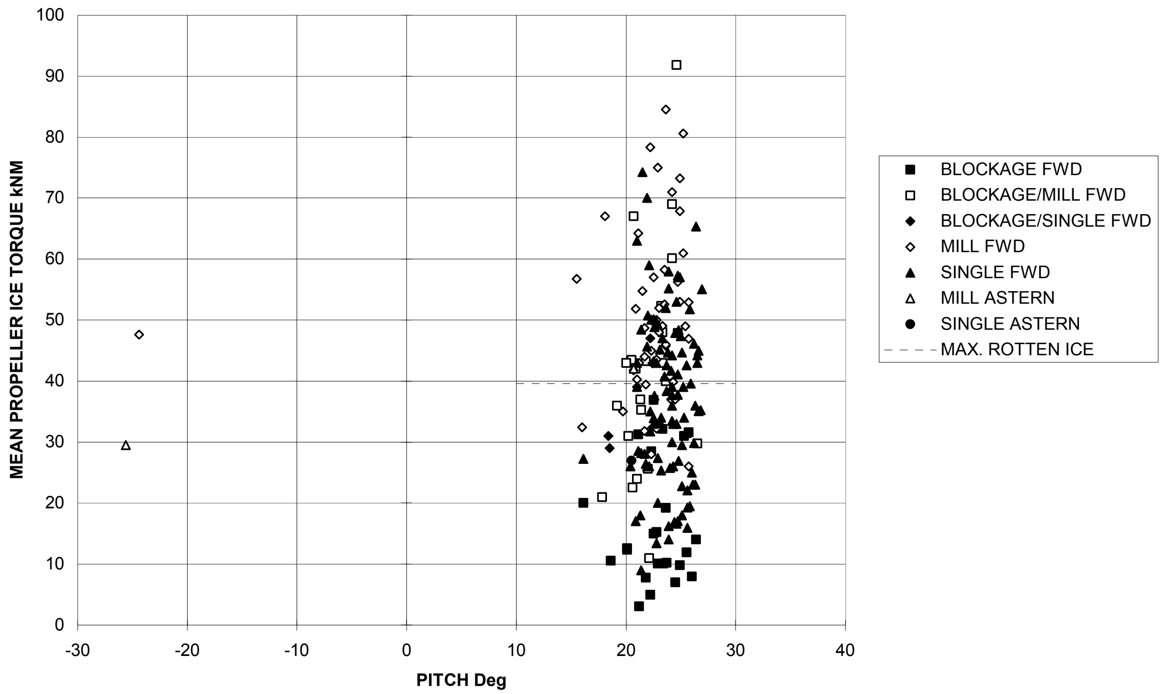

Figure 56 Robert Lemeur - Mean Propeller Ice Torque versus Pitch Angle

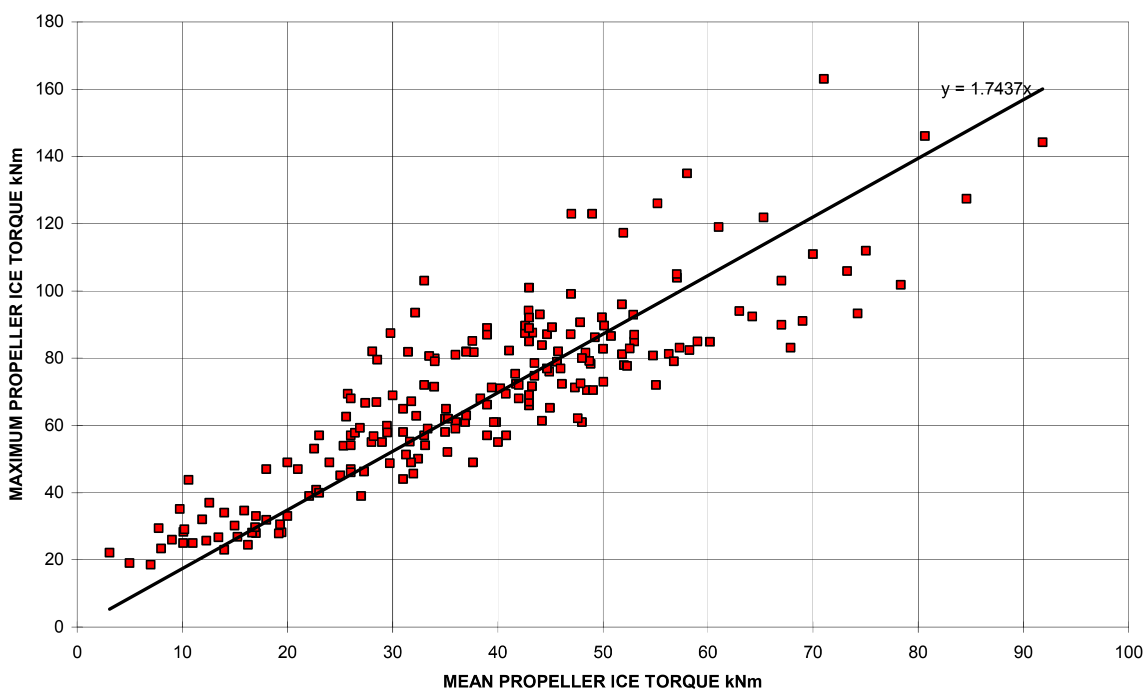

Figure 57 Robert Lemeur - Comparison of Maximum and Mean Propeller Ice Torque

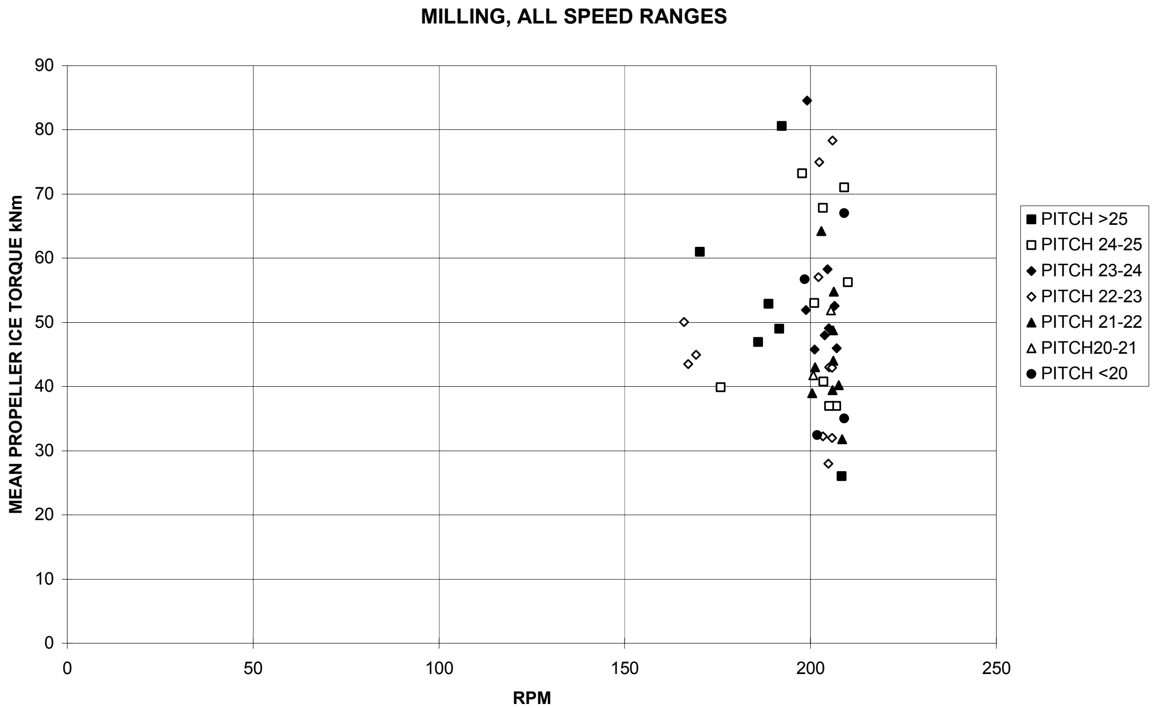

Figure 58 Robert Lemeur - Mean Propeller Ice Torque versus RPM

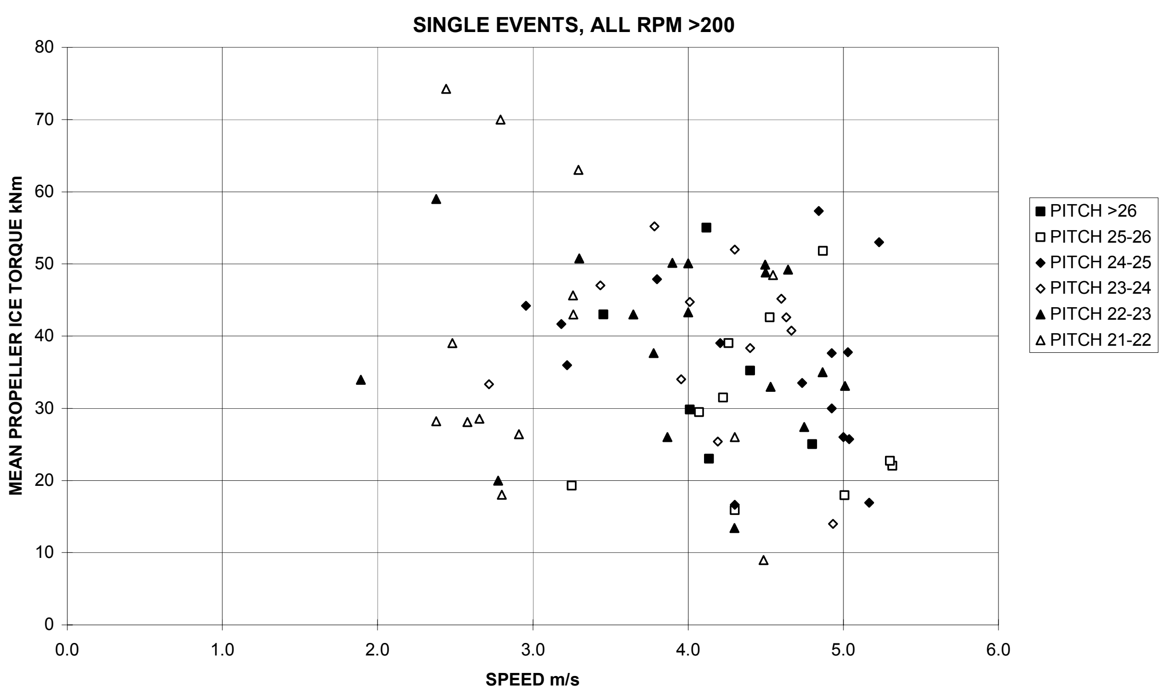

Figure 59 Robert Lemeur - Mean Propeller Ice Torque versus Ship Speed

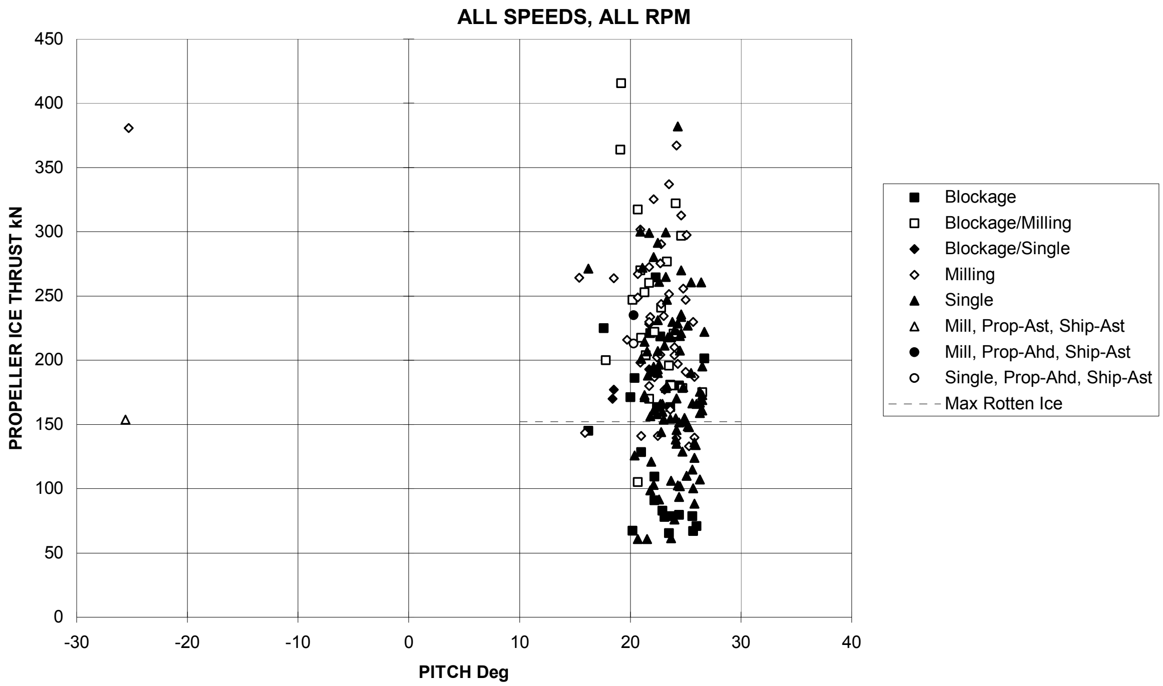

Figure 60 Robert Lemeur - Positive Propeller Ice Thrust versus Pitch Angle

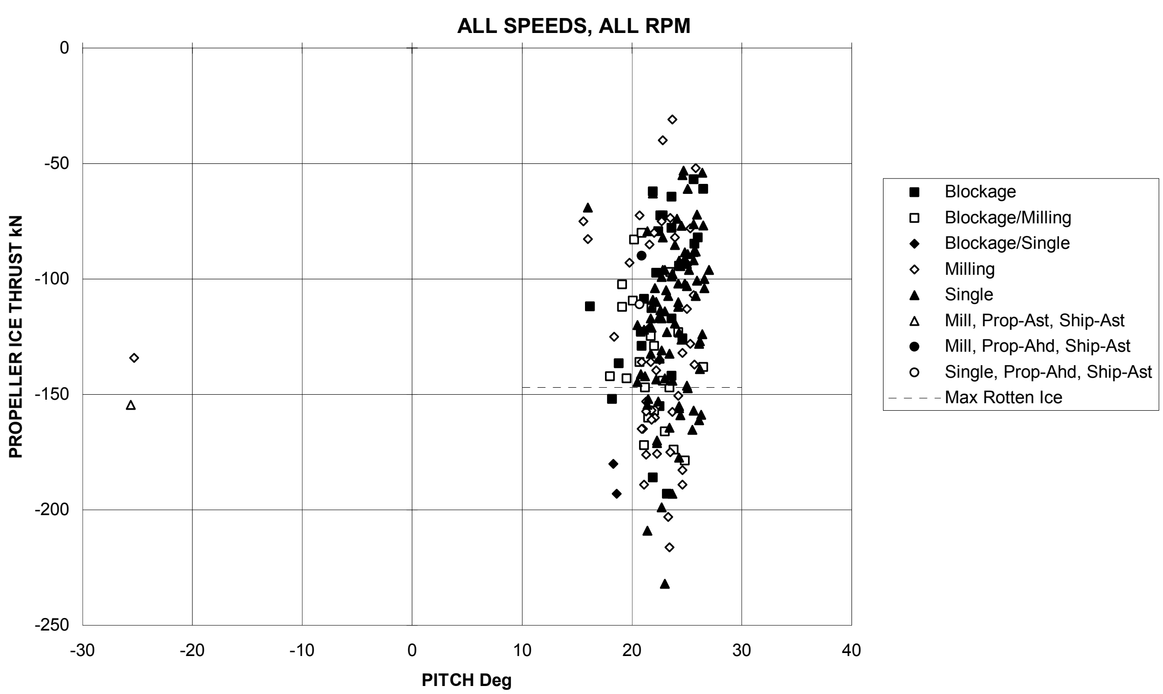

Figure 61 Robert Lemeur - Negative Propeller Ice Thrust versus Pitch Angle

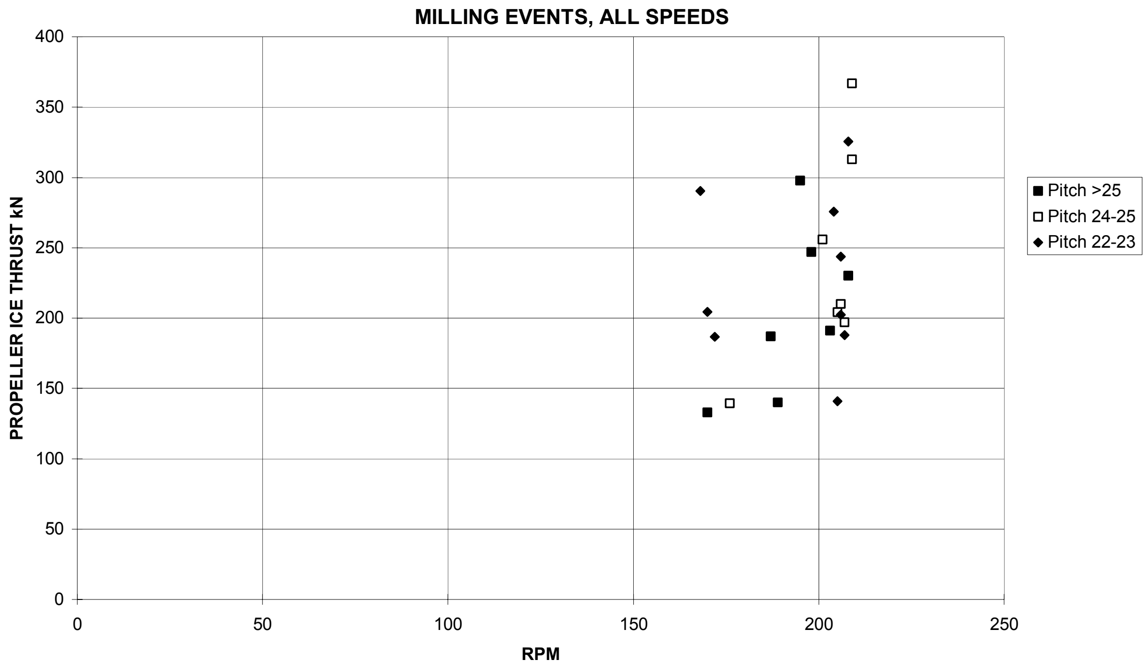

Figure 62 Robert Lemeur - Positive Propeller Ice Thrust versus RPM

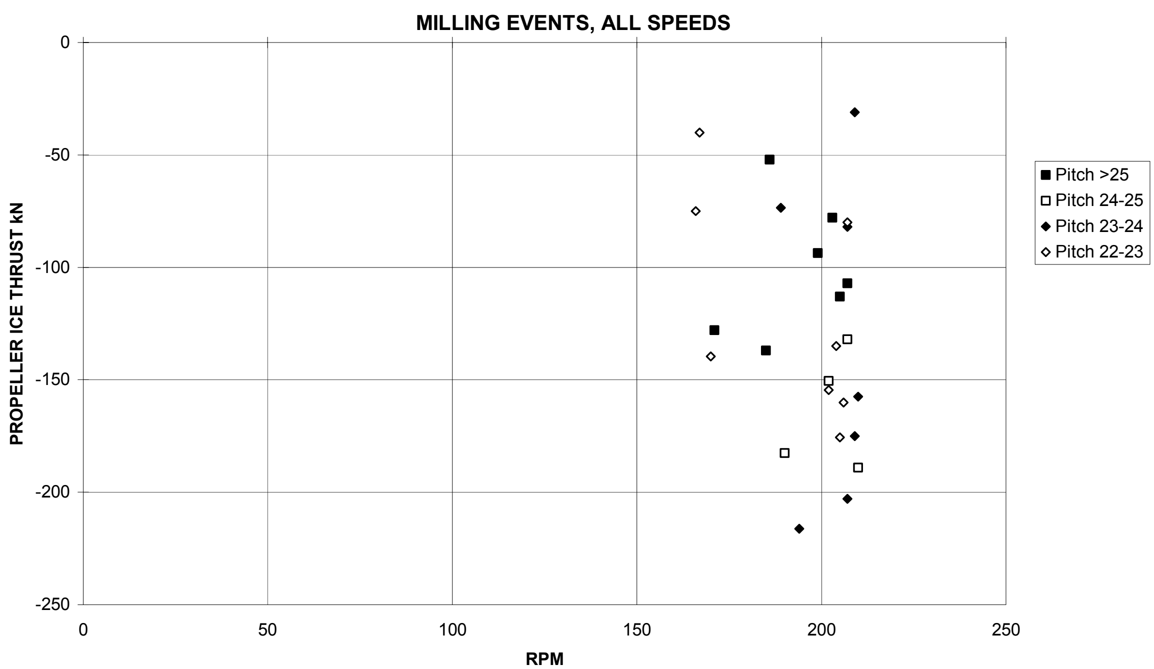

Figure 63 Robert Lemeur - Negative Propeller Ice Thrust versus RPM

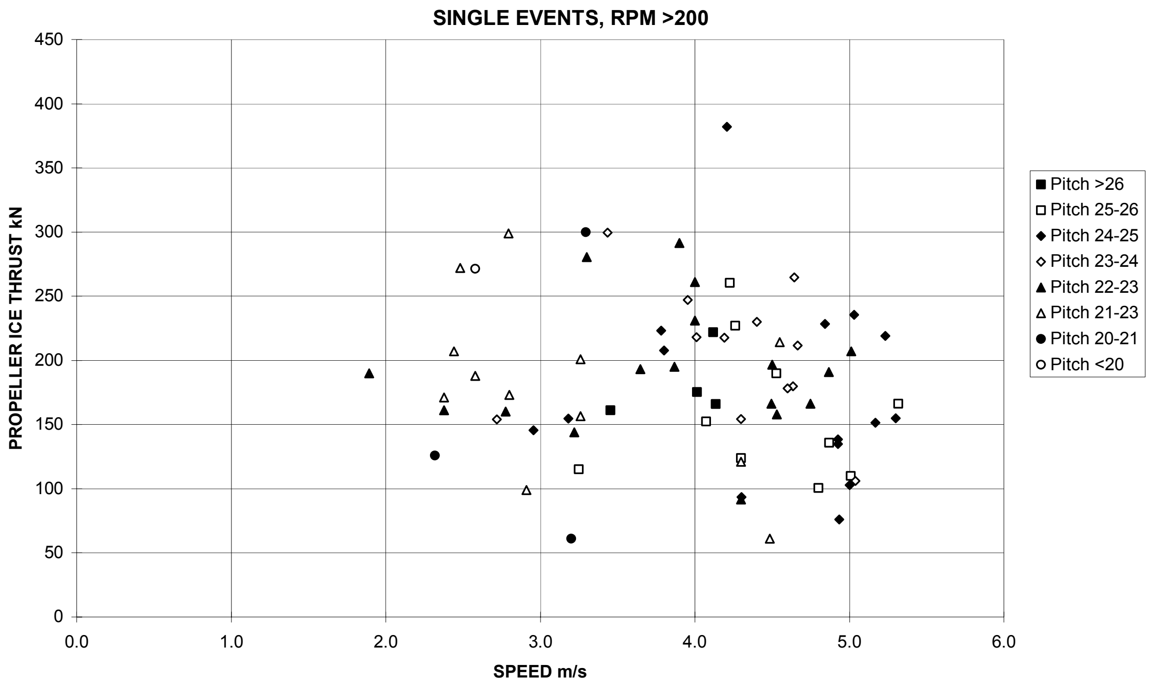

Figure 64 Robert Lemeur - Positive Propeller Ice Thrust versus Ship Speed

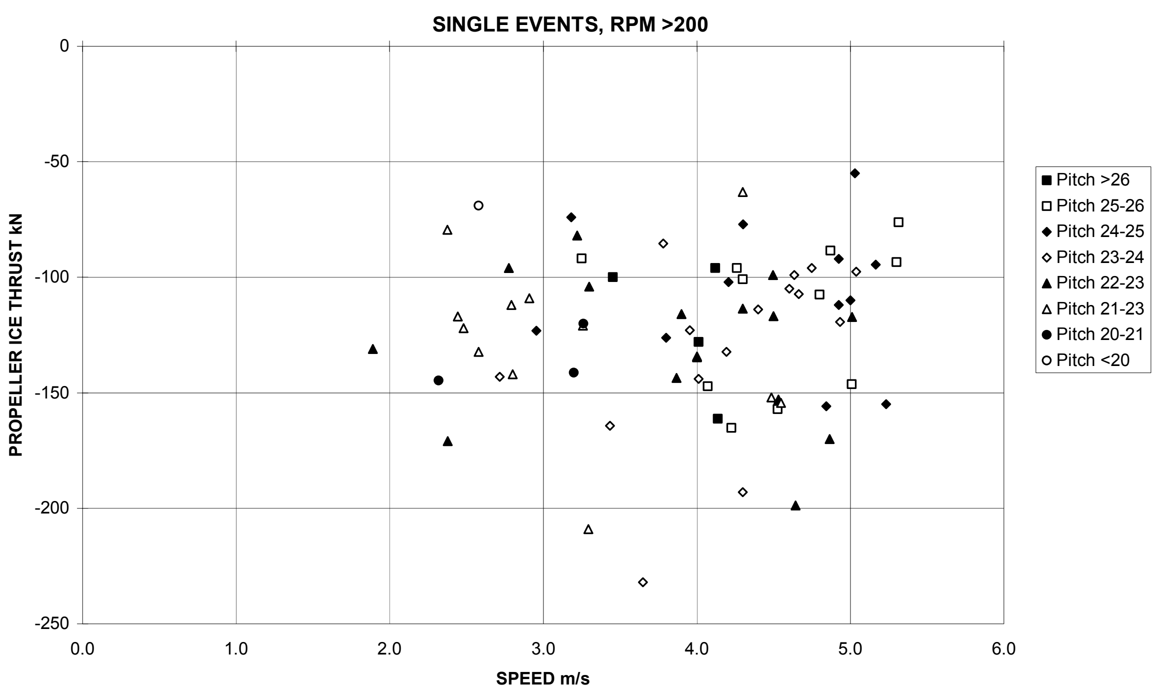

Figure 65 Robert Lemeur - Negative Propeller Ice Thrust versus Ship Speed

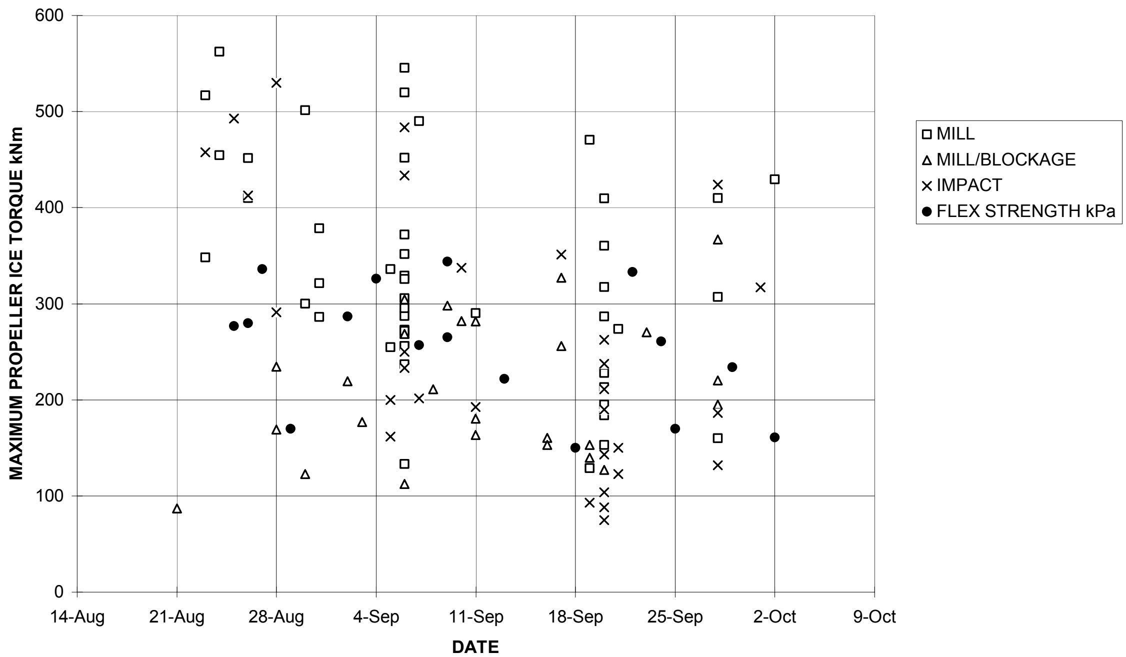

Figure 66 **Oden - Maximum Port Propeller Ice Torque versus Voyage Date and Ice Strength**

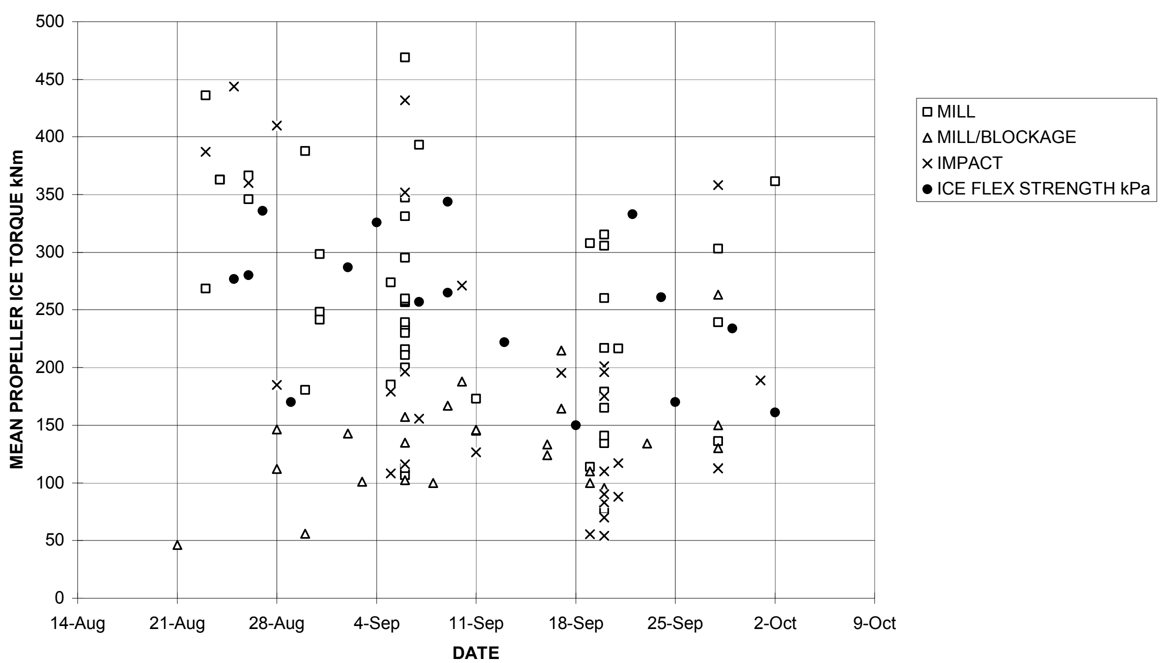

Figure 67 **Oden - Mean Port Propeller Ice Torque versus Voyage Date and Ice Strength**

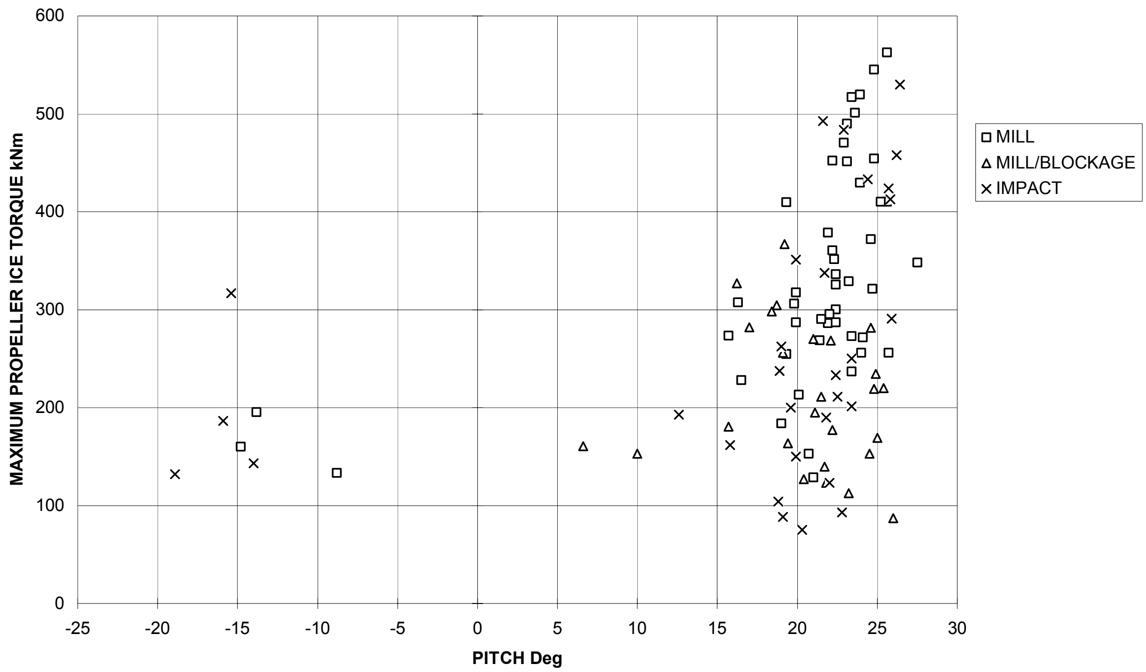

Figure 68 Oden - Maximum Port Propeller Ice Torque versus Pitch Angle

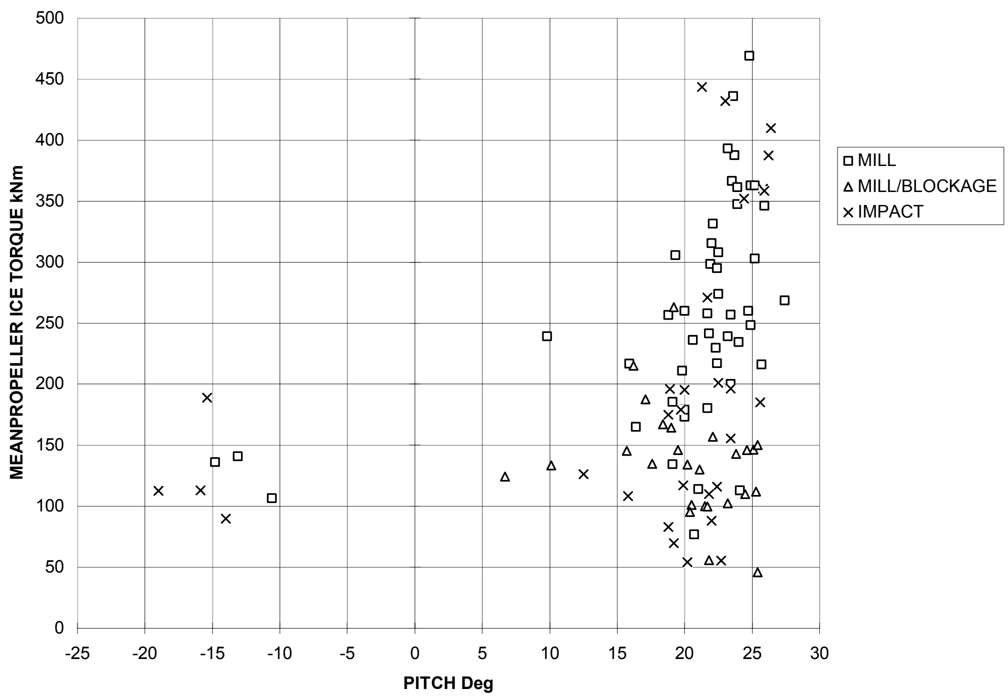

Figure 69 Oden - Mean Port Propeller Ice Torque versus Pitch Angle

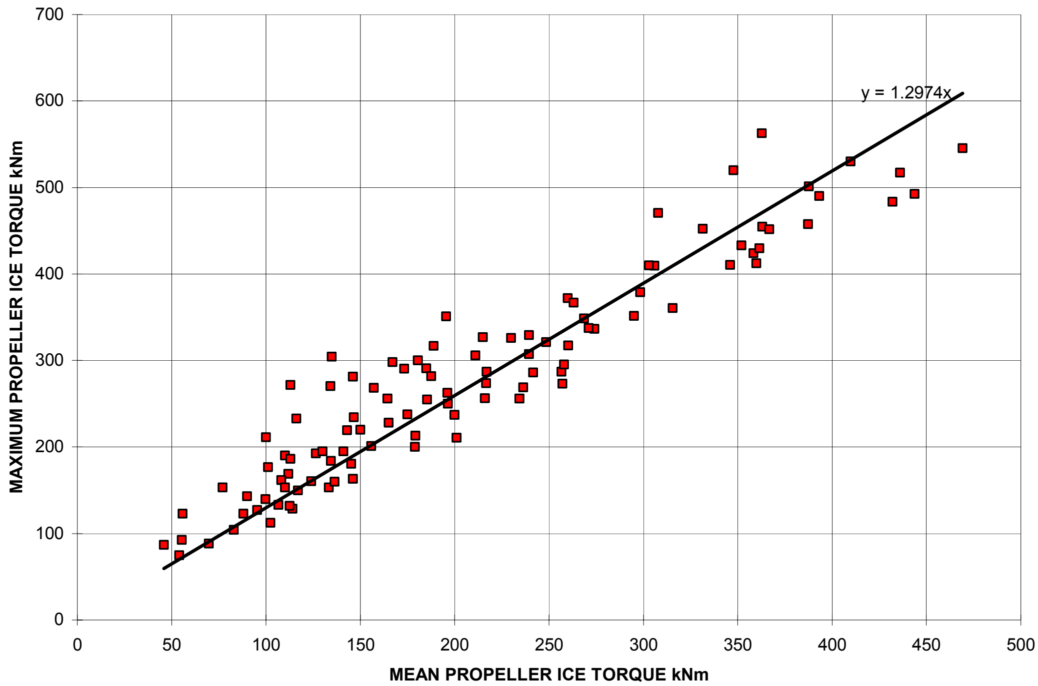

Figure 70 Oden - Comparison of Maximum and Mean Port Propeller Ice Torque

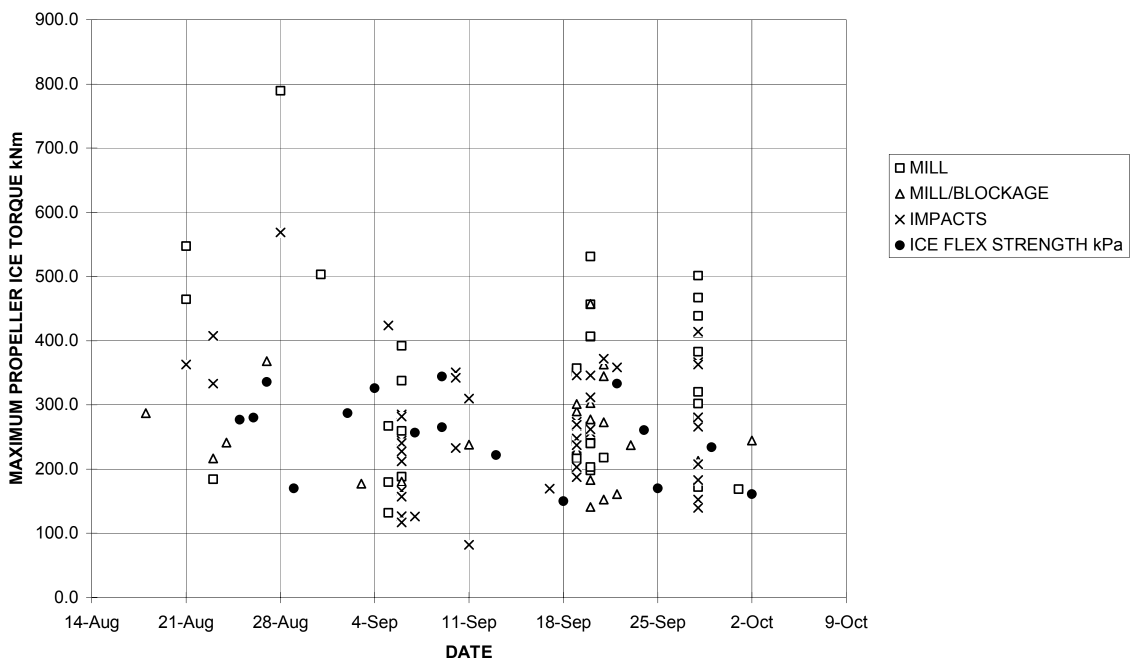

Figure 71 Oden - Maximum Starboard Propeller Ice Torque versus Voyage Date and Ice Strength

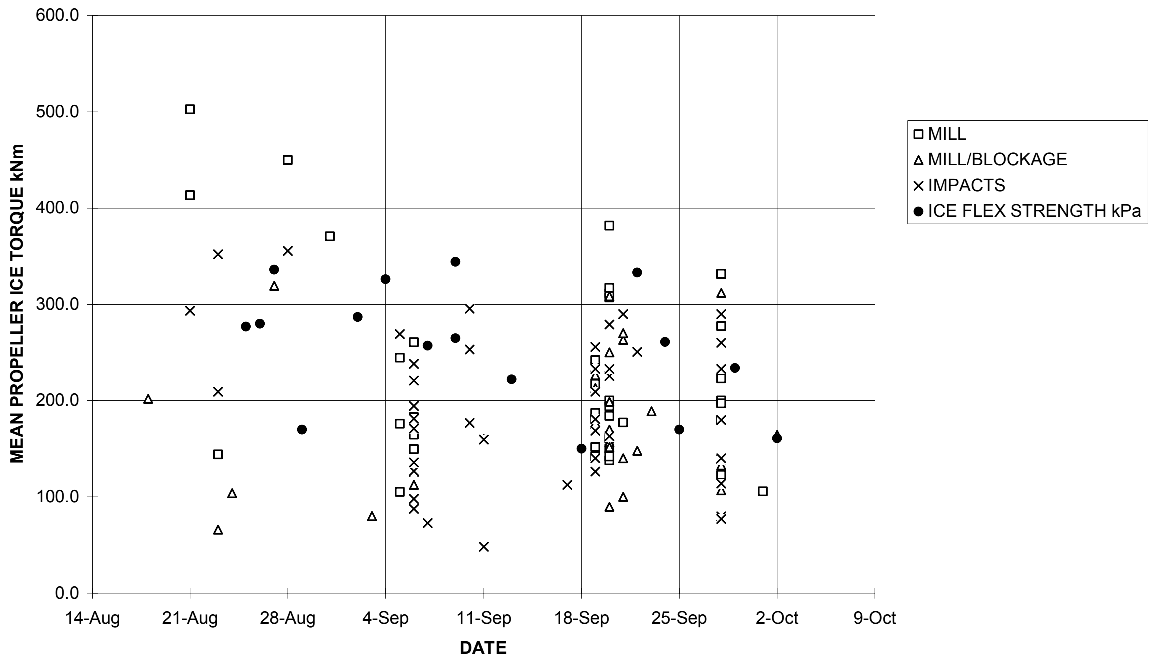

Figure 72 **Oden - Mean Starboard Propeller Ice Torque versus Voyage Date and Ice Strength**

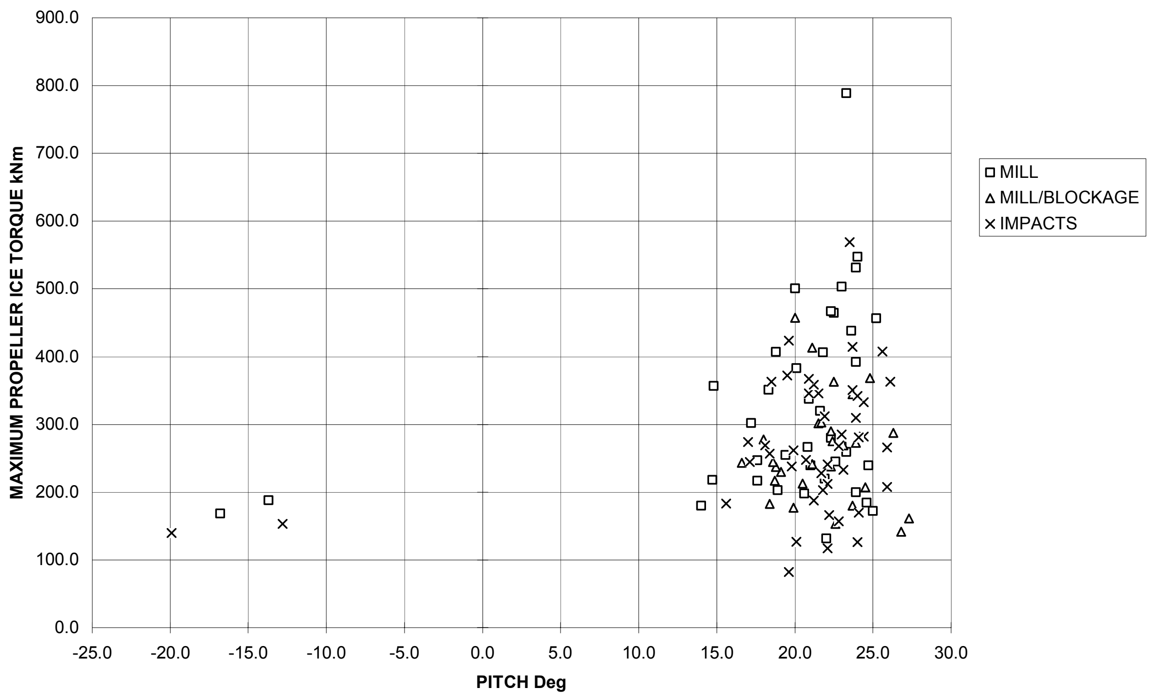

Figure 73 **Oden - Maximum Starboard Propeller Ice Torque versus Pitch Angle**

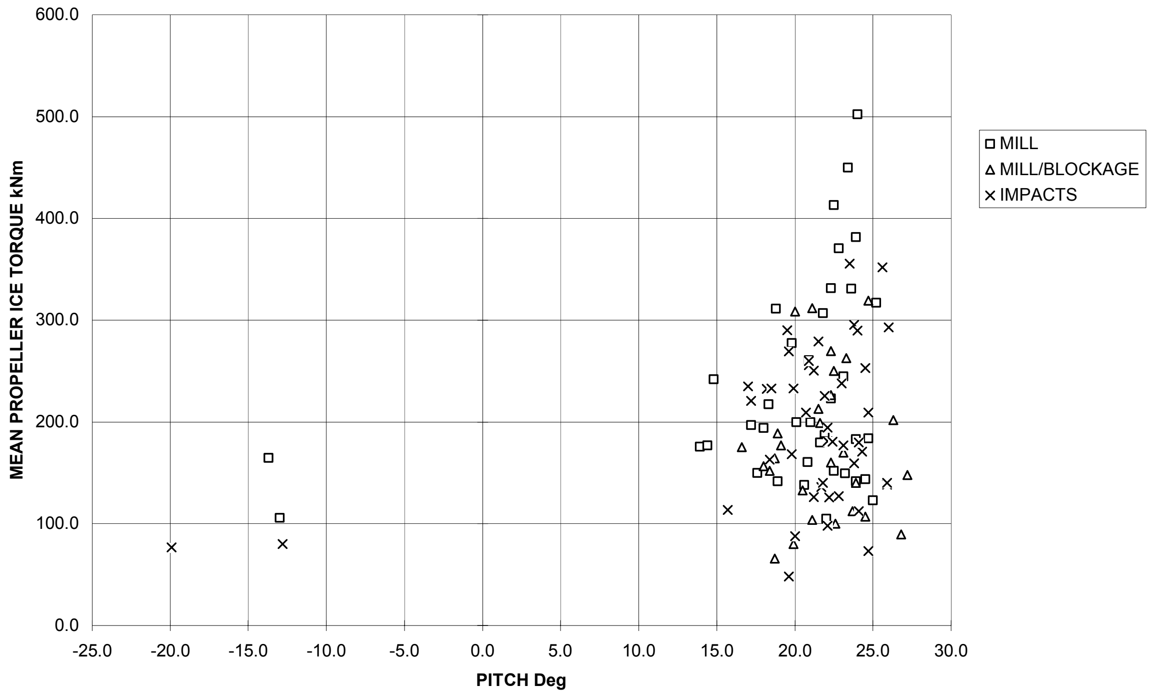

Figure 74 Oden - Mean Starboard Propeller Ice Torque versus Pitch Angle

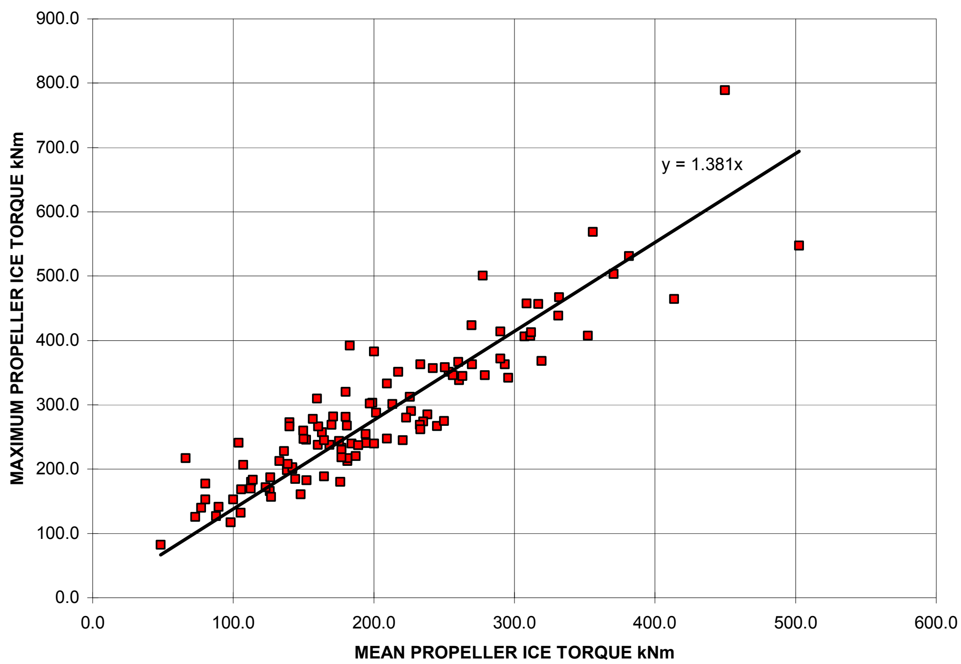

Figure 75 Oden - Comparison of Maximum and Mean Starboard Propeller Ice Torque

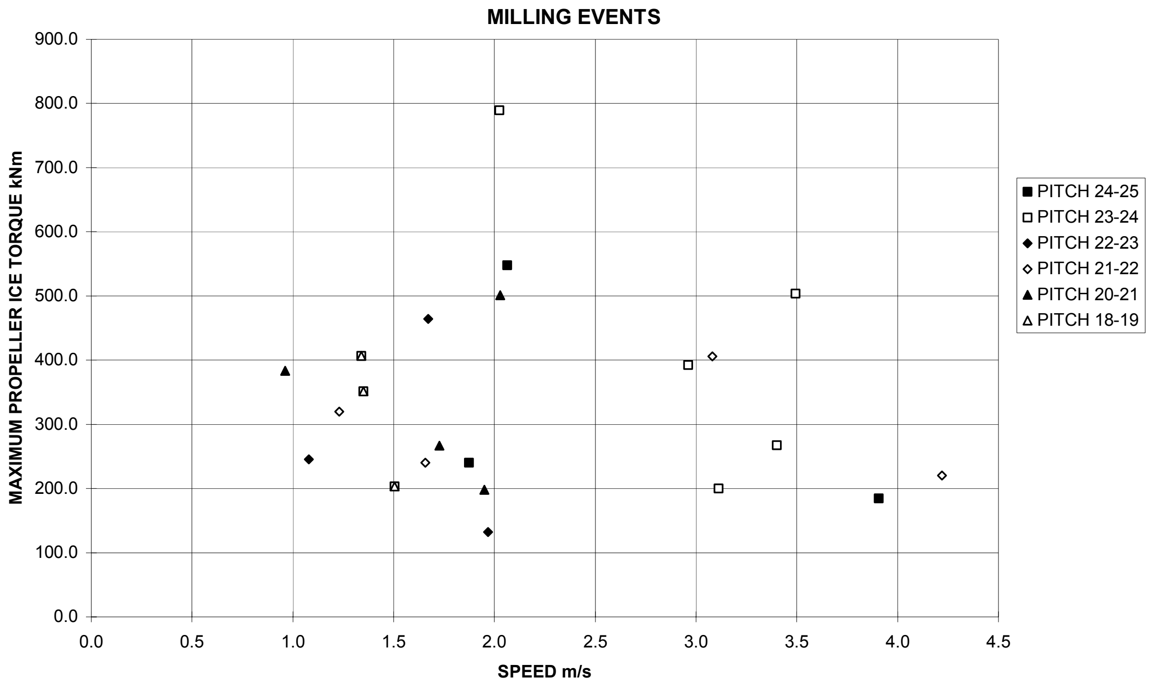

Figure 76 Oden - Maximum Starboard Propeller Ice Torque versus Ship Speed

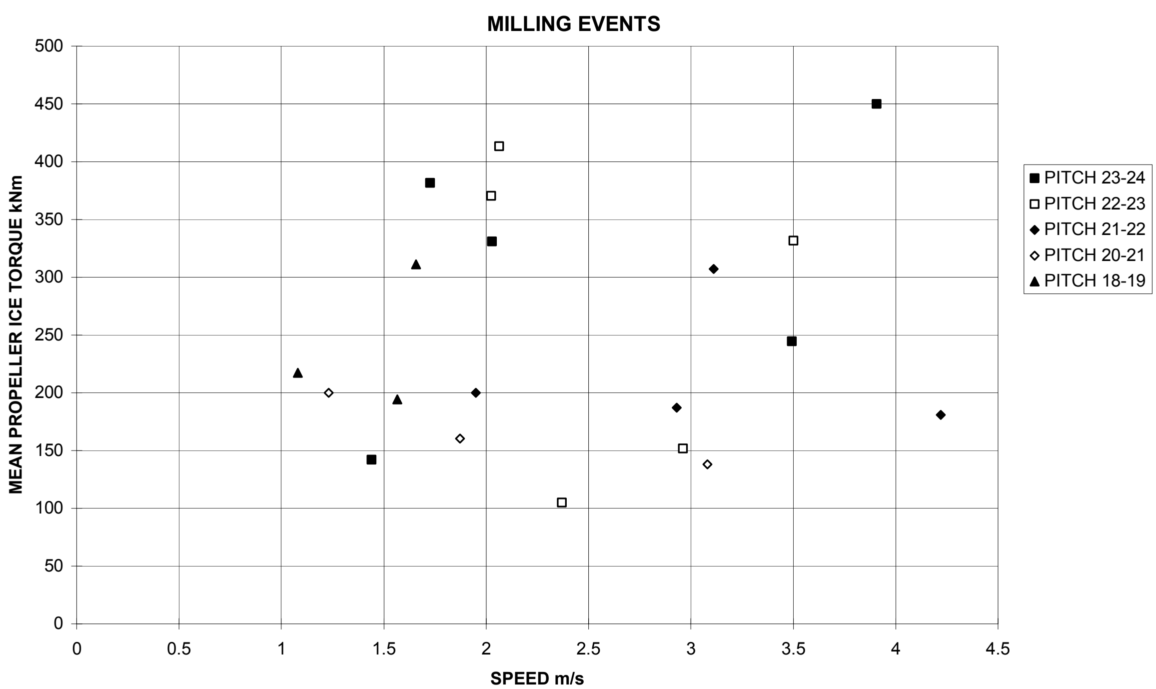

Figure 77 Oden - Mean Starboard Propeller Ice Torque versus Ship Speed

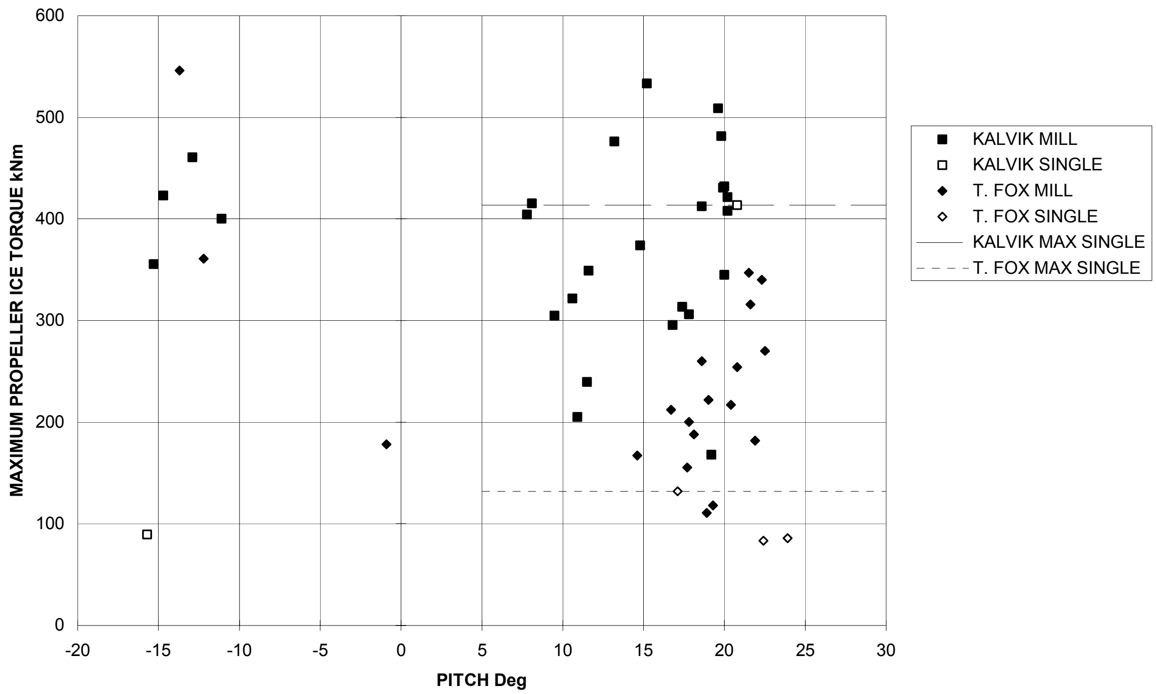

Figure 78 Comparison of Kalvik and Terry Fox Maximum Propeller Ice Torque

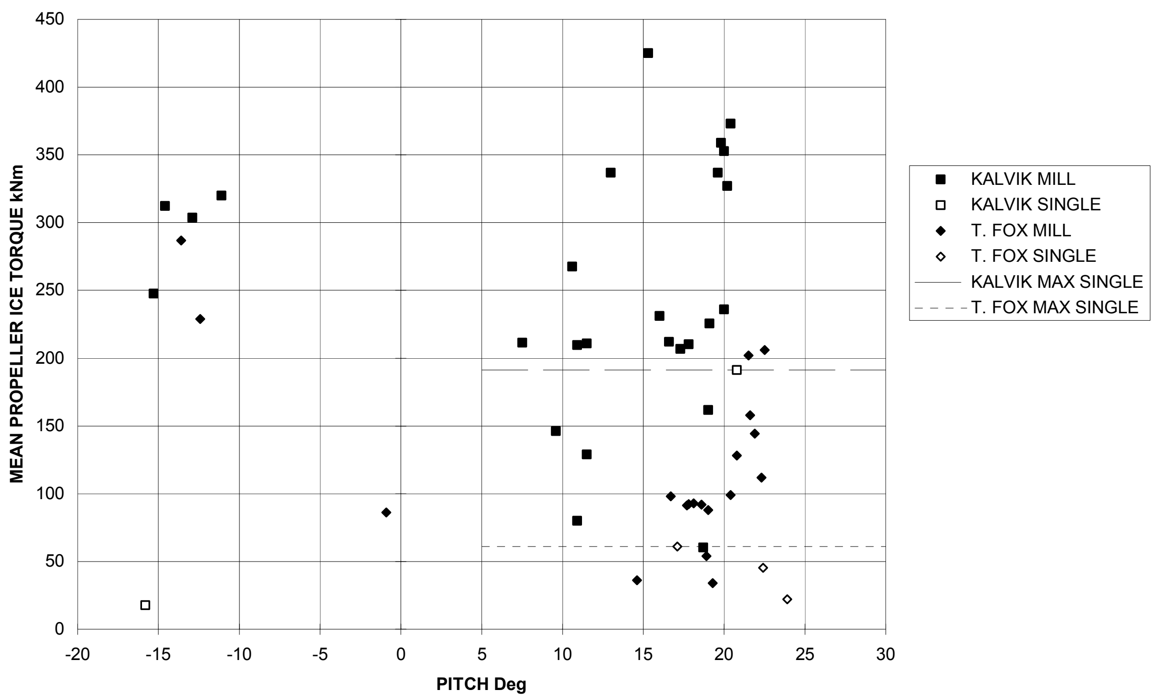

Figure 79 Comparison of Kalvik and Terry Fox Mean Propeller Ice Torque

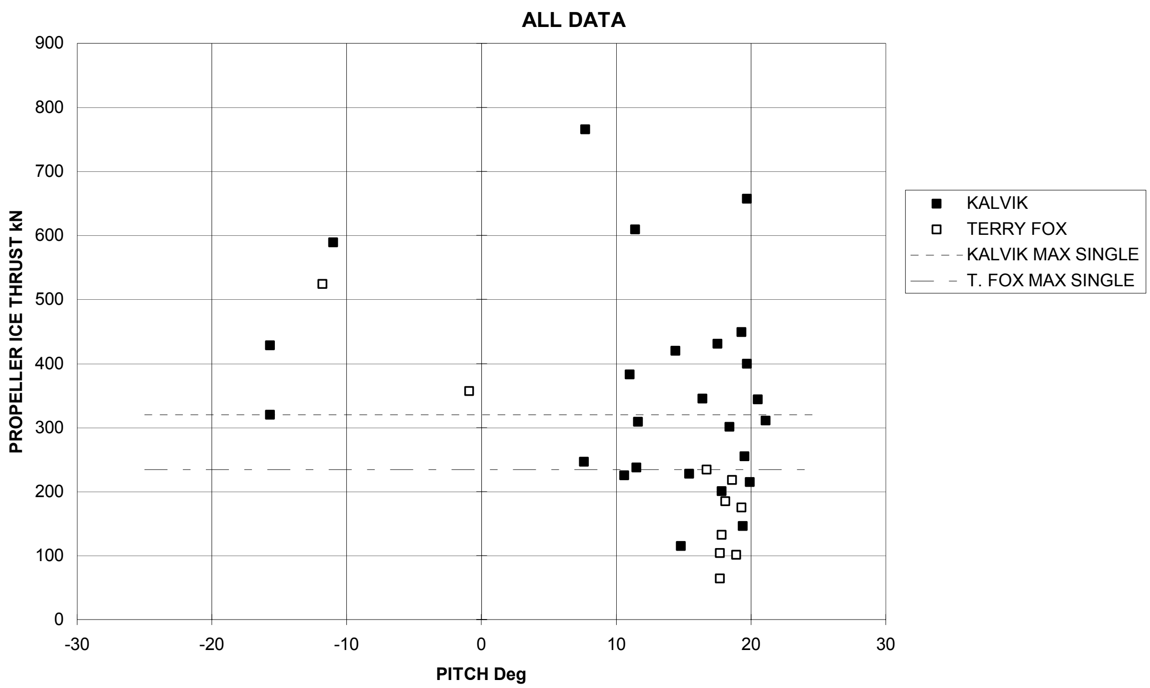

Figure 80 Comparison of Kalvik and Terry Fox Positive Propeller Ice Thrust

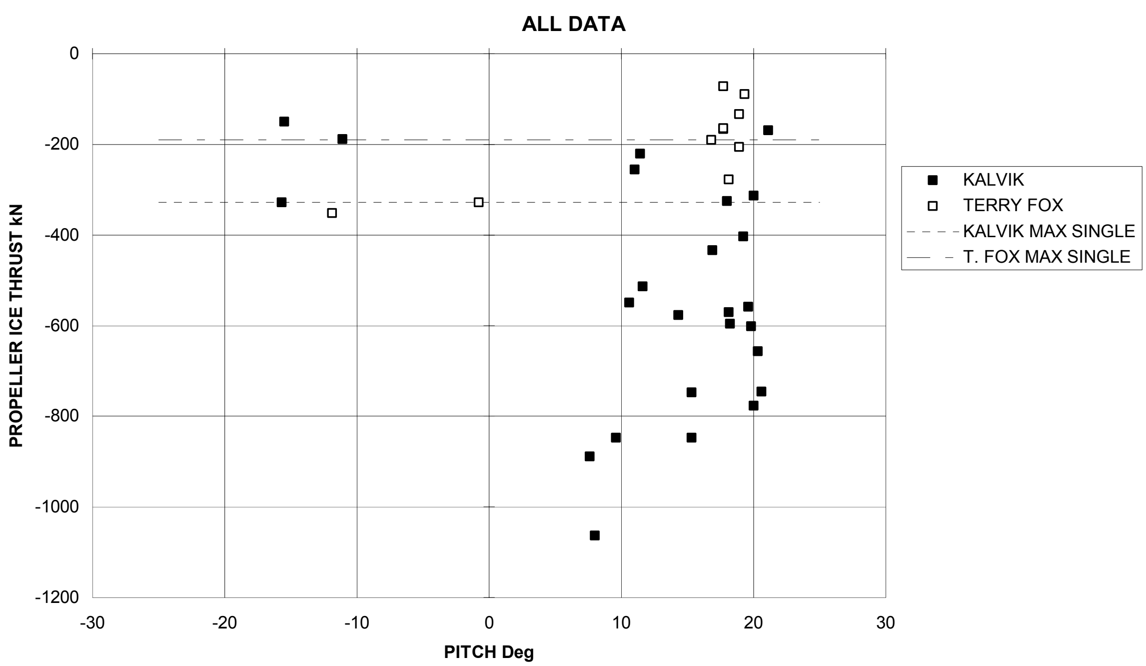

Figure 81 Comparison of Kalvik and Terry Fox Negative Propeller Ice Thrust

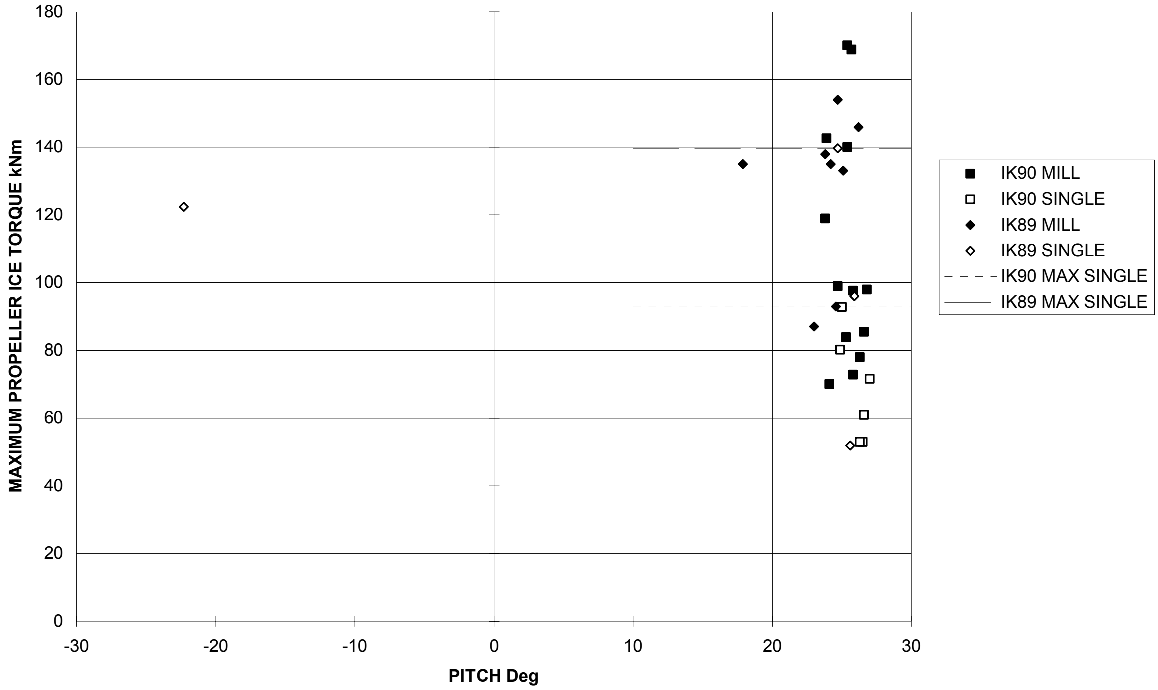

Figure 82 Comparison of Ikaluk '89 and Ikaluk '90 Maximum Propeller Ice Torque

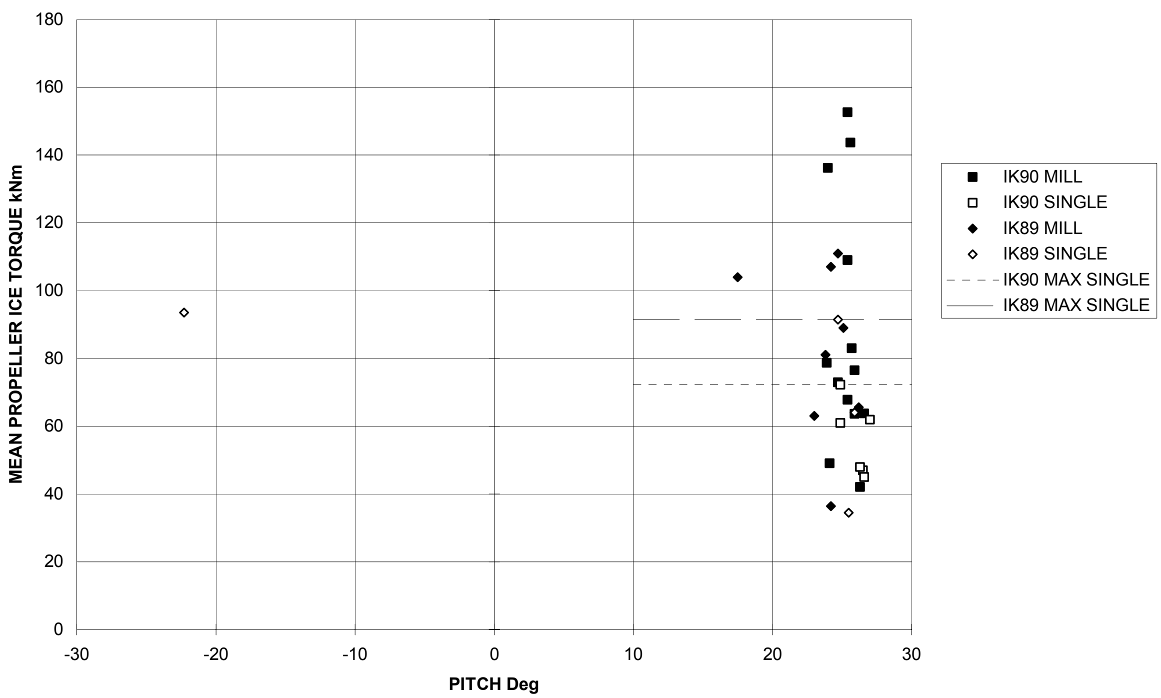

Figure 83 Comparison of Ikaluk '89 and Ikaluk '90 Mean Propeller Ice Torque

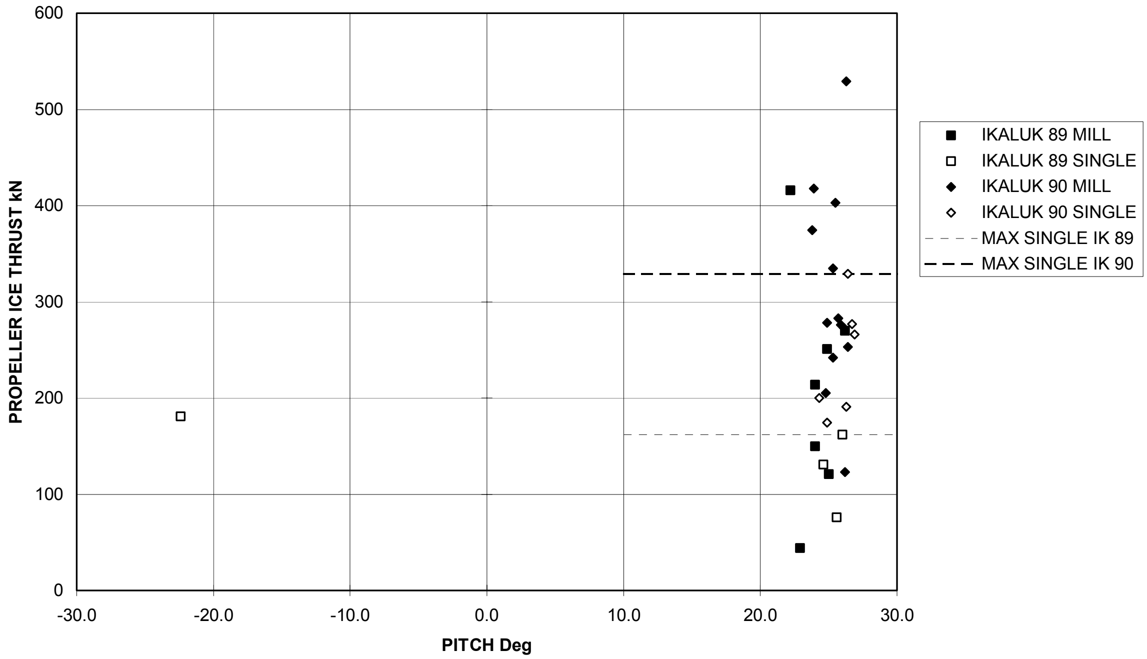

Figure 84 Comparison of Ikaluk '89 and Ikaluk '90 Positive Propeller Ice Thrust

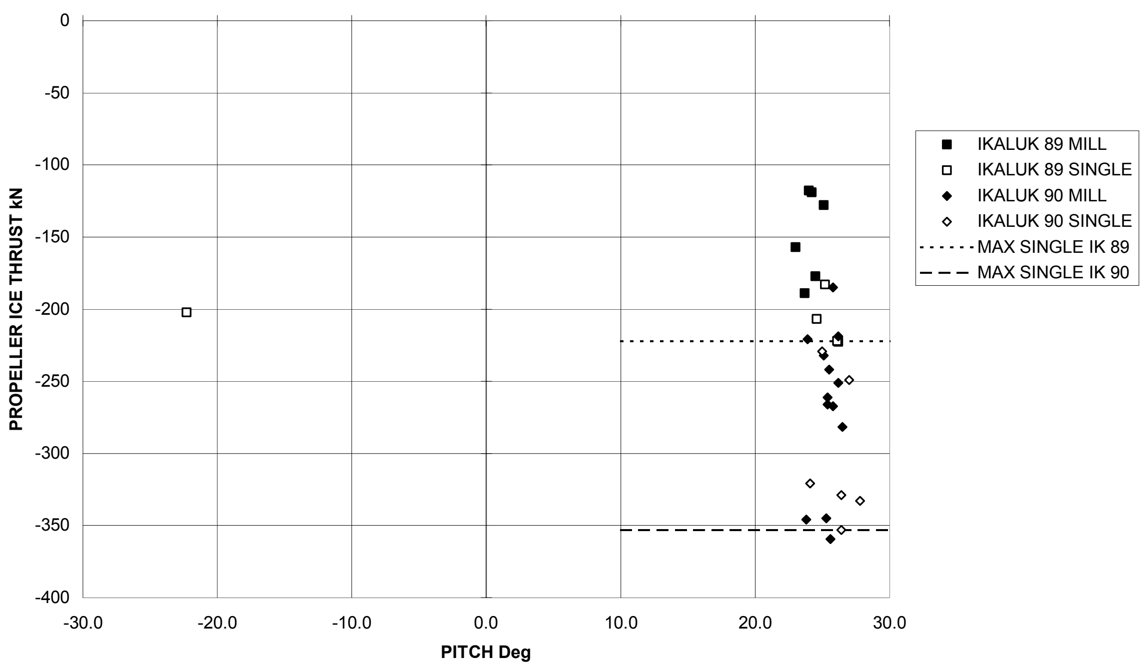

Figure 85 Comparison of Ikaluk '89 and Ikaluk '90 Negative Propeller Ice Thrust

4. LONG-TERM PROPELLER ICE LOAD PREDICTIONS

4.1. The Weibull Distribution

Long-term predictions of propeller ice loads have been made by fitting Type 3, lower-bound, Weibull distributions to the propeller ice load data. This distribution is applicable to data sets having a low level cut-off, which is the case for all the full-scale data. These were recorded above specific threshold values of shaft thrust and torque, thus preventing the recording of smaller load events.

4.1.1. Procedure

The procedure for fitting the long-term Weibull distributions is as follows.

The Weibull distribution has the form:

$$\text{Probability of Exceedence} \quad Q(T) = \exp(-((T-\varepsilon)/\theta)^{\alpha})$$

Where:

- T = is the load value
- ε = lower limiting value of the data set
- θ = scale parameter which describes the degree of spread of the data
- α = parameter which describes the basic shape of the distribution

The procedure to determine the parameters ε, θ, α, is illustrated by Figures 86a to 86c, for the Robert Lemeur maximum negative propeller ice thrust data set.

α is determined from the slope of the straight line fit of $\ln(T-\varepsilon)$ versus $\ln(-\ln(Q(T)))$, as in Figure 86a. The appropriate low level cut-off value ε is not known exactly, and is therefore determined by varying its value until the best straight line relationship is found. Figure 86b shows an unacceptable relationship for $\varepsilon = 0$, as opposed to the value of $\varepsilon = -30$ determined in Figure 86a. α determined from Figure 86a is 2.54.

θ is now determined from the slope of the straight line fit of T and $(-\ln(Q(T)))^{1/\alpha}$. Slope = $1/\theta$, Figure 86c. $\theta = 103$.

The Weibull distribution is now plotted versus the data set in Figure 87 for the parameter values of $\varepsilon = -30$, $\theta = 103$ and $\alpha = 2.54$.

4.2. Long-term Predictions from the Trials Data

From analysis of the propeller ice load data, derived from the following instrumented trials,

Robert Lemeur	1984 Spring Breakout
Ikaluk	1989 Herschel Basin
Ikaluk	1990 Herschel Basin
Oden	1991 Arctic Expedition
Louis S. St. Laurent	1994 Trans-Arctic Voyage
Kalvik	1986 Viscount Melville Sound
Terry Fox	1990 Herschel Basin

predictions have been made for the expected maximum, positive and negative, propeller ice thrust, and both the maximum and mean propeller ice torque, for 10,000 hours of operation, in ice having the characteristics of that met on the trials.

The propeller load data are plotted, versus probability of exceedence, in the Figures noted in Table 7. The long-term Weibull distributions are also shown.

Table 7 Weibull Plot Figure Numbers

Ship Trial	Ice Torque		Ice Thrust	
	Max	Mean	Max + ve	Max - ve
Robert Lemeur, 1984	88	89	90	91
Ikaluk, 1989	92	93	94	95
Ikaluk, 1990	96	97	98	99
Oden, 1991	100/101	102/103	No Measurements	
Louis S. St. Laurent,1994	104/105	106/107	108/109	110/111
Kalvik, 1986	112	113	114	115
Terry Fox, 1990	116	117	118	119

For each trial and propeller load, the probability of exceedence associated with 1,000 and 10,000 hours of operation, is given in **Table** . This table then provides the predicted long-term loads.

Table 8 Long Term Predictions Using Weibull Distribution

							Max. Positive Ice Thrust							Max. Negative Ice Thrust						
							Measured				Predicted			Measured				Predicted		
Vessel	Data for Shafts	Trial	No. of Props	Propeller Ducted/Open D = Dructed, O = Open	Type of Propeller, FP=Fixed Pitch,	Diameter (m)	No. of Events	Max value Recorded (kN)	Average Event Interval (mins)	1,000 hrs Probability of Exceedence	1,000 hrs Max. (kN)	10,000 hrs Probability of Exceedence	10,000 hrs Max. (kN)	No. of Events	Max value Recorded (kN)	Average Event Interval (mins)	1,000 hrs Probability of Exceedence	1,000 hrs Max. (kN)	10,000 hrs Probability of Exceedence	10,000 hrs Max. (kN)
R.Lemeur	STBD	1984 Spring Breakout	2	D	CP	3	190	415.6	2.68	4.5E-05	504	4.47E-06	544	190	-232	2.68	4.5E-05	-285	4.47E-06	-307
Ikaluk 1	STBD	1989 May, Herschel Basin	2	D	CP	3.725	30	530	6.36	1.1E-04	830	1.06E-05	930	30	-320	6.36	1.1E-04	-408	1.06E-05	-440
Ikaluk 2	P & S	1990 June, Herschel Basin	2	D	CP	3.725	19	529	2.36	3.9E-05	735	3.93E-06	790	19	-359	2.36	3.9E-05	-476	3.93E-06	-496
Oden	PORT	1991 Arctic Expedition	2	D	CP	4.5														
Oden	STBD	1991 Arctic Expedition	2	D	CP	4.5														
Louis	STBD	1994 Trans-Arctic Voyage	3	O	FP	4.57	326	2165	70.7	1.2E-03	2410	1.18E-04	2720	326	-3420	70.7	1.2E-03	-2890	1.18E-04	-3160
Louis	CENTRE	1994 Trans-Arctic Voyage	3	O	FP	4.57	103	1130	223.7	3.7E-03	1150	3.73E-04	1320	103		223.7	3.7E-03	-1680	3.73E-04	-1890
Kalvik	STBD	1986 Viscount Melville Sound	2	O	CP	4.8	25	766	15	2.5E-04	1330	2.50E-05	1540	25	-1063	15	2.5E-04	-1730	2.50E-05	-1950
T. Fox	P & S	1990 June, Herschel Basin	2	O	CP	4.8	10	524	4.49	7.5E-05	1020	7.48E-06	1160	10	-352	4.49	7.5E-05	-900	7.48E-06	-1035

The overall level of fit of the Weibull distributions to the full-scale data is considered to be good. The level of fit to the thrust data is slightly better in general than to the torque data. Also, data from the two longest trials for Louis S. St. Laurent and Oden are, overall, matched best by the Weibull distributions.

The total operational time on each trial is given in Table 9, together with the magnitude of the extrapolation required to 10,000 hours of operating time.

Table 9 Ship Trials Operational Times

Ship Trial	Operational Time - hours	Multiplier to 10,000 hours
Robert Lemeur, 1984	9	1,100
Ikaluk, 1989	3.5	2,900
Ikaluk, 1990	1	10,000
Oden, 1991	422	24
Louis S. St. Laurent, 1994	390	26
Kalvik, 1986	7	1,400
Terry Fox, 1990	1	10,000

The value of any long-term prediction is clearly a function of the extent to which the recorded data set is representative statistically of the vessel's normal operation. This condition is likely to be achieved to an increasing extent as the sampling period increases. The required extrapolation also decreases. The degree of confidence which can be placed in the long-term predictions is shown in relative order in Table 10.

Table 10 Relative Degree of Confidence in Long-term Predictions

Louis S. St. Laurent, 1994	High
Oden, 1991	High
Robert Lemeur, 1984	Moderate
Kalvik, 1986	Moderate
Ikaluk, 1989	Low
Ikaluk, 1990	Lowest
Terry Fox, 1990	Lowest

It must also be borne in mind, that although the overall level of fit of the Weibull distributions to the full-scale data is good, this does not guarantee the degree of extrapolation possible beyond the measured data. Physical limitations are expected to exist, which restrict the theoretically worst combinations of interaction parameters, and therefore the maximum ice loads possible. These limitations are currently not known, beyond the measured data. However, the process of extrapolating all trials data sets to the same exposure time is expected to provide at least valid comparisons of relative maximum load levels.

4.3. Discussion of Results

The data for open and ducted propellers are plotted versus propeller diameter in Figures 120 to 122. A diameter squared curve is drawn through the Robert Lemeur ice thrust data points in Figure 120, and a diameter cubed curve is drawn through the mean of the Oden port and starboard ice torque data points in Figures 121 and 122.

The ducted propeller results for Robert Lemeur and Ikaluk provide general support for ice thrust to vary approximately with propeller diameter squared, when the ice is thick as on the trials. The results for Robert Lemeur, Ikaluk, and Oden provide general support for ice torque to vary approximately with diameter cubed. The ice torque predictions from the Ikaluk 1989 trials data, however, are significantly lower than might be expected.

It is also noted that:

- For the open propellers, negative ice thrust is greater than positive ice thrust by up to 27% in the case of Kalvik, and 43% in the case of Louis S. St. Laurent centre propeller.
- For the ducted propellers, positive propeller ice thrust is about 75% larger than negative propeller ice thrust.
- Maximum negative ice thrust for the open propellers is up to 4 times that of a similar diameter ducted propeller.
- For the ducted propellers, the ratio of maximum/mean ice torque varies considerably, with maximum ice torque on average being 30% higher than mean ice torque.
- For the open propellers, maximum ice torque is as much as 55% higher than mean ice torque.
- The open propellers can generate higher ice torques than ducted propellers, but this difference is by no means as large as that seen between open and ducted propellers for ice thrust.
- The centre screw of the triple open screw vessel Louis S. St. Laurent experiences only about 60% of the ice thrust and 75% of the ice torque of the wing propellers, which are much exposed to ice interaction. The twin open screws of Kalvik, which have some protection due to their limited separation and location beneath the buttock flow stern, experience similar loads to those on the Louis centre propeller. It is probable that these data show an influence of hull protection.

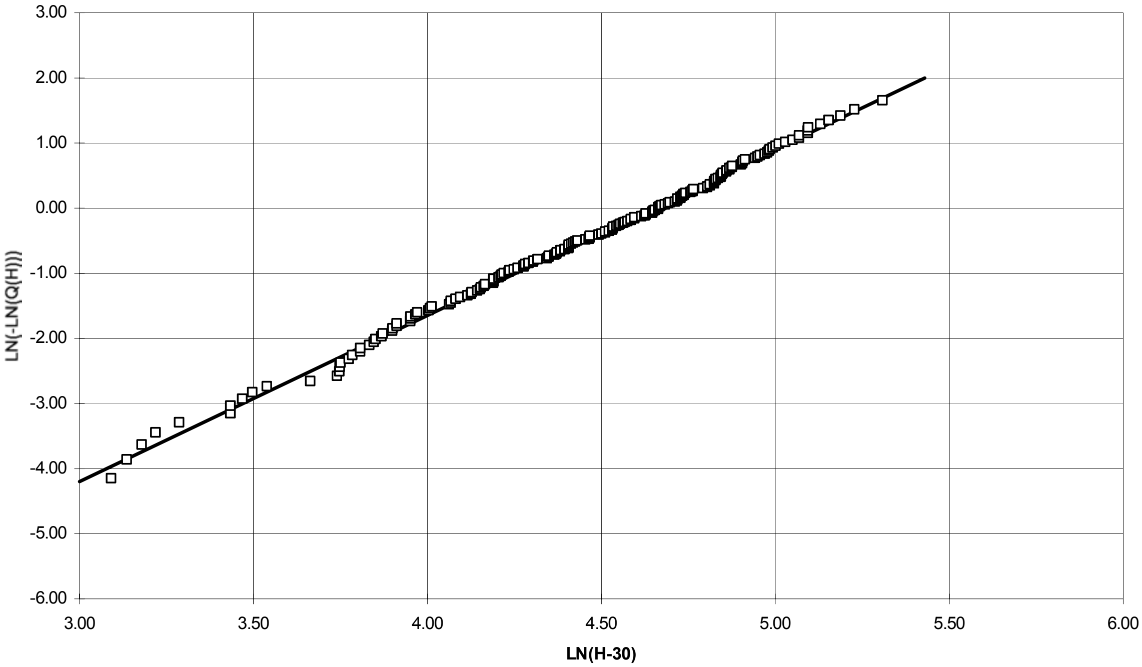

Figure 86(a)

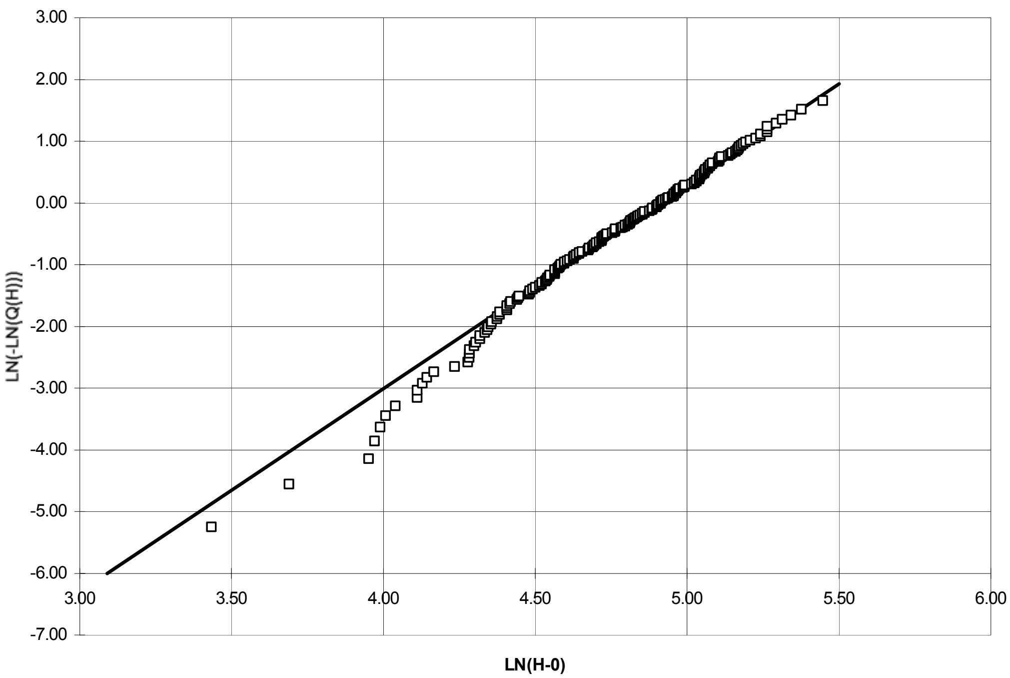

Figure 86(b)

Figure 86 Robert Lemeur - Negative Propeller Ice Thrust data plots for Weibull Distribution Coefficients

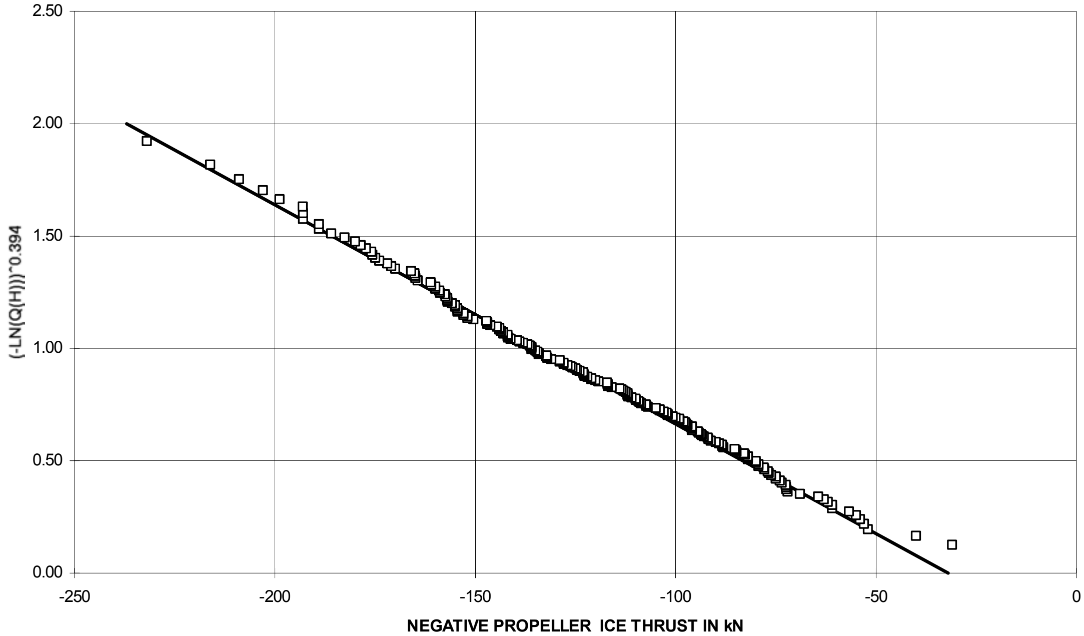

Figure 86(c) Robert Lemeur - Negative Propeller Ice Thrust data plots for Weibull Distribution Coefficients

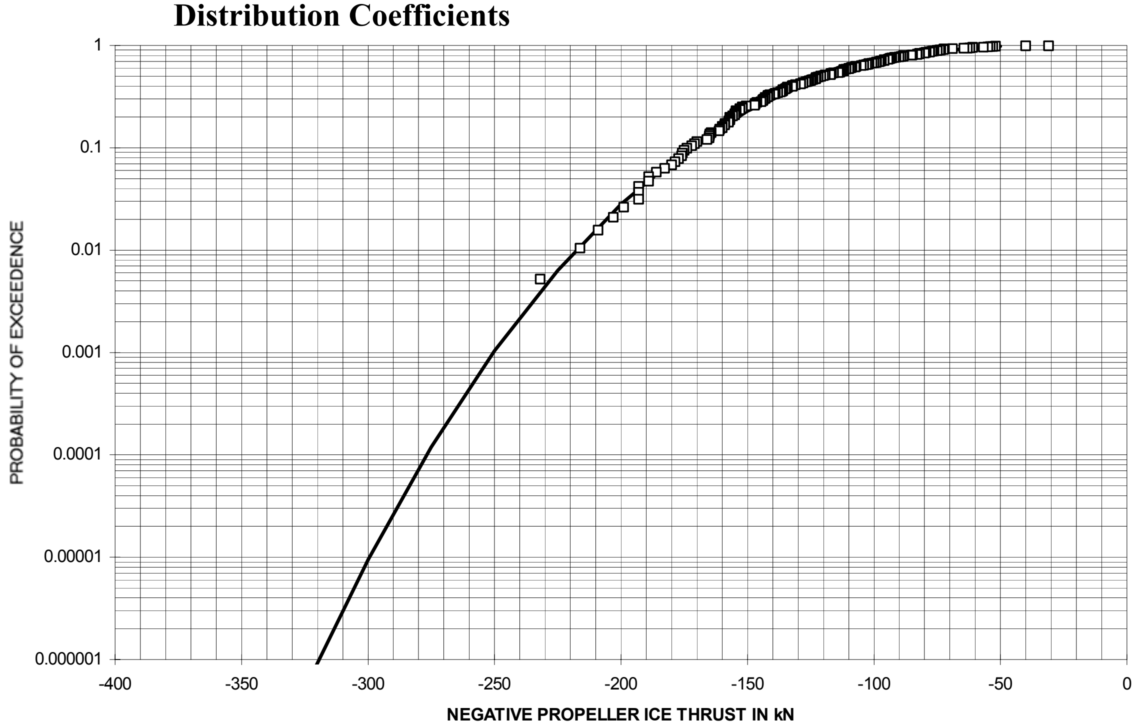

Figure 87 Robert Lemeur - Negative Propeller Ice Thrust Long-term Prediction

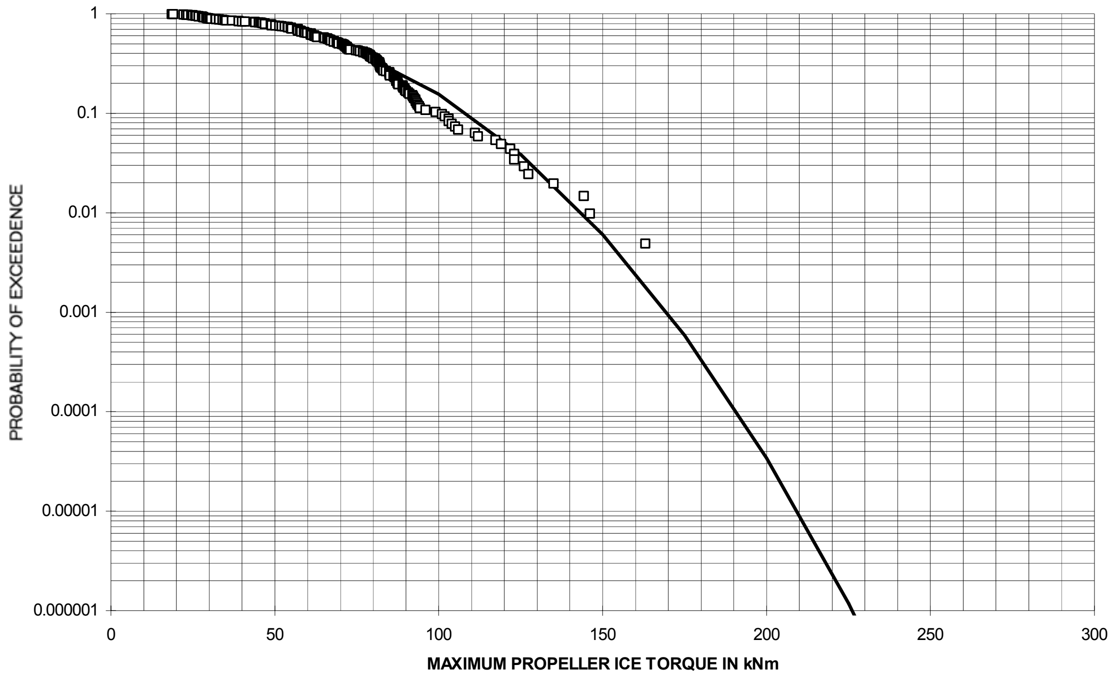

Figure 88 Robert Lemeur - Maximum Propeller Ice Torque Long-term Prediction

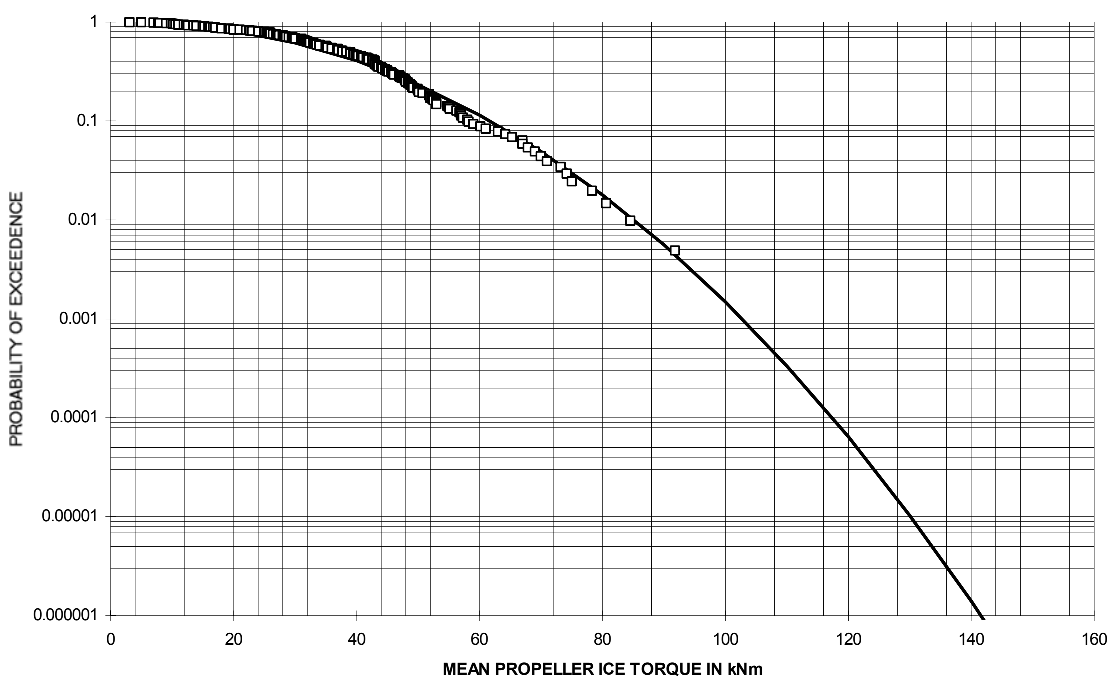

Figure 89 Robert Lemeur - Mean Propeller Ice Torque Long-term Prediction

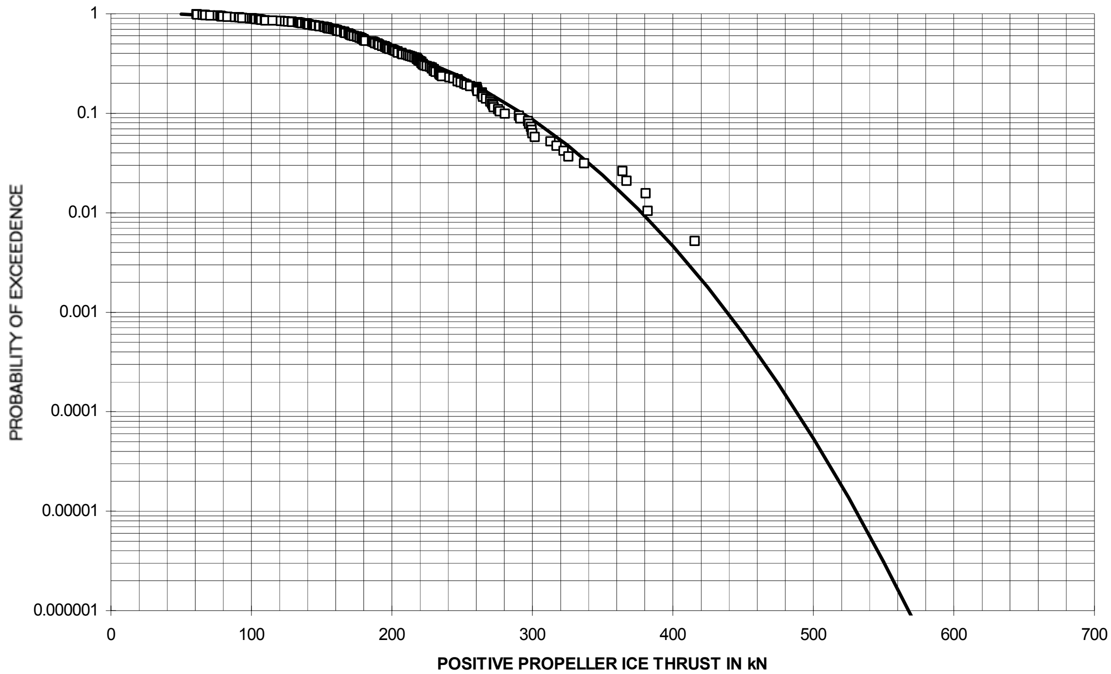

Figure 90 Robert Lemeur - Positive Propeller Ice Thrust Long-term Prediction

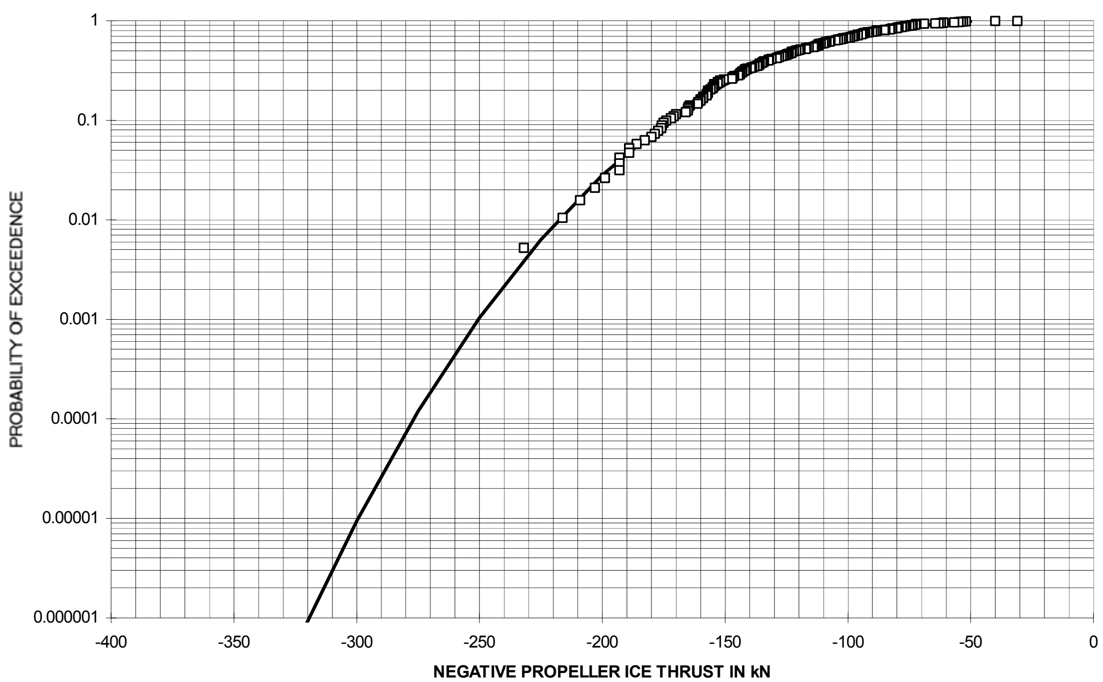

Figure 91 Robert Lemeur - Negative Propeller Ice Thrust Long-term Prediction

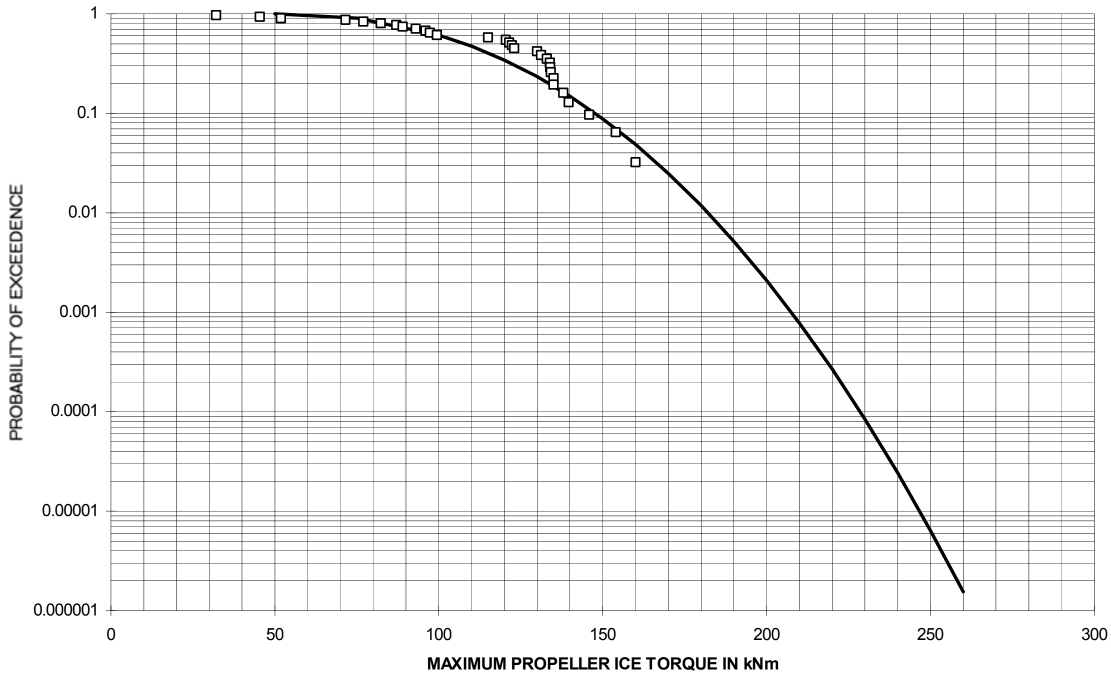

Figure 92 Ikaluk '89 - Maximum Propeller Ice Torque Long-term Prediction

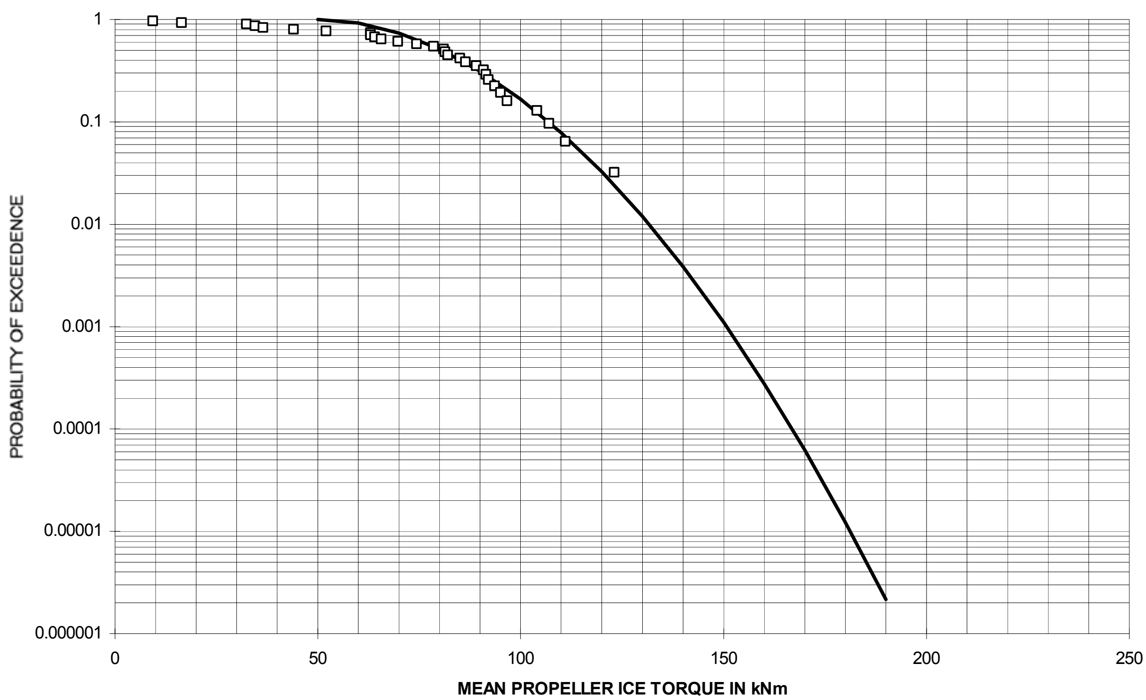

Figure 93 Ikaluk '89 - Mean Propeller Ice Torque Long-term Prediction

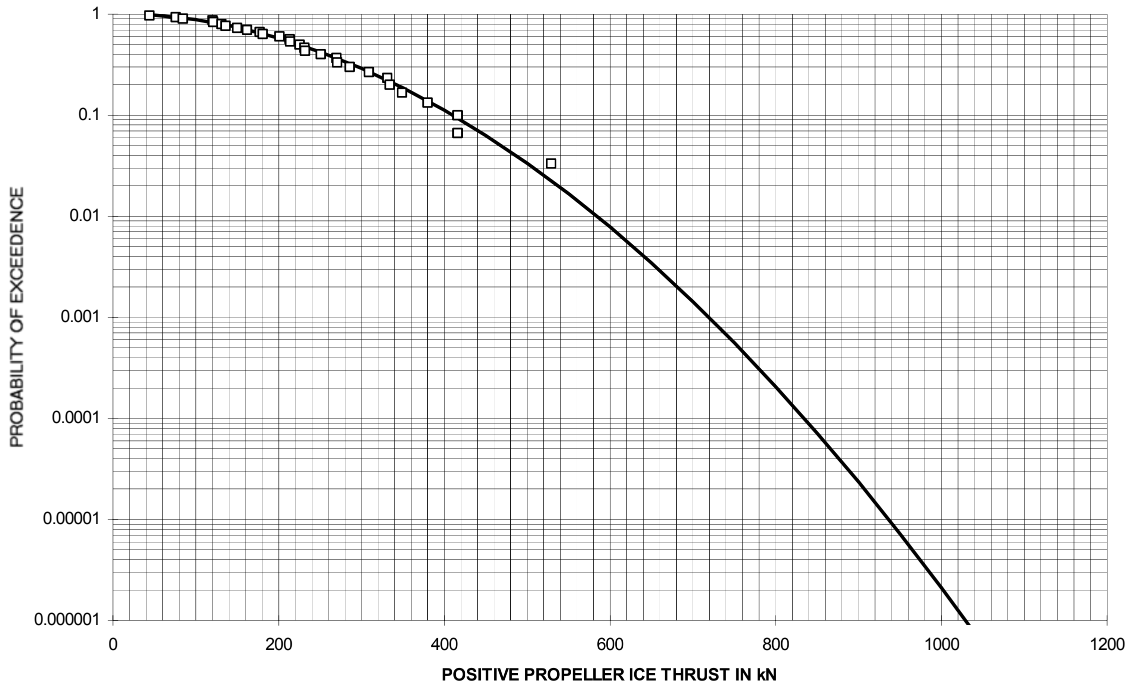

Figure 94 Ikaluk '89- Positive Propeller Ice Thrust Long-term Prediction

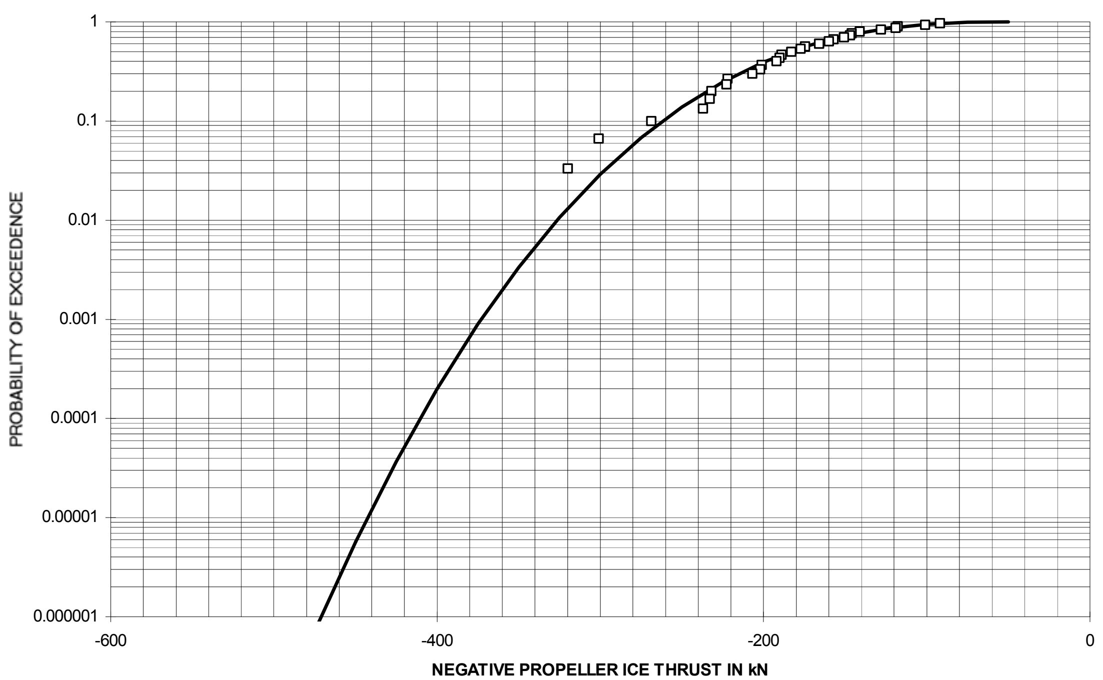

Figure 95 Ikaluk '89 - Negative Propeller Ice Thrust Long-term Prediction

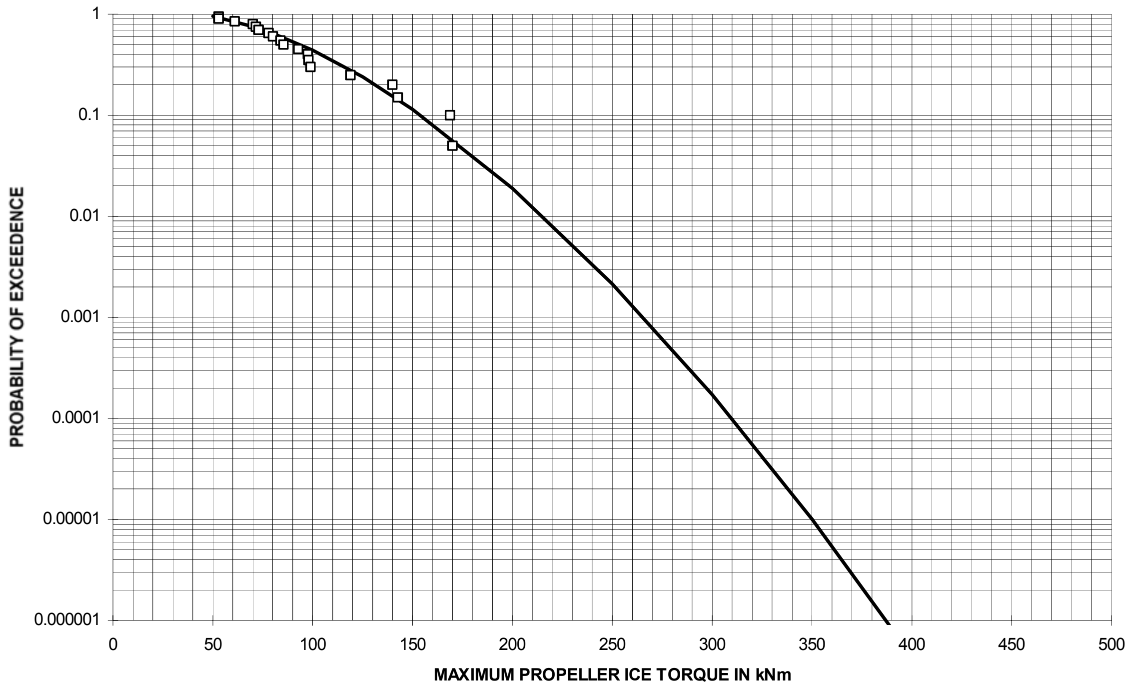

Figure 96 Ikaluk '90 - Maximum Propeller Ice Torque Long-term Prediction

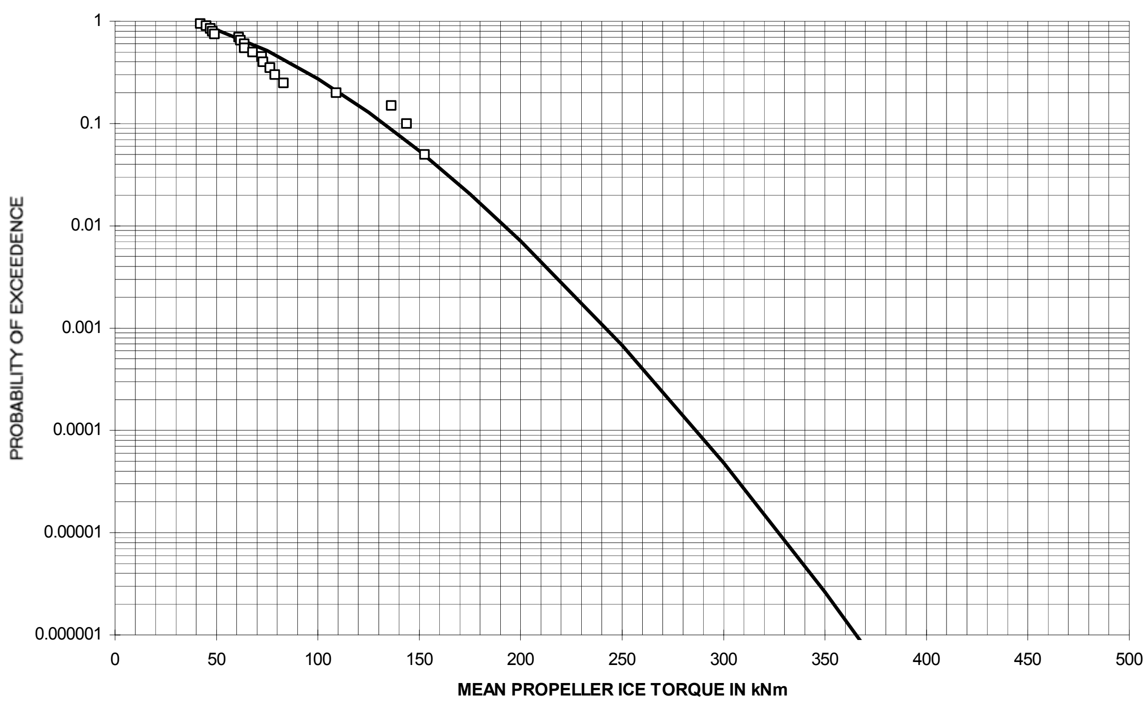

Figure 97 Ikaluk '90 - Mean Propeller Ice Torque Long-term Prediction

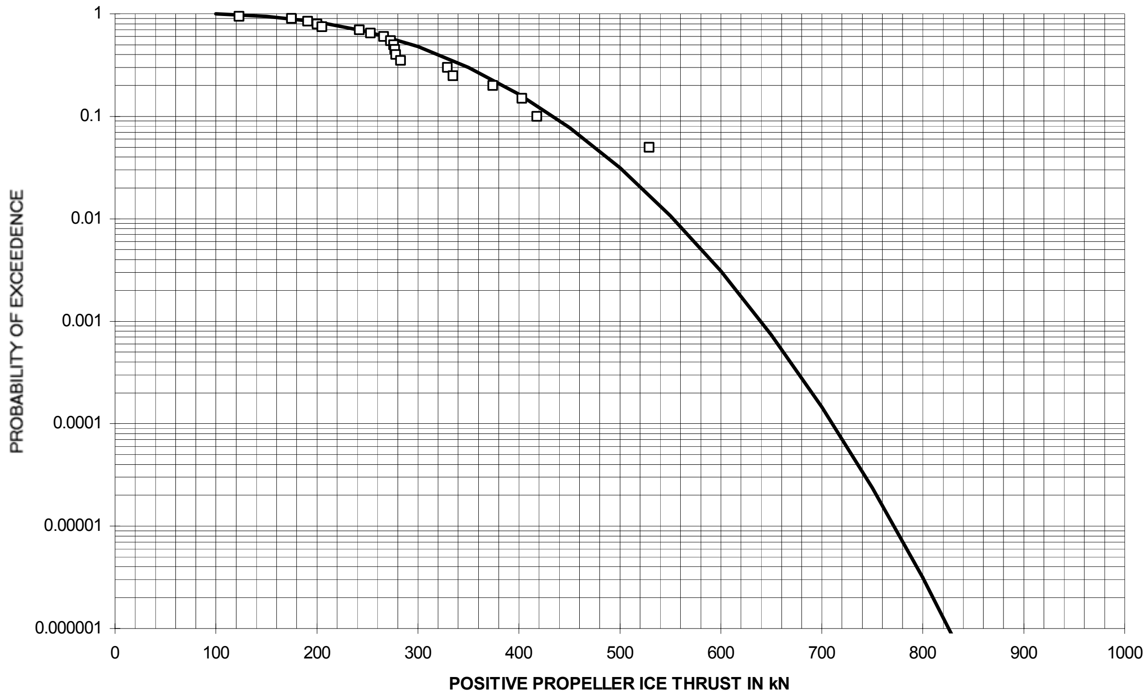

Figure 98 Ikaluk '90- Positive Propeller Ice Thrust Long-term Prediction

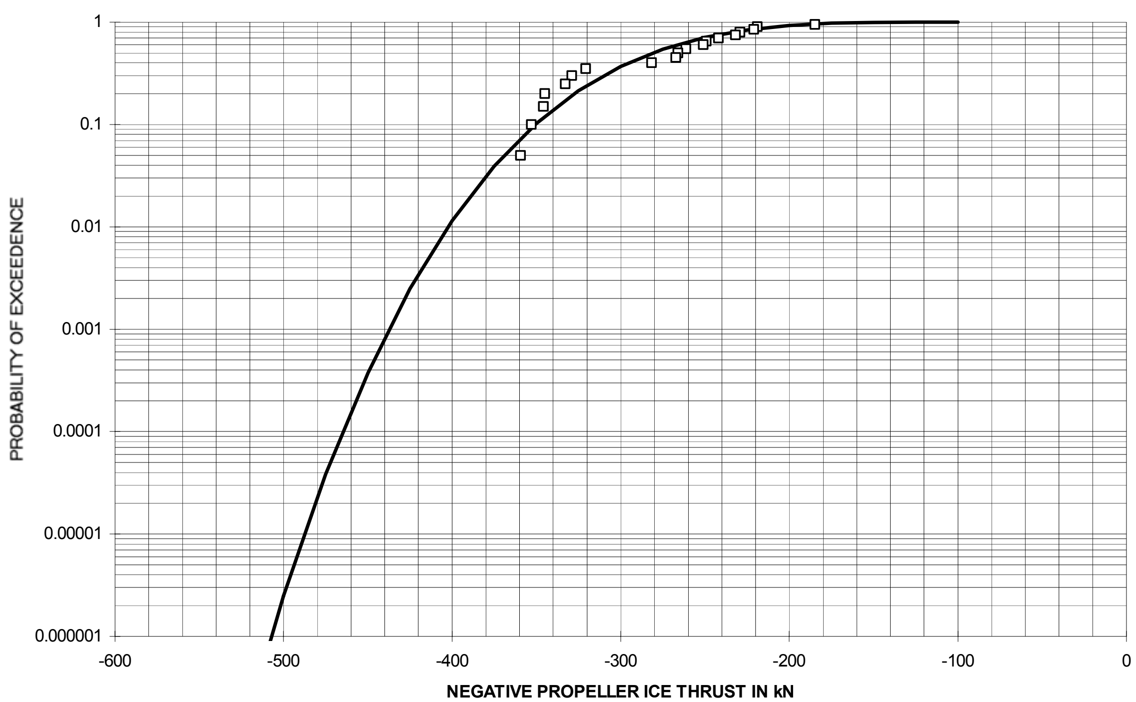

Figure 99 Ikaluk '90 - Negative Propeller Ice Thrust Long-term Prediction

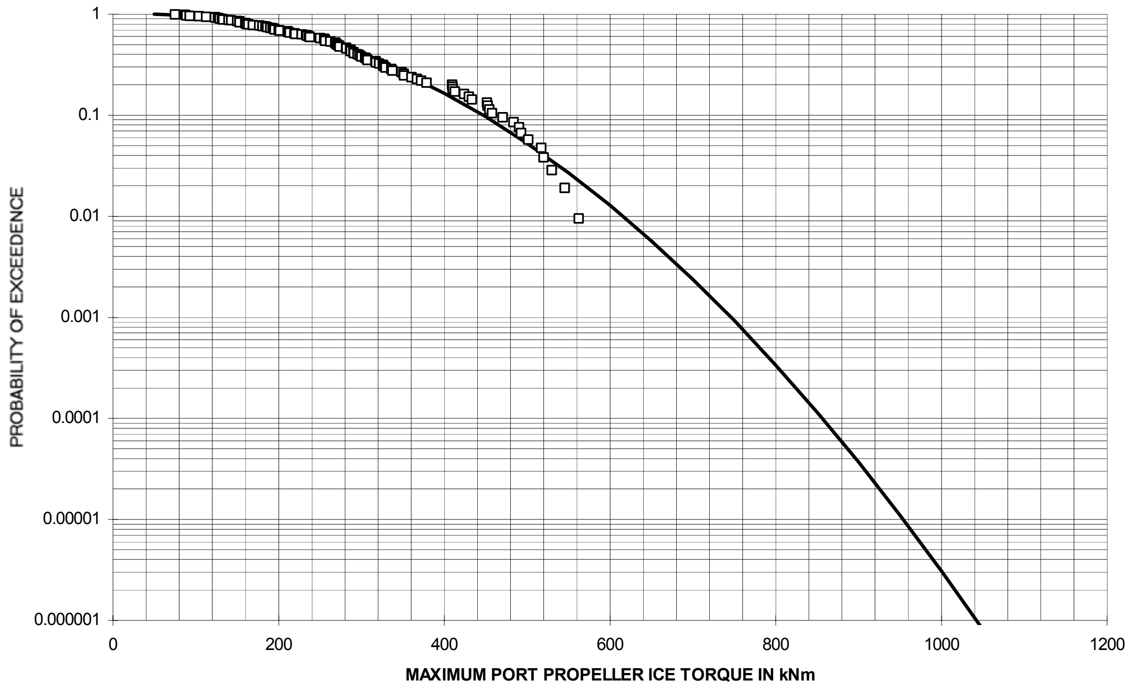

Figure 100 Oden - Maximum Port Propeller Ice Torque Long-term Prediction

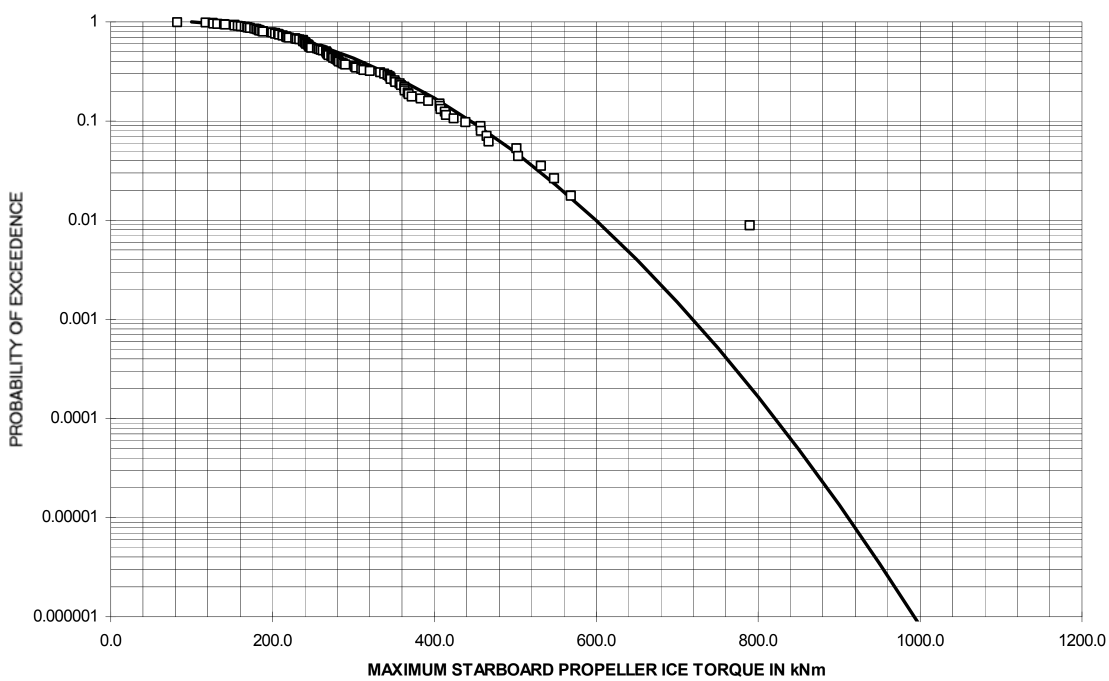

Figure 101 Oden - Maximum Starboard Propeller Ice Torque Long-term Prediction

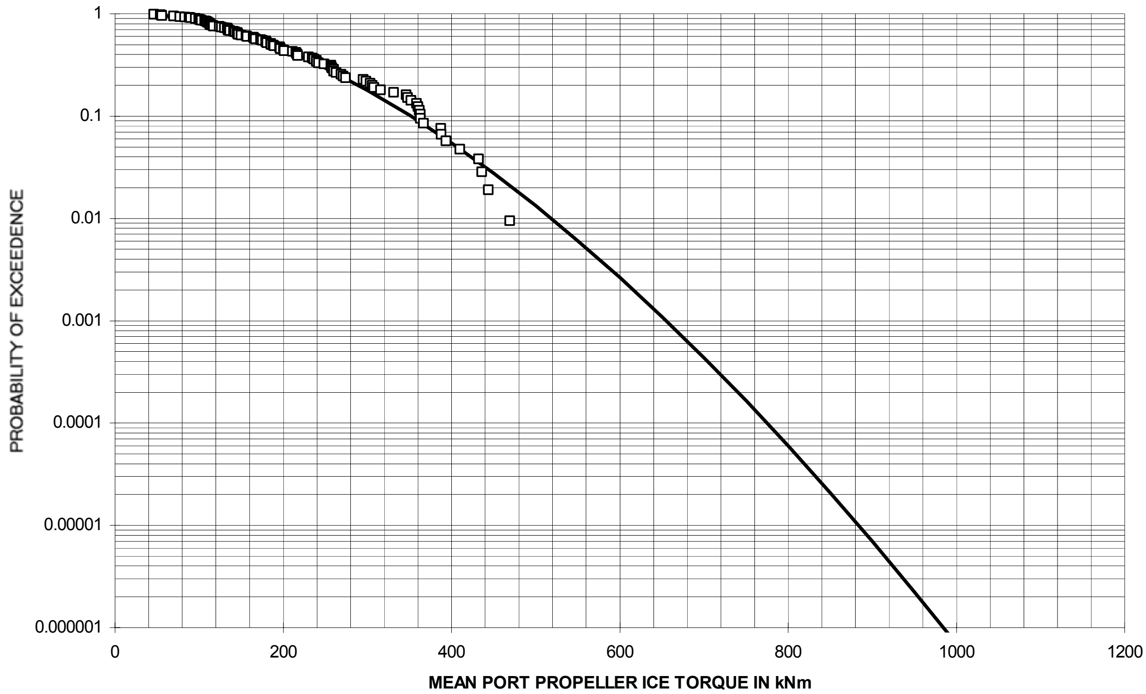

Figure 102 Oden - Mean Port Propeller Ice Torque Long-term Prediction

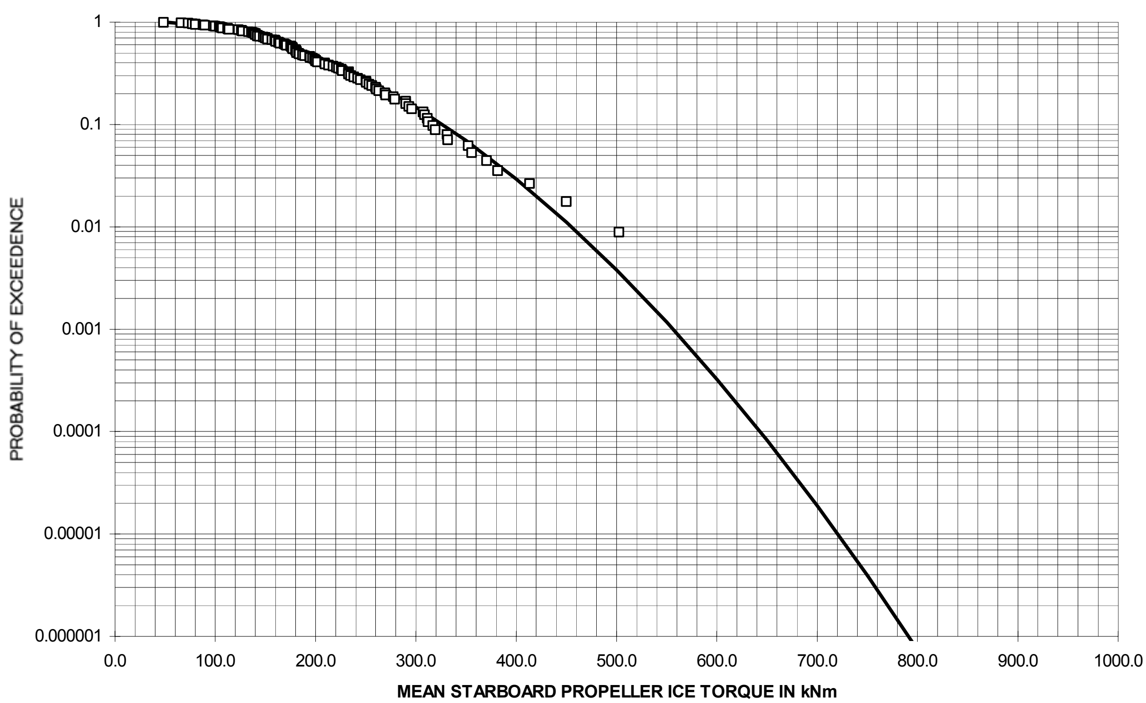

Figure 103 Oden - Mean Starboard Propeller Ice Torque Long-term Prediction

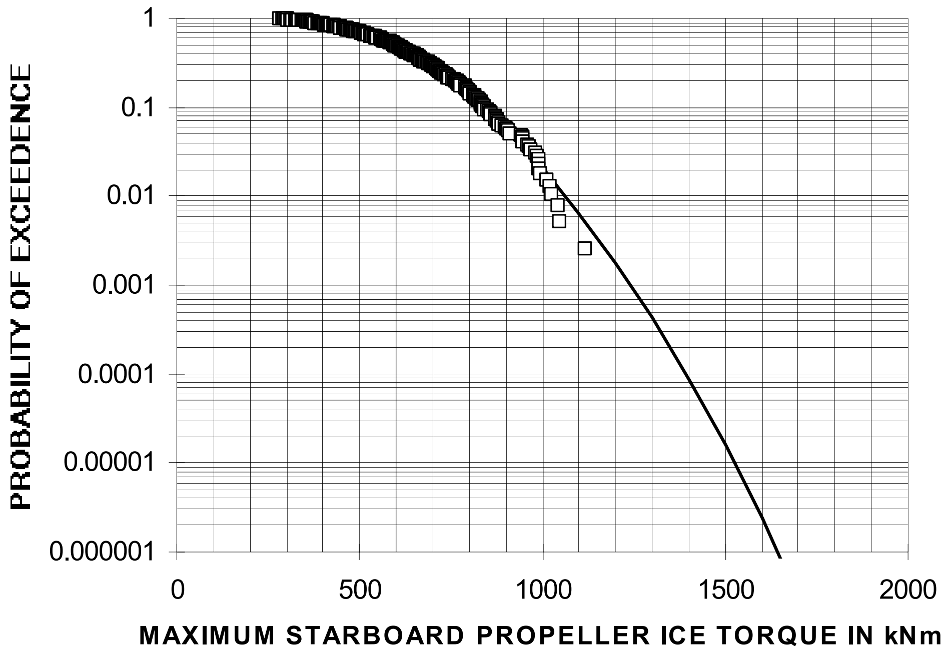

Figure 104 Louis S. St. Laurent - Maximum Starboard Propeller Ice Torque Long-term Prediction

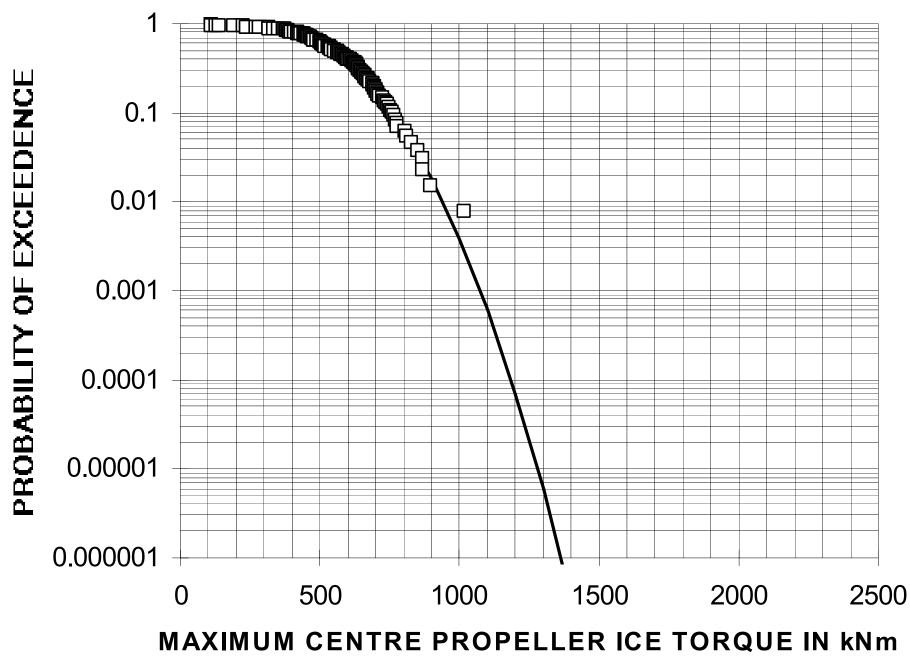

Figure 105 Louis S. St. Laurent - Maximum Centre Propeller Ice Torque Long-term Prediction

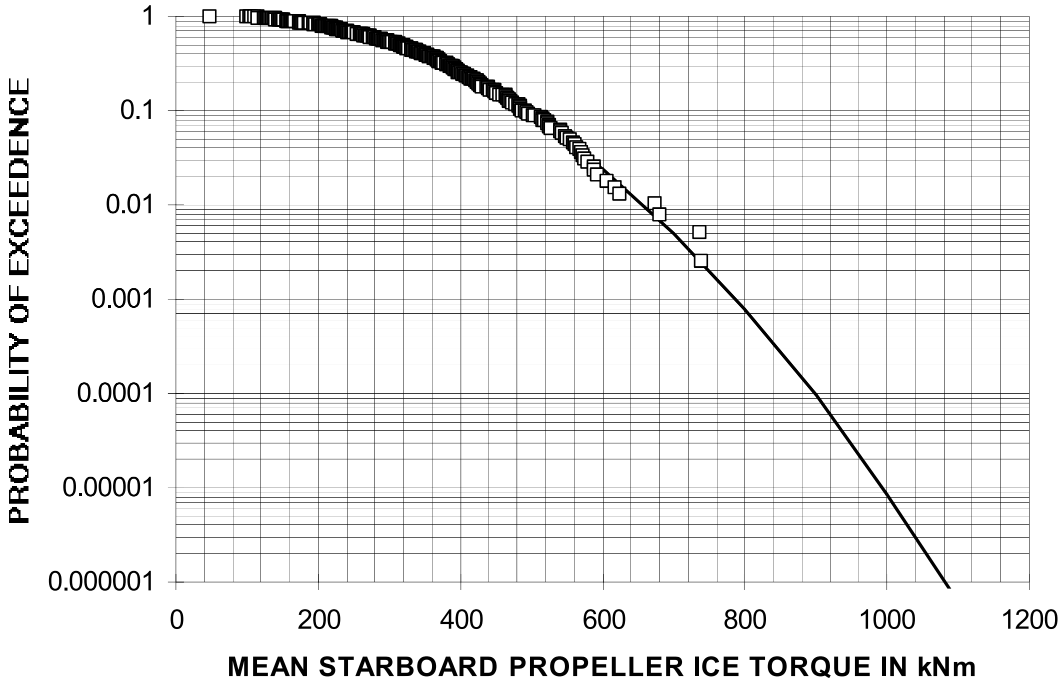

Figure 106 Louis S. St. Laurent - Mean Starboard Propeller Ice Torque Long-term Prediction

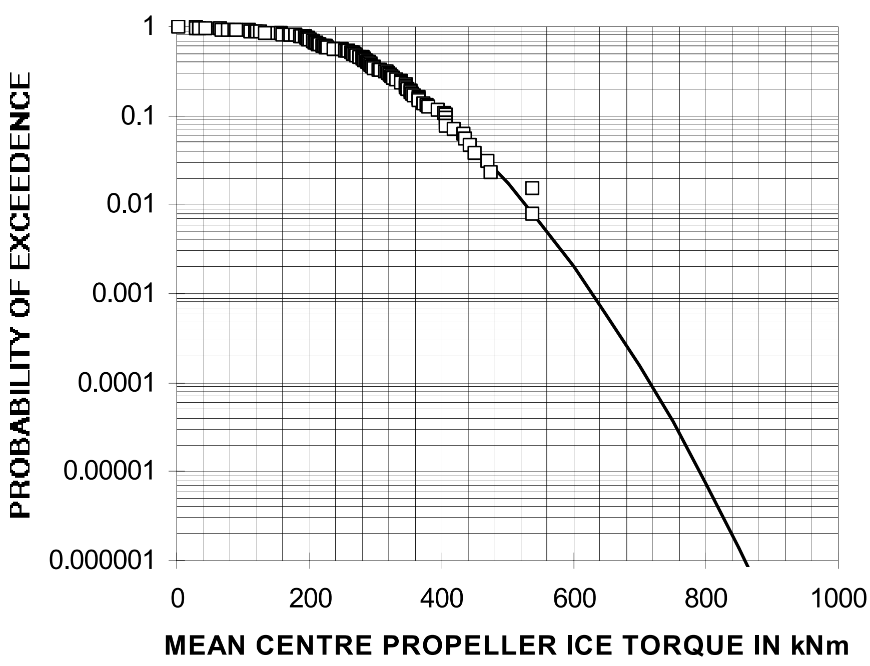

Figure 107 Louis S. St. Laurent - Mean Centre Propeller Ice Torque Long-term Prediction

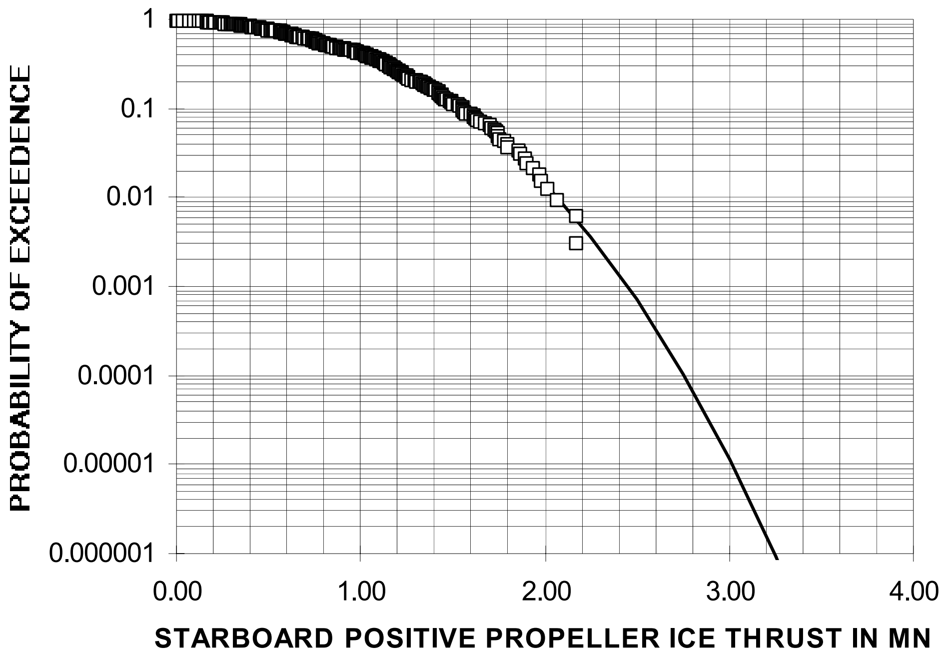

Figure 108 Louis S. St. Laurent - Starboard Positive Propeller Ice Thrust Long-term Prediction

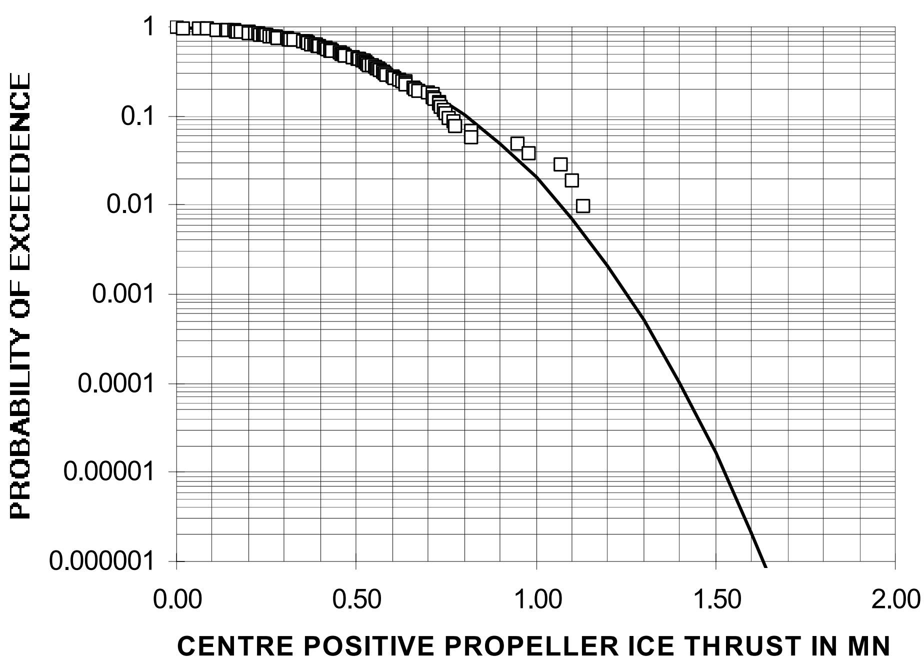

Figure 109 Louis S. St. Laurent - Centre Positive Propeller Ice Thrust Long-term Prediction

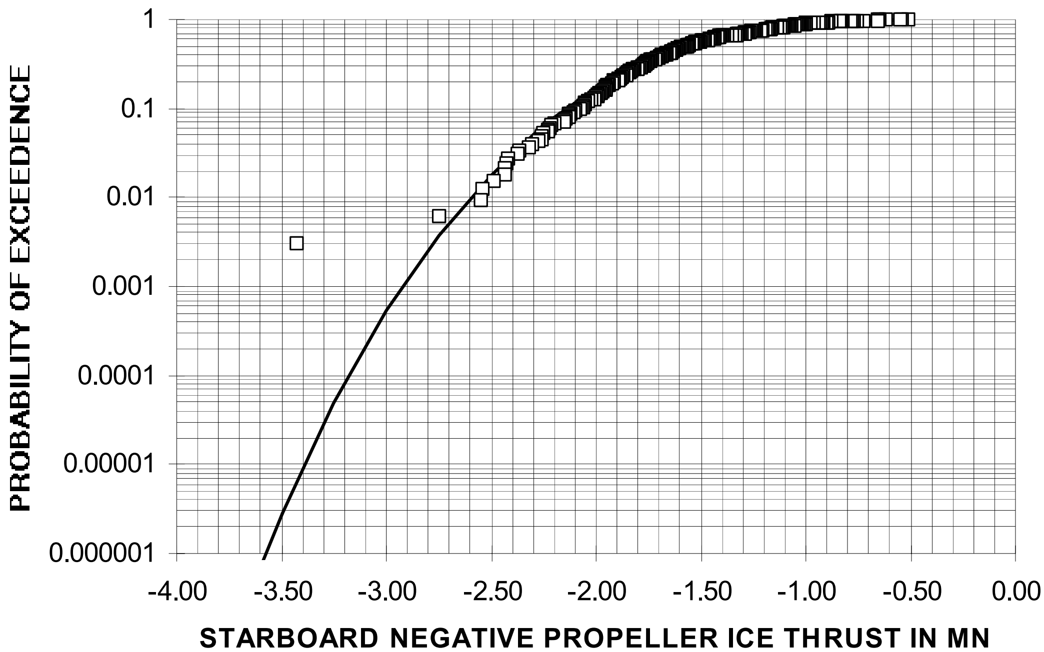

Figure 110 **Louis S. St. Laurent - Starboard Negative Propeller Ice Thrust Long-term Prediction**

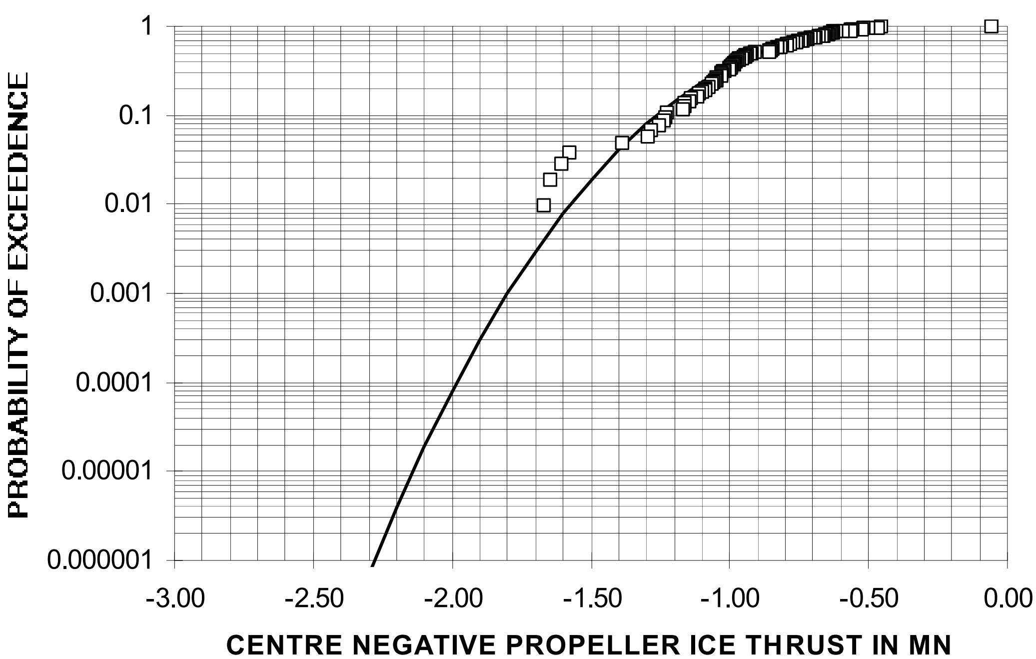

Figure 111 **Louis S. St. Laurent - Centre Negative Propeller Ice Thrust Long-term Prediction**

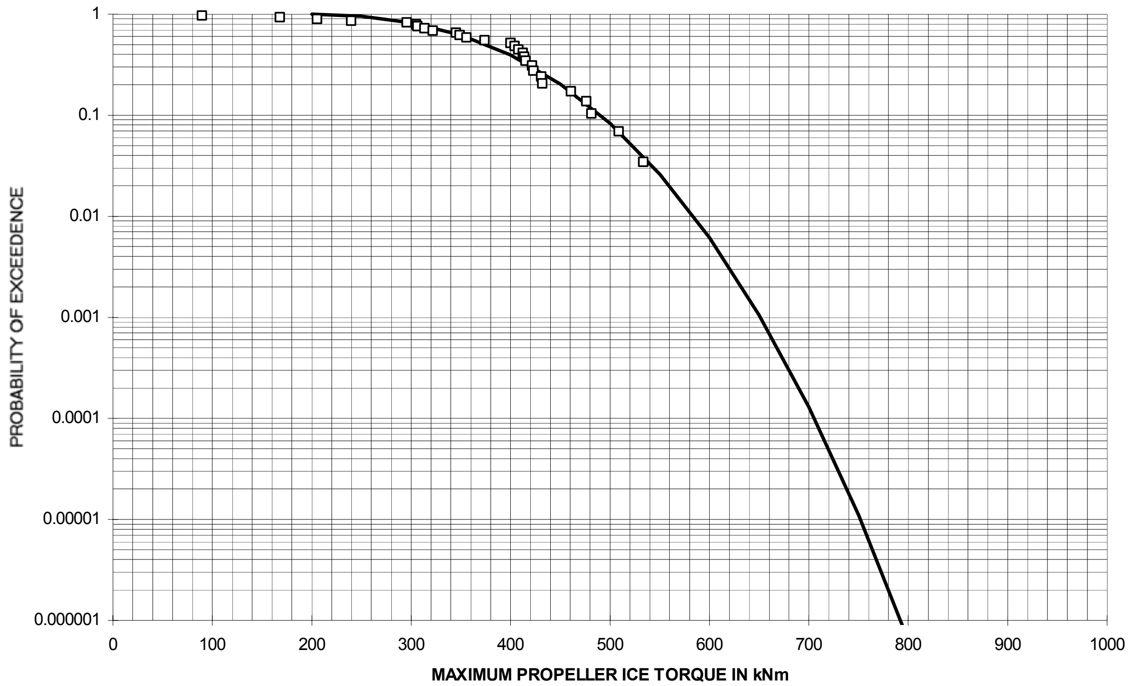

Figure 112 Kalvik - Maximum Propeller Ice Torque Long-term Prediction

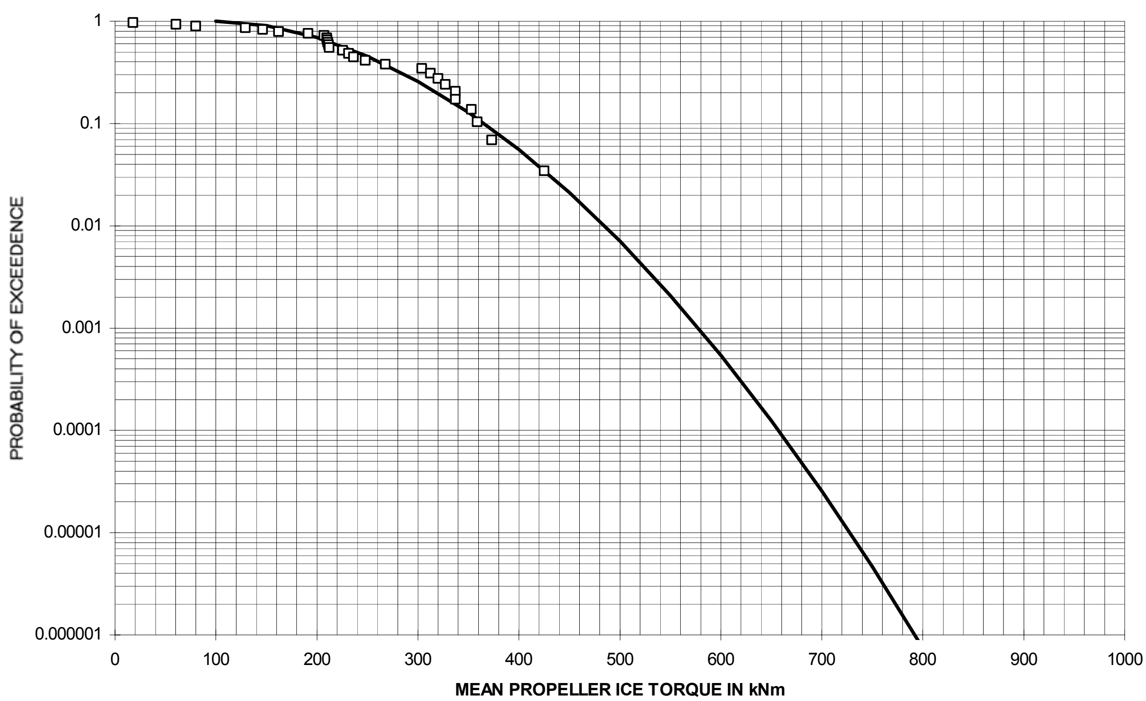

Figure 113 Kalvik - Mean Propeller Ice Torque Long-term Prediction

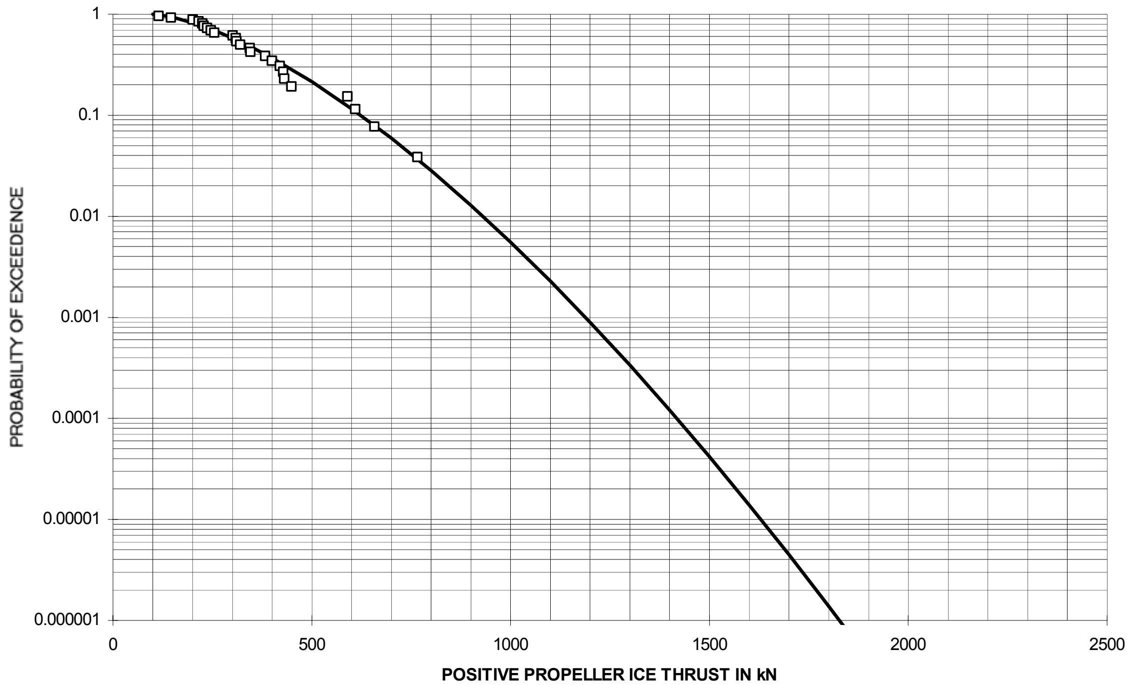

Figure 114 Kalvik - Positive Propeller Ice Thrust Long-term Prediction

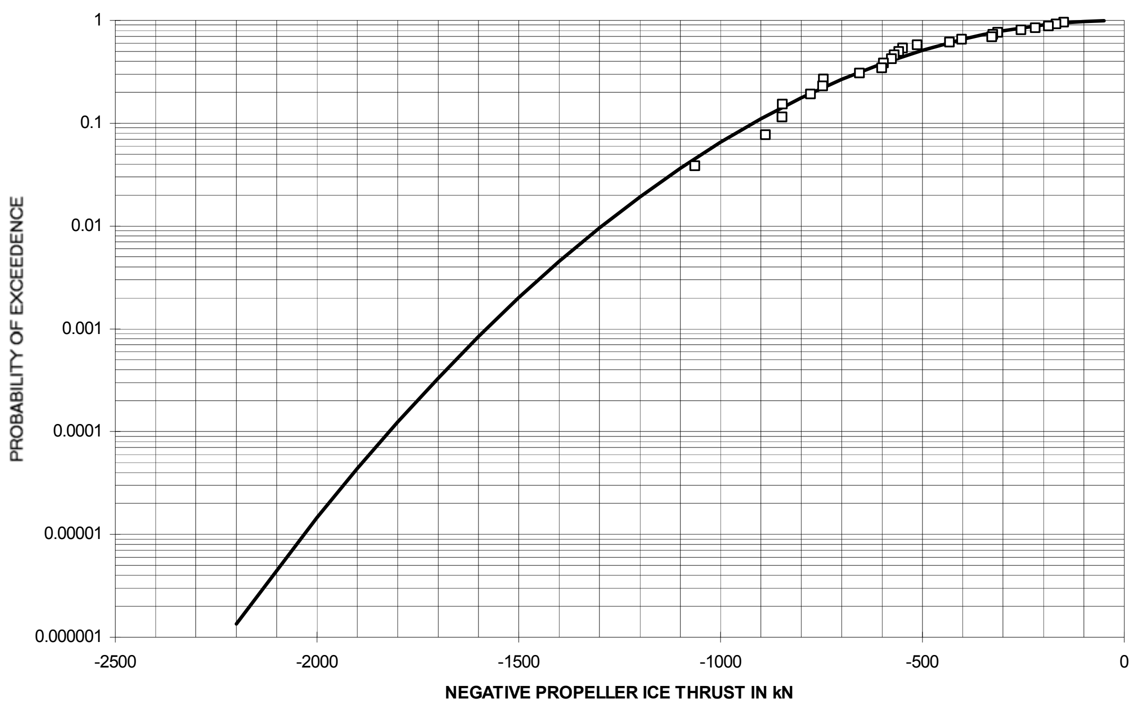

Figure 115 Kalvik - Negative Propeller Ice Thrust Long-term Prediction

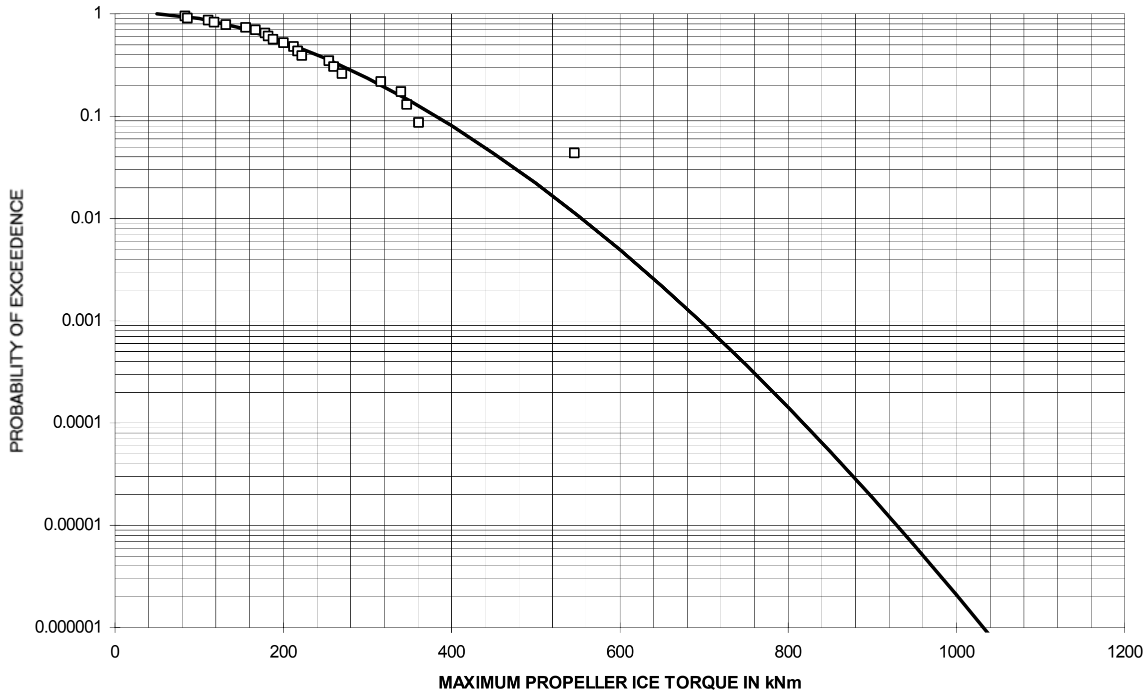

Figure 116 Terry Fox - Maximum Propeller Ice Torque Long-term Prediction

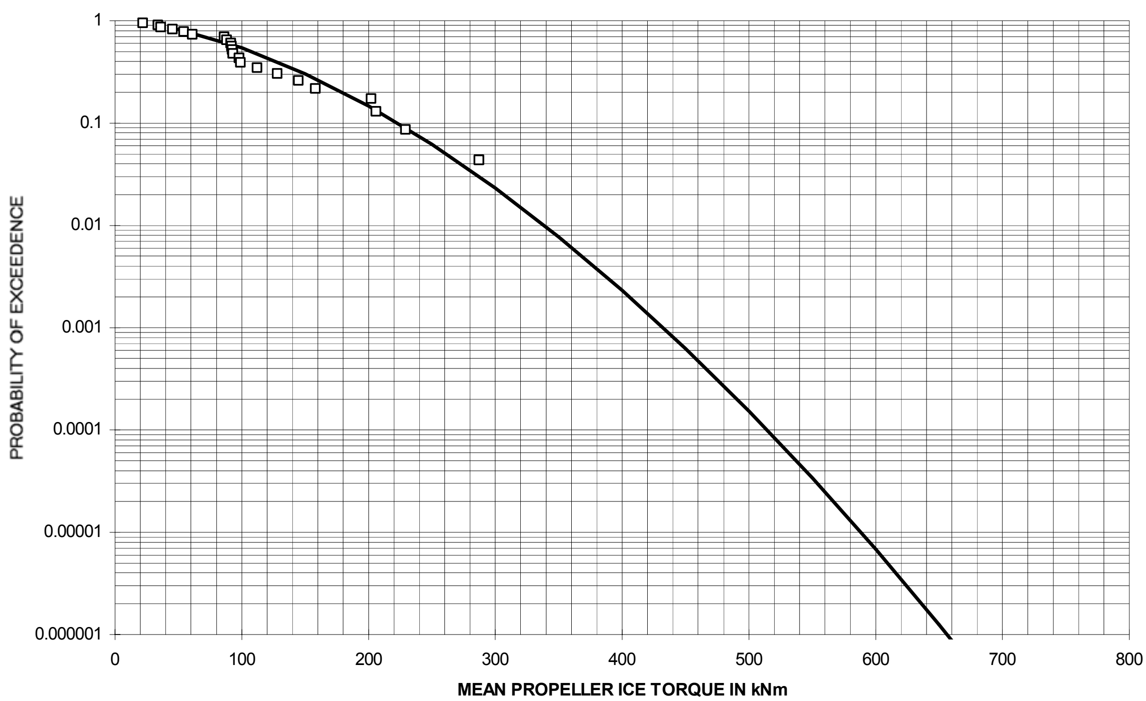

Figure 117 Terry Fox - Mean Propeller Ice Torque Long-term Prediction

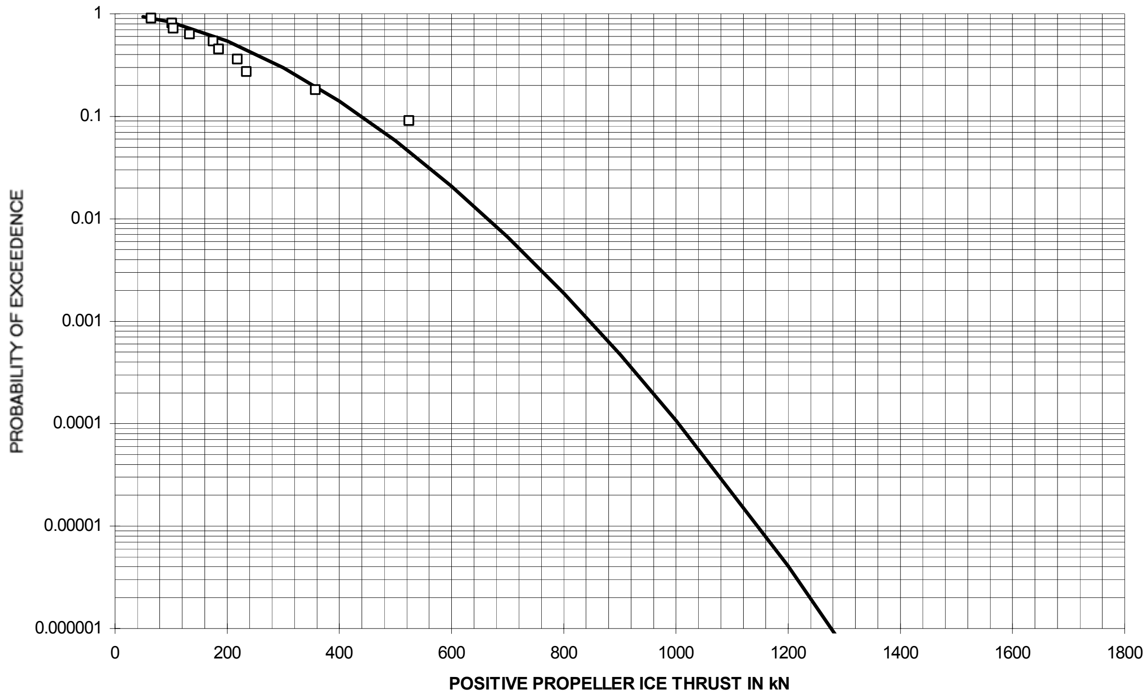

Figure 118 Terry Fox - Positive Propeller Ice Thrust Long-term Prediction

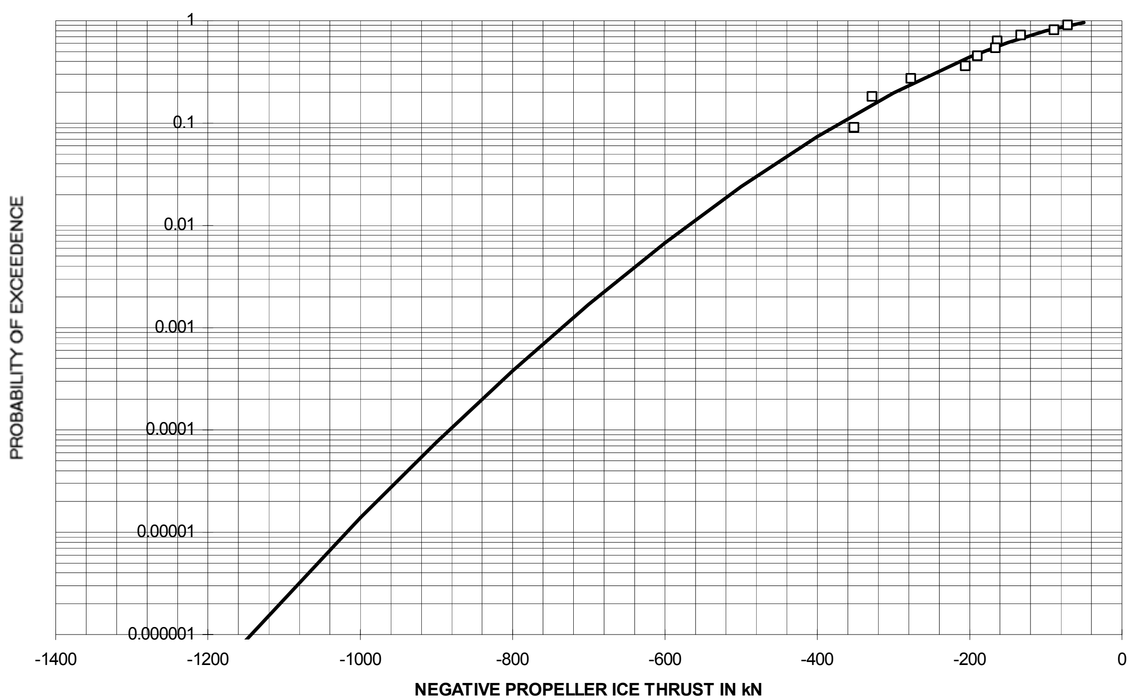

Figure 119 Terry Fox - Negative Propeller Ice Thrust Long-term Prediction

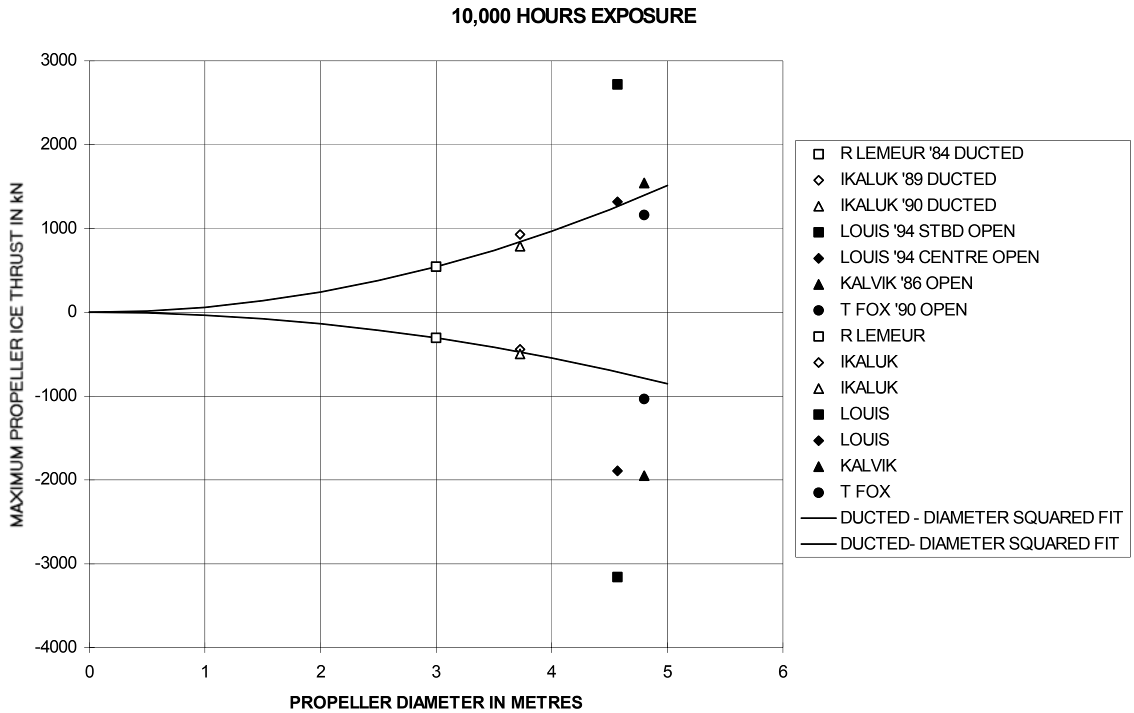

Figure 120 Maximum Propeller Ice Thrust Prediction from Trials Data

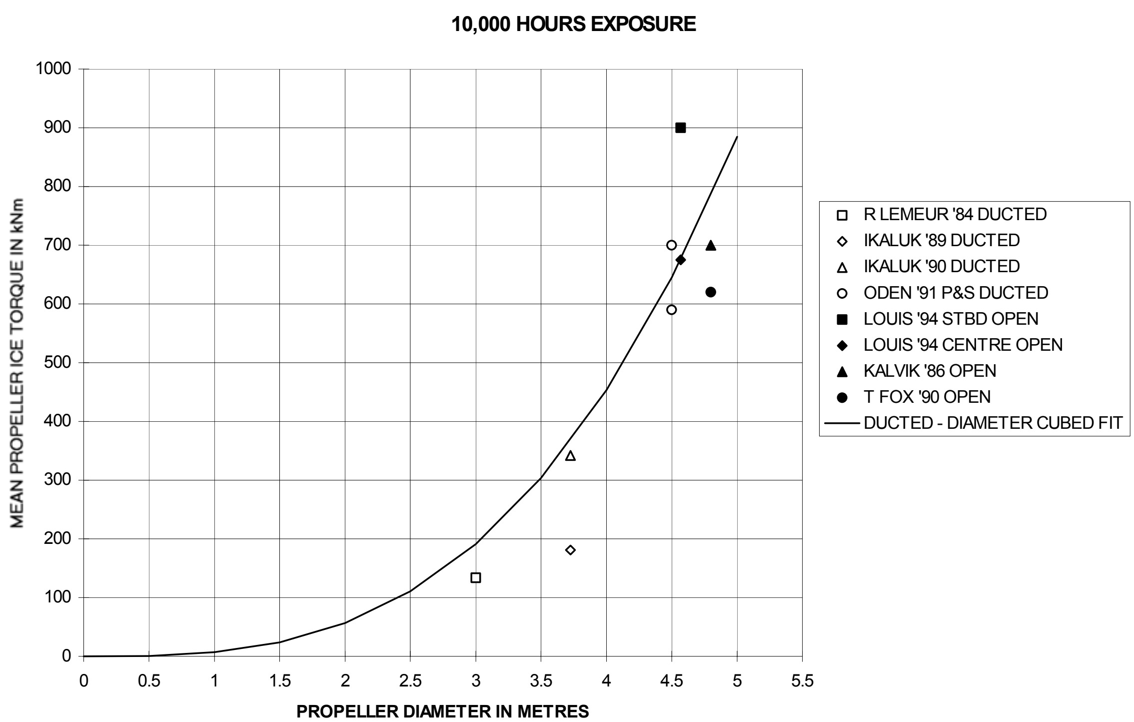

Figure 121 Mean Propeller Ice Torque Prediction from Trials Data

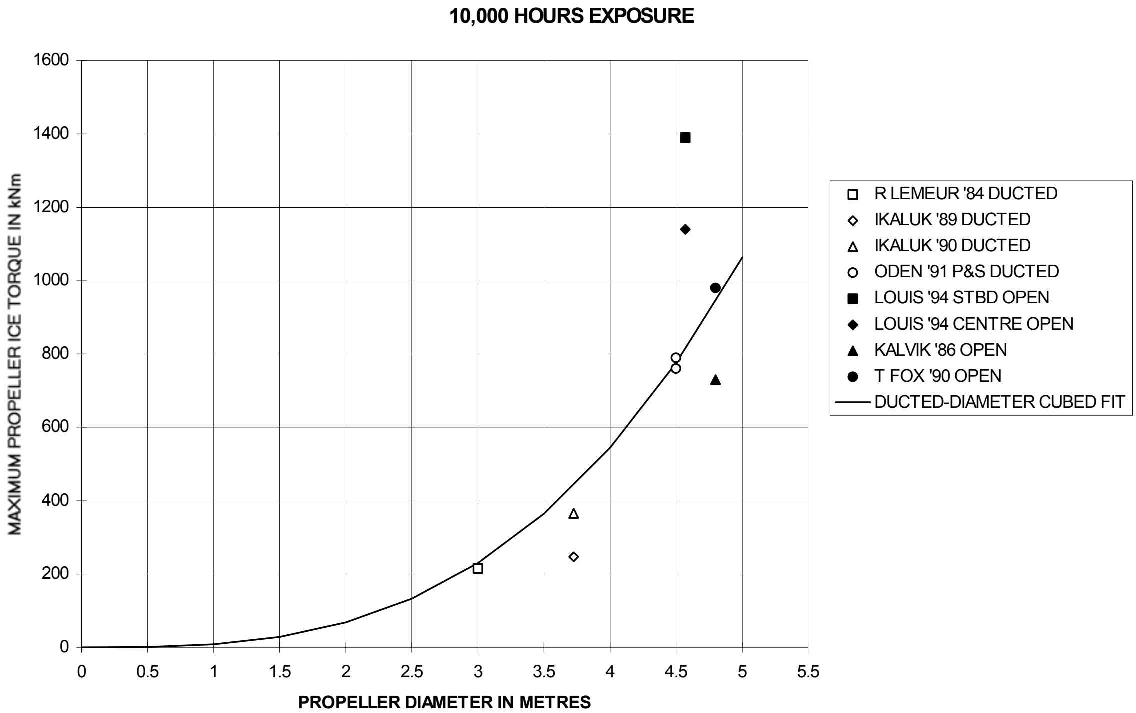

Figure 122 Maximum Propeller Ice Torque Prediction from Trials Data

5. COMPARISON WITH THE UNIFIED LOAD MODEL

5.1. The Basic Concepts

To compare the long-term predicted propeller ice loads from the different vessel trials in a satisfactory manner, the comparisons must take into account all design, operational, and environmental particulars. With so few trials data available, this cannot be resolved on its own.

However, Unified Load Model predictions and long-term return period loads from ship trials are considered to be directly equivalent. The Unified Load Model is based on a deterministic, propeller and ice interaction, numerical simulation model, and provides the maximum interaction loads for any combination of propeller design, ice conditions, and operating conditions. In the case of the trials, certain interaction parameters are not known with any accuracy, in particular the local ice block and blade contact geometry and velocities. However, over a sufficiently long period of time, as given by the return period, the limiting conditions for the maximum loads are expected to occur.

Consequently, the long-term propeller ice load predictions may be compared with predictions using the Unified Load Model. In this way, the influences of design parameters - propeller diameter, hub diameter, number of blades, expanded area ratio, pitch and blade thickness; operational parameters - propeller rpm and ship speed, and environmental parameters - ice thickness and ice strength can be taken into account.

However, it should be borne in mind that the Unified Load Model currently includes the influence of propeller nozzles and ducted protection in an approximate manner, and does not consider the protective influence of propeller location, hull form, and dimensions. Moreover, the Unified Load Model is based on the interaction of the propeller with a single ice block, whereas it is possible for the occasional full-scale trials event to involve more than one ice block. It is considered unlikely, however, for the occurrence of simultaneous, multi-block interactions to be sufficiently common to significantly influence the long-term predictions.

5.2. Design, Operational and Environmental Conditions for Comparisons

Table provides the design, operational, and environmental information for each vessel and trial required for the comparisons. The operational data used in the comparisons are in the form of the average values of ship speed, pitch angle, rpm, and nominal J coefficient (based on ship speed rather than the unknown inflow velocity) for all events in a particular trials data set.

Table 11 Design, Operational, and Environmental Information

			Ship Particulars				Propeller Particulars					Blade Particulars							Operating Conditions			Ice Conditions		
Vessel	Data for Shafts	Trial	LWL (m)	B (m)	d (m)	Displacement (tonnes)	No. of Propellers	D = Ducted O = Open	FP = Fixed Pitch CP = Controlable Pitch	Diameter (m)	No. of Blades	EAR	Hub diameter (m)	Blade Length (m)	Blade Thickness @ 0.7R (mm)	Pitch @ 0.7R (m)	Average Actual Pitch (deg)	Average Actual Pitch @ 0.7R (m)	Design RPM	Average Actual RPM	Average Actual J Vlaue	General Ice Conditions	Hice max (m)	Beam Flexural Strength (kPa)
R.Lemeur	STBD	1984 Spring Breakout	79.13	19.03	5.5	5538	2	D	CP	3	4	0.604	1.1	0.95	68.7	3.287	24	2.9370832	209	202	0.37	giant composite loosely formed floes	3+	150-631
Ikaluk 1	STBD	1989 May, Herschel Basin	76.2	16.61	7.5	5047	2	D	CP	3.725	4	0.618	1.3	1.2125	75	4.201	23	3.4768857	165	162	0.14	FY landfast + grounded ridged old ice	3+	460-790
Ikaluk 2	P & S	1990 June, Herschel Basin	76.2	16.61	7.5	5047	2	D	CP	3.725	4	0.618	1.3	1.2125	75	4.201	25	3.8195333	165	165	0.14	deteriorated spring FY landfast ice Summer polar ice -	1.55	150
Oden	PORT	1991 Arctic Expedition	93.65	29.4	8.5	13000	2	D	CP	4.5	4	0.663	1.6	1.45	99	4.615	21	3.7984184	139.5	144	0.19	Mixed multi-year regimes	3+	350 ave
Oden	STBD	1991 Arctic Expedition	93.65	29.4	8.5	13000	2	D	CP	4.5	4	0.663	1.6	1.45	99	4.615	21	3.7984184	139.5	142	0.19	Summer polar ice -	3+	350 ave
Louis	STBD	1994 Trans-Arctic Voyage	107.9	24.4	9.8	15000	3	O	FP	4.57	4	0.552	1.14	1.715	140	3.421	18.8	3.421	155	132	0.22	Mixed multi-year regimes	3+	400 ave
Louis	CENTRE	1994 Trans-Arctic Voyage	107.9	24.4	9.8	15000	3	O	FP	4.57	4	0.552	1.14	1.715	140	3.421	18.8	3.421	140	139	0.27		3+	400 ave
Kalvik	STBD	1986 Viscount Melville Sound	81.4	17.45	8	6824	2	O	CP	4.8	4	0.57	2	1.4	129.5	4.988	16	3.026578	130	125	0.3	vast composite floes - refrozen melt pools	3+	230-700
T. Fox	P & S	1990 June, Herschel Basin	81.4	17.45	8	6824	2	O	CP	4.8	4	0.57	2	1.4	129.5	4.988	17	3.2269648	130	129	0.3	deteriorated spring FY landfast ice	1.55	150

In carrying out the comparisons between the long-term predicted loads and the Unified Load Model, interpretation must be made of the ship trials environmental conditions, ice thickness and strength, the interaction condition for thrust angle of attack, and the probable influence of protection from the worst ambient ice.

5.2.1. Environmental Conditions

The 1990 Terry Fox and Ikaluk trials were carried out in well-defined conditions of 1.55 m thick, highly deteriorated weak ice.

All other trials were carried out in Arctic spring and fall, in mixed ice conditions, including different mixes of first-year, second-year, and multi-year ice, with a wide range of measured thicknesses and strengths.

In all of these trials, however, the maximum ice thicknesses are consistently above 3 m, which from the Unified Load Model (and supporting VTT Numerical Simulation Model) point of view, represents virtually infinite ice conditions, with regard to the influence of ice block size and inertia on loads, for both the ducted and open propellers,

Ice strength is a more difficult parameter to address, because the compressive strength measure required for the prediction formulae was not recorded on any of the trials. A borehole jack measurement was made on the Kalvik '86 trial (2.3 MPa). However, the values obtained from such measurements include influences of indentor size and confinement, which cannot be correlated with the uniaxial, unconfined, compressive strength tests that form the background to the compressive strength index range used in the Unified Load Model.

On all of the trials, ice temperature and salinity profiles were measured and, from these, equivalent beam flexural strengths were calculated. The maximum of these values for the trials range from 500 kPa to 800kPa, with minimums at approximately half these values. Each temperature/salinity profile is, however, different, and includes ice of often widely different strength at different depths. Equivalent beam flexural strength is therefore not necessarily a good indication of the relative compressive strength of the ice from the propeller and ice interaction viewpoint.

From recent analysis of the Polar Star Antarctic trials ice data, the uniaxial compressive strength of the ice was measured as anywhere from three to six times the beam flexural strength based on temperature/salinity profiles. These factors would give a maximum range of from 1.5 to 4.8 MPa for the trials.

In view of this dilemma regarding the compressive strength values to use, a pragmatic decision was made. The compressive ice strength (index) used in the Unified Load Model is from 1 to 9 MPa. It was argued that we cannot reliably differentiate between the compressive strengths of ice in the trials in mixed ice conditions, in the Arctic Spring (deteriorating ice) and Fall (strengthening ice). The same strength index was therefore applied to them all. The figure of 3 MPa was used in the subsequent comparisons, on the basis that the overall ice strength conditions were only moderate, and probably less than one half of those in the Arctic mid-winter. It could be argued that a figure of 4 MPa might equally well be used. However, this would alter the subsequent comparisons only slightly.

For the 1990 Terry Fox and Ikaluk trials in 1.55 m thick, highly deteriorated first-year ice, the minimum compressive strength value of 1MPa was applied.

5.3. Ice Thrust and Angle of Attack

The Unified Load Model formula for maximum negative thrust includes an angle of attack term. This is unknown from any of the trials, but it was argued that the extreme predicted loads will result from interactions at the worst (smallest) angles which occur in normal operations.

The Louis S. St. Laurent predicted maximum negative wing propeller thrust is shown in Figure 123, relative to Unified Load Model predictions for a range of attack angles and ice strengths. Matching of results is achieved in 3 m thick ice, at 3 MPa ice strength and approximately 2.5 degrees angle of attack.

It is generally held that lower angles of attack can occur in normal operation. Whether this would occur in the thickest ice is not known. On the Louis trials, the average speed for propeller and ice interaction events was relatively low at 2.3 m/s, with a nominal J value of 0.25. At higher speeds, lower angles of attack would be possible, but would probably be associated with thinner ice allowing the higher speed. It might also be considered that, although the wing propellers on the Louis appear to be exposed to ice to a significant extent, due to their wide separation, low immersion, and the hull waterline flow stern, some level of protection is received from direct, unimpeded impact with ice. This protection, whether it be manifested in terms of less heavy ice reaching the propellers or reduced ice block impact speeds, would be equivalent to a small positive increase in attack angle in Figure 123. The question of the attack angle value to be used for regulatory purposes is expected to be determined from consideration of all full-scale data comparisons.

Figures 124 and 125 show similar comparisons for the Louis centre propeller and the Kalvik wing propeller. Matching of results occurs at larger angles of attack of between 5 and 6 degrees. However, these propellers clearly benefit from a greater degree of protection than the Louis wing propellers. The Louis centre propeller protection is immediately obvious. Moreover, the Kalvik has a large ice-clearing bow wedge, low separation of the twin shafts, and a buttock flow stern. These features clearly shield the propellers from contact with ice (ice block size and/or speed and/or frequency of encounter) to a significantly greater extent than for the wing propellers on the Louis.

In Figures 126 and 127, the worst ice thickness is reduced to 2 m, and the angle of attack is now matched at 3 MPa and approximately 2.5 degrees angle of attack. This does not mean that the propeller saw ice no thicker than 2 m, but that the influence of protection from ice might be equivalent to such a reduction in ice thickness. In the regulatory context, it is anticipated that the Unified Load Model might be calibrated with a low attack angle, representing normal operation for an exposed propeller, and that coefficients might be introduced to cover ice loads for installations with greater protection.

In all following propeller thrust comparisons, the Unified Load Model is set at a nominal 2.5 degrees angle of attack. The Unified Load Model, as developed and given in Reference 1, and given below, has remained in the same form, and with the same coefficients, since its development.

5.4. Ice Thrust Comparisons

Figures 128 and 129 provide comparison of the 10,000 hour predicted maximum positive and negative propeller ice thrust values and the Unified Load Model (ULM).

In both figures, separate ULM predictions are given for ducted and open propellers.

In Figures 128 and 129, the ducted and open propeller curves are given for average blade expanded area ratios (EAR) of 0.61 and 0.56 respectively.

In Figure 129, the ULM predictions are for 3 MPa ice strength, 2.5 degrees angle of attack, and the actual trials propeller rpms.

5.4.1. Positive Thrust
Notes regarding Figure 128.

Forward Blade Thrust $= 1.13*400*(EAR/Z)*pi*(D/2)^2$ for open screws
$= 1.13*350*(EAR/Z)*pi*(D/2)^2$ for ducted screws

Ducted screw comparison
The trials predictions are higher than the ULM, by an average of 30%.

Open screw comparison
The Kalvik twin and Louis centre propeller predictions are 30% higher than the ULM. The Louis wing propeller prediction is 160% higher than the ULM. This result may be associated incorrectly with response from the higher negative thrust excitation.

5.4.2. Negative Thrust
Notes regarding Figure 129.

Ice thickness = 0.7 * blade length for ducted props.

$$\text{Backward Blade Thrust} = -1.13 * 93.0 * (\sigma * EAR/Z)^{0.287} * (Hice/D)^{1.36} * e^{-0.183\alpha} * (nD)^{0.712} * D^{2.02}$$

Hice/D maximum = 0.65

Open screw comparison
The Louis starboard propeller load comparison at 3 m ice thickness, of near equality, has been set by the interaction condition of 2.5 degrees angle of attack.

The Louis centre and Kalvik '86 propeller loads are 38% lower than those for the Louis wing propeller. The influence of hull protection is equivalent to a reduction in ice thickness to 2 m.
The T Fox comparison for thinner ice is very close.

Ducted screw comparison
The Lemeur and Ikaluk trials predictions are very close to the ULM.

5.5. Ice Torque Comparisons

Figures 130 and 131 provide comparisons of the 10,000 hour predicted mean and maximum propeller ice torque values with the Unified Load Model.

In both figures, separate ULM predictions are given for ducted and open propellers. Ice thickness is 3 m, ice strength is 3 MPa and the actual trials propeller rpms are used.

The ducted curves are for average values of blade length/propeller radius of 0.643, J of 0.23, t/D of 0.0217, and P/D of 0.925.

There are separate open propeller ULM prediction curves for Louis and Kalvik/Fox. In view of the widely different design of these propellers - Louis is fixed pitch, whereas Kalvik/Fox is controllable pitch - separate curves are given for the individual design and operating conditions given in Table 11.

Notes regarding Figures 130 and 131

$$\text{Mean Torque} = 152 * (1 - d/D) * \sigma^{0.183} * (Hice/D)^{1.20} * (-0.881 * J^2 + J + 0.520) * (P/D)^{0.275} * (t/D)^{0.562} * (nD)^{0.201} * D^{3.04}$$

$$\text{Max Torque} = 234 * (1 - d/D) * \sigma^{0.195} * (Hice/D)^{1.07} * (-0.902 * J^2 + J + 0.438) * (P/D)^{0.162} * (t/D)^{0.605} * (nD)^{0.173} * D^{3.04}$$

Hice/D maximum = 0.55

5.5.1. Mean Ice Torque - Figure 130

Ducted screw comparison
The ULM predictions are 30% higher on average than the Trials data predictions.
The comparison for Oden is close, but significantly poorer for Robert Lemeur and Ikaluk.

Open screw comparison
The ULM prediction for the Louis wing prop is 15% high, and for Kalvik 22% high.
The Louis centre trials prediction is 25% lower than for the wing propeller.

5.5.2. Maximum Ice Torque - Figure 131

Ducted screw comparison
The ULM predictions are 17% higher on average than the Trials data predictions.
The comparison is close for Oden and Robert Lemeur, but significantly poorer for Ikaluk.

Open screw comparison
The ULM prediction for the Louis wing propeller is 7% lower than the trials prediction.
The Louis centre trials prediction is 18% lower than for the wing propeller.
The ULM prediction for Kalvik is 27% higher than the Trials prediction.

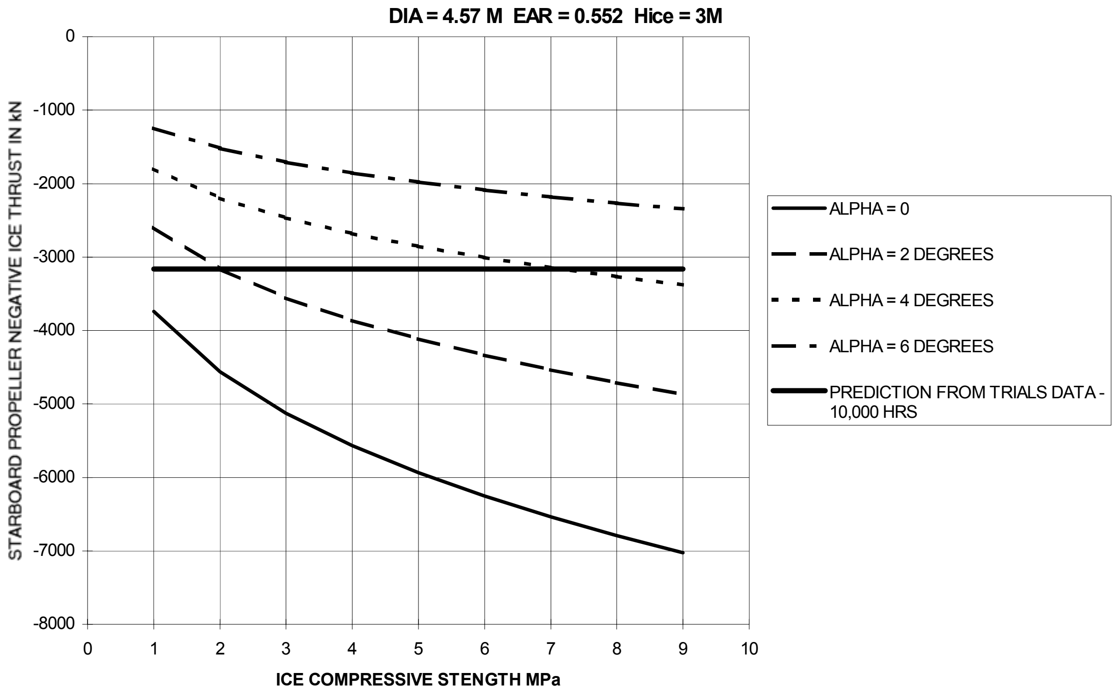

Figure 123 Louis S. St. Laurent - Starboard Propeller Negative Ice Thrust Comparison with Unified Load Model

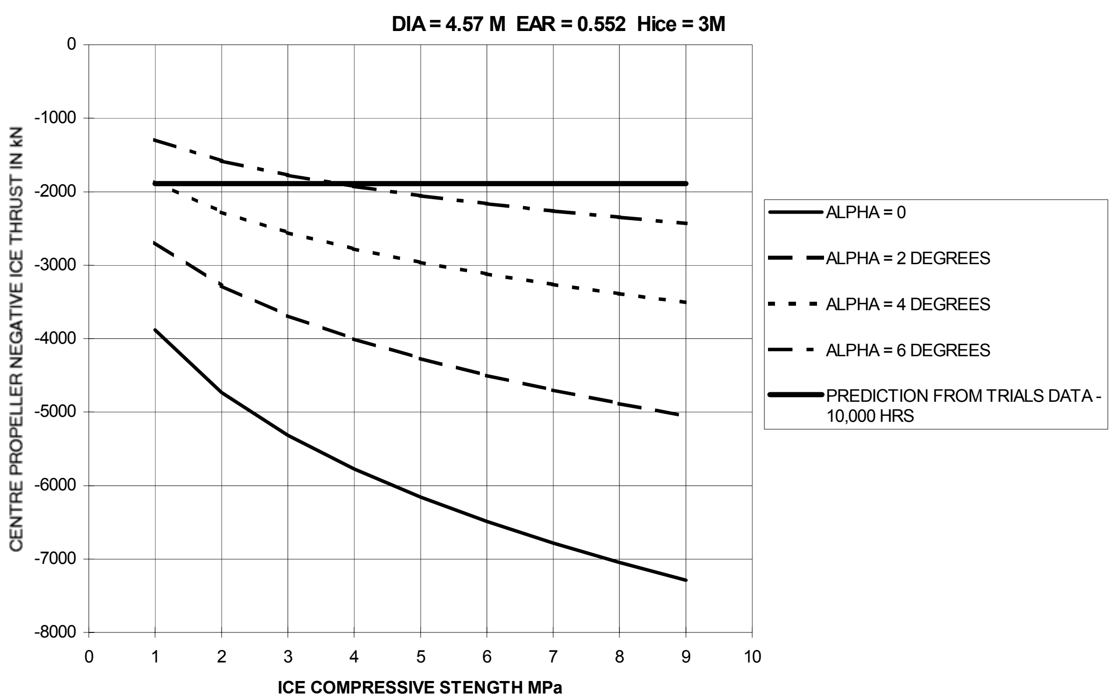

Figure 124 Louis S. St. Laurent - Centre Propeller Negative Ice Thrust Comparison with Unified Load Model

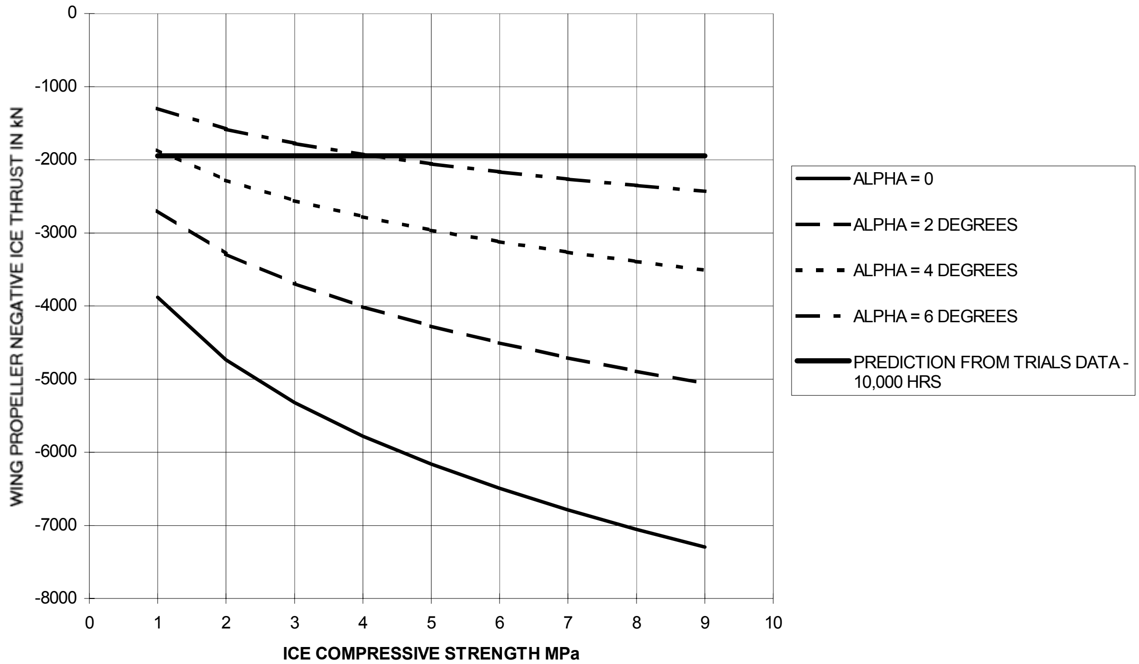

Figure 125 Kalvik - Wing Propeller Negative Ice Thrust Comparison with Unified Load Model

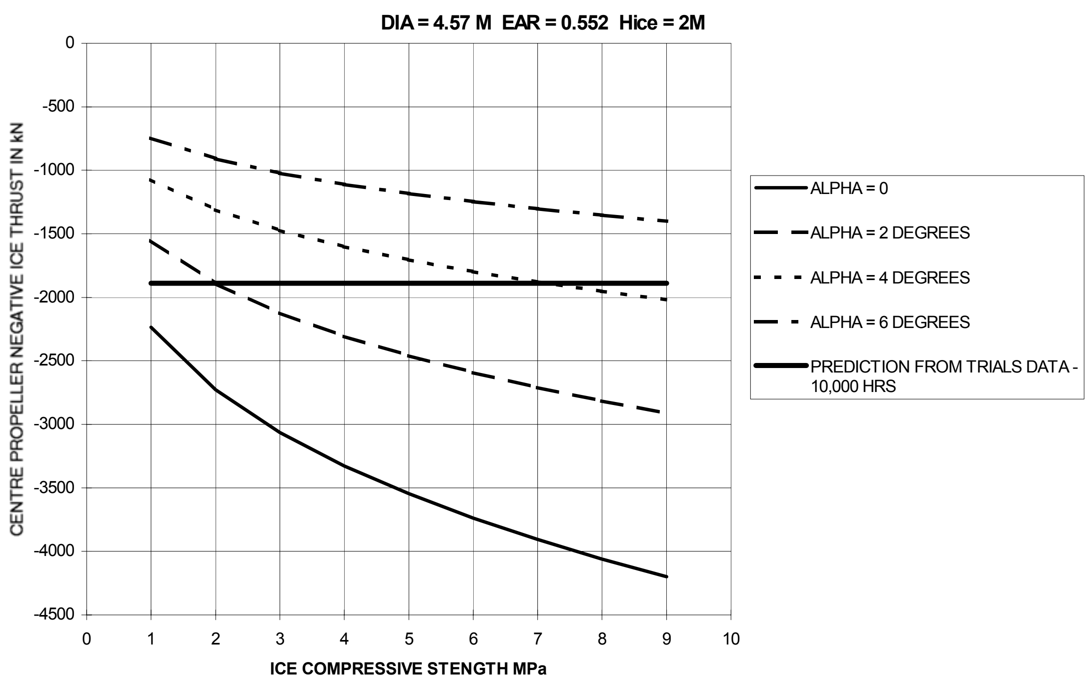

Figure 126 Louis S. St. Laurent - Centre Propeller Negative Ice Thrust Comparison with Unified Load Model

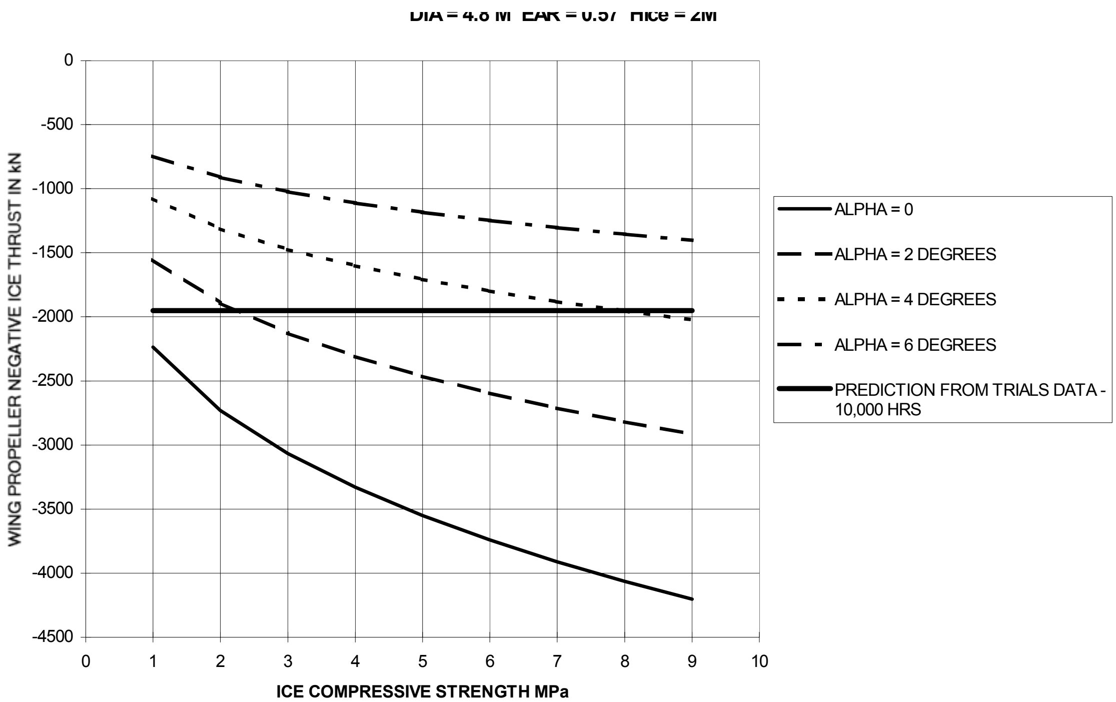

Figure 127 Kalvik - Wing Propeller Negative Ice Thrust Comparison with Unified Load Model

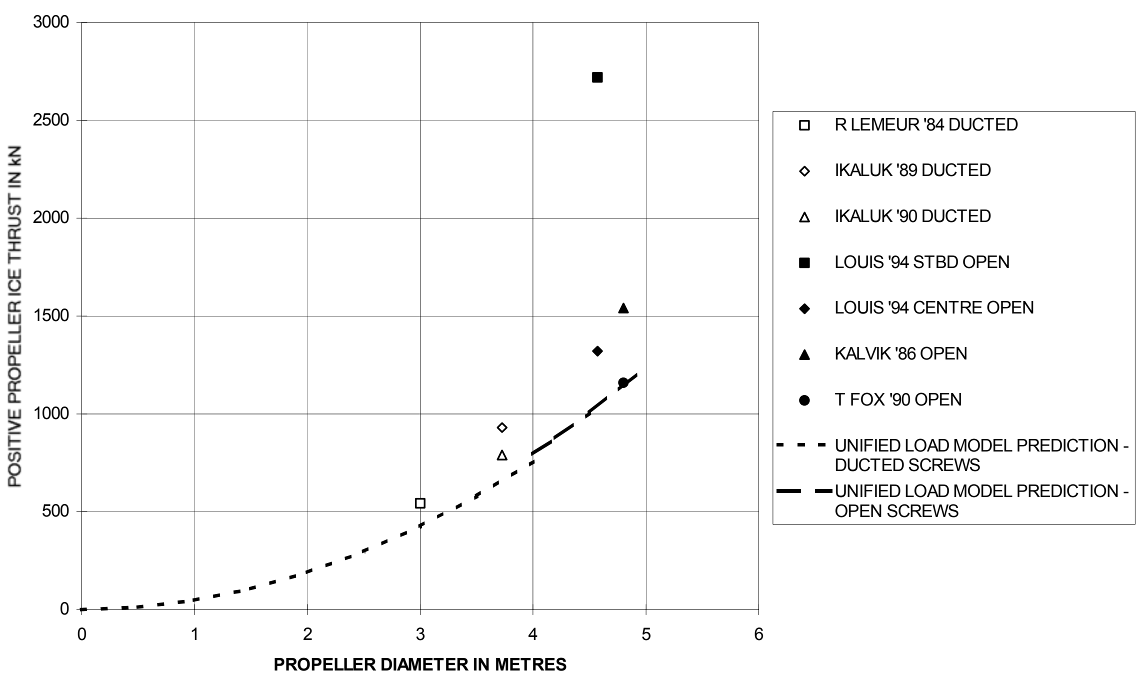

Figure 128 Positive Propeller Ice Thrust Predictions from Trials Data and Comparison with the Unified Load Model

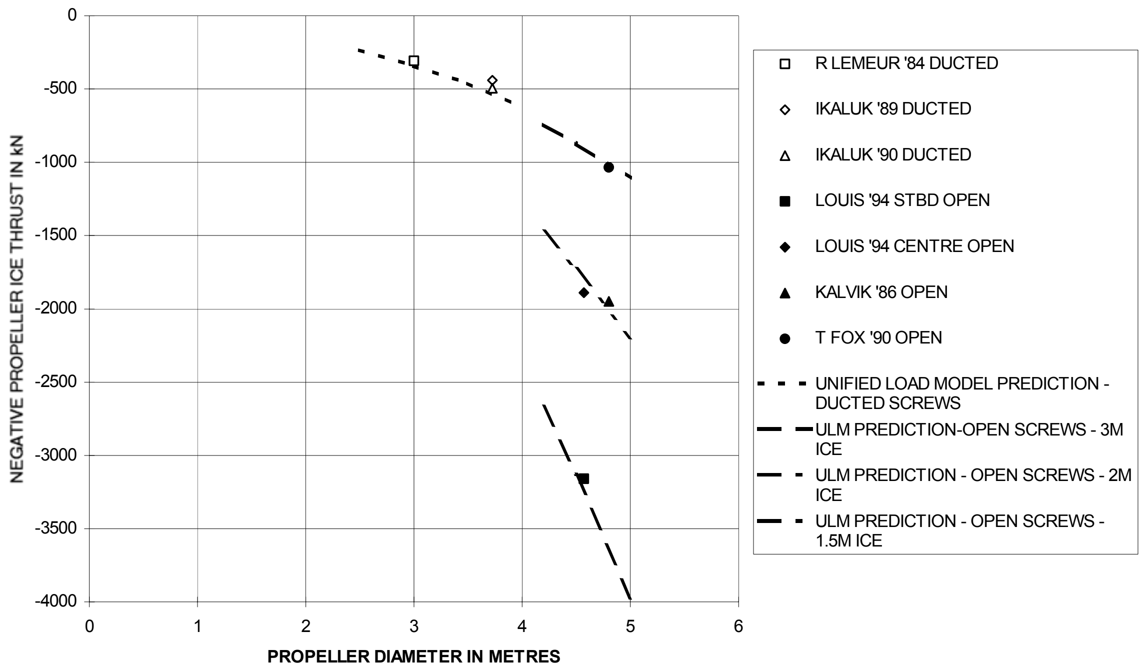

Figure 129 Negative Propeller Ice Thrust Predictions from Trials Data and Comparison with the Unified Load Model

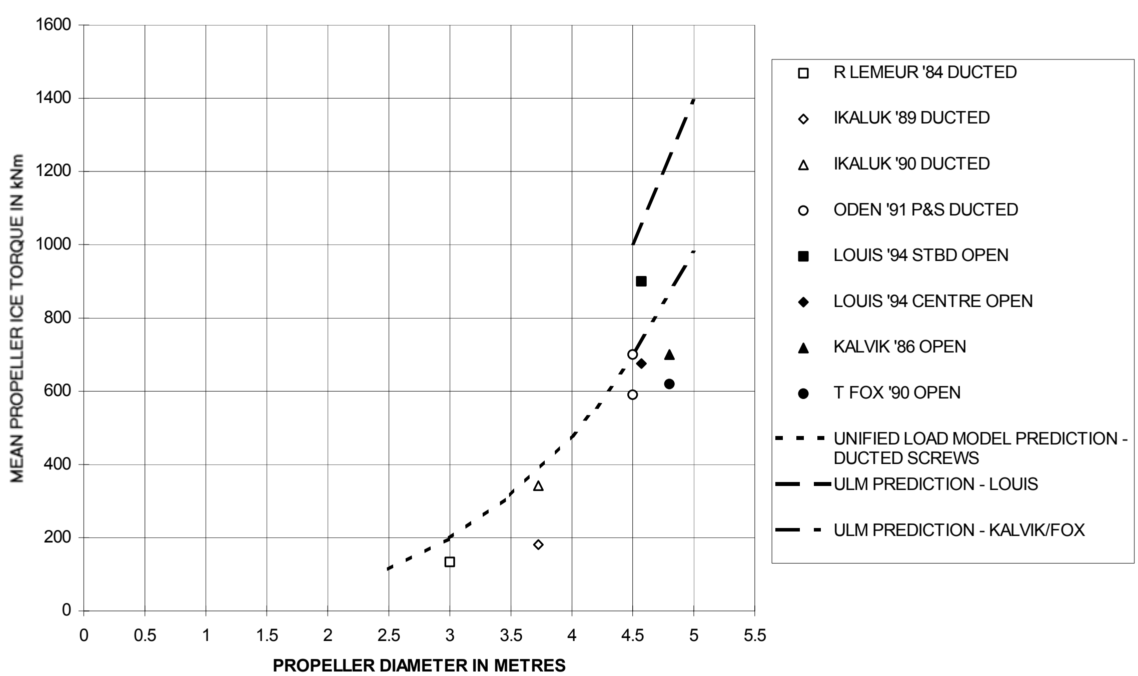

Figure 130 Mean Propeller Ice Torque Predictions from Trials Data and Comparison with the Unified Load Model

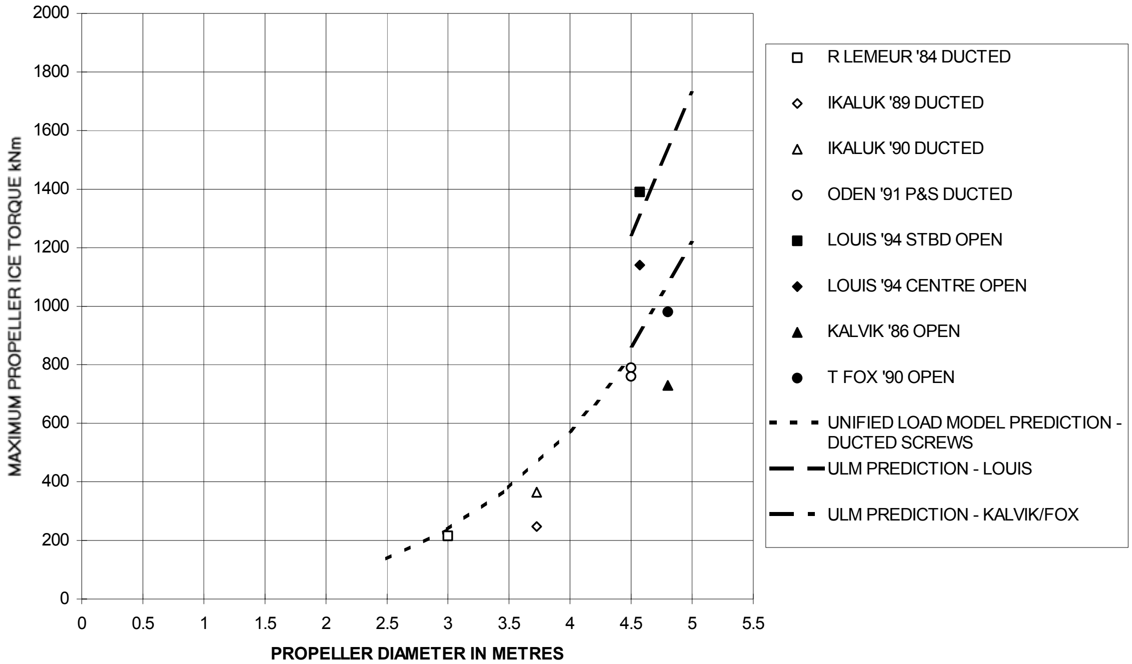

Figure 131 Maximum Propeller Ice Torque Predictions from Trials Data and Comparison with the Unified Load Model

6. CONCLUSIONS

Propeller ice thrust and torque loads have been calculated from the measured shaft thrust and torque loads from seven sets of Canadian full-scale trials data, for the vessels, Louis S. St. Laurent, Oden, Robert Lemeur, Terry Fox, Kalvik, and Ikaluk (two trials).

Parametric analysis carried out on the resulting propeller ice loads has shown that:

- For the ducted propellers, positive ice thrust loads were larger than negative ice thrust loads.
- For the open propellers, negative ice thrust loads were larger than positive ice thrust loads.
- In general, for both the ducted and open propellers, propeller ice torque increased with increasing pitch angle.
- Investigation for the influence of pitch angle upon ducted propeller ice thrust was inconclusive.
- For the open propeller, in heavy ice conditions, the highest ice thrust loads occurred at low pitch angles.
- In general, the magnitudes of ice thrust and torque at negative pitch angles were less than those at positive pitch values.
- Investigation for the separate influence of rpm upon ice loads was inconclusive.
- It was not possible determine trends in ice loads with ship speed, although high load values occurred at all speeds.
- Single impact events generated ice loads as high as during milling, for both the ducted and open propellers.
- Although blockage loads for the ducted propellers were lower than the contact loads, they were still significant.
- Ice loads varied less than linearly with ice strength. An additional analysis, based on gear tooth contact loads for the Canmar Kigoriak, suggests a weaker dependency relative to ice crushing strength than that derived for the propeller loads relative to ice flexural strength. The Kigoriak dependency is very similar to the influence incorporated in the Design Load Model.

Long-term predictions of propeller ice loads, for 10,000 hours of operation, were made from Weibull Type 3 distributions of the propeller ice load data. These data show the following influences:

- For the ducted propellers in thick ice, ice thrust varied approximately with the square of propeller diameter, and ice torque varied approximately with the cube of propeller diameter. The diameter range for the open propellers was too small to investigate the diameter influence.
- Maximum negative ice thrust for the open propellers was up to four times that of a similar diameter ducted propeller, and over twice the maximum positive thrust for the ducted propeller.

- The open propellers could generate higher ice torques than ducted propellers, but this difference was much less than that between open and ducted propellers for ice thrust.
- The degree of exposure to ice interaction had a significant influence upon ice loads. The centre screw of the triple open screw vessel Louis S. St Laurent experienced only about 60% of the ice thrust and 75% of the ice torque of the wing propellers. The twin open screws of Kalvik, which have some protection due to their limited separation and location beneath the buttock flow stern, experienced similar loads as the similar diameter Louis centre propeller.

The long-term propeller ice load predictions from trials data have been compared with predictions using the Unified Load Model, for the specific propeller design, operational, and environmental conditions on the trials. The Unified Load Model predictions were made for an angle of attack of 2.5 degrees.

The comparisons have shown that:

- For both the open and ducted propellers, maximum positive ice thrust is predicted on average 30% higher than the Unified Load Model.
- For the ducted propellers, maximum negative ice thrust predictions agree well with the Unified Load Model.
- With some logical interpretation of the influence of hull form and propeller arrangement on exposure to ice, the open propeller negative ice thrust predictions are similar to the Unified Load Model.
- For both the open and ducted propellers, maximum and mean ice torque long-term predictions are lower than Unified Load Model predictions by 20-30%
- The best agreement between trials predictions and the Unified Load Model occurs for the cases of the largest, most reliable trials data sets - Louis S. St. Laurent, Oden, and Robert Lemeur.

The overall finding is that the Canadian data, with a bias towards larger propellers and ducted propellers, appears to support well the Unified Load Model, which is based on numerical modeling and a separate set of Finnish full-scale data.

REFERENCES

1. Koskinen, P., Jussila, M., & Soininen, H. Espoo, *Propeller Ice Load Models,* Technical Research Centre of Finland, Research Notes 1739. 1996.

2. Browne R. P., & Ritch R, *Analysis of Propeller Shaft Load Measurements taken on board the Louis S. St. Laurent during the 1994 Trans-Arctic Voyage*, NRC/IMD Report CR-1996-14. October 1996.

3. Browne, R.P., *Analysis of Canadian Full-scale Propeller and Ice Interaction Trials Data for Correlation with Empirical Models*. R.P. Browne Marine Consultants Limited for IMD/NRC. CR-1997-12. December 1997.

4. Cowper, B., *The Shaft Modeling Tool Kit*, Arctec Canada Limited. Arctec Report ACL#2488, 1988.

5. *1979/1980 Full-scale Tests of the Icebreaker Kigoriak*. Dome Petroleum. Sept. 1982. Restricted. Access through AKAC Inc. Calgary, Alberta.

Appendix A

Propeller and Ice Interaction Loads

**(*Not available in electronic format/*
***Non disponible en format électronique*)**

Appendix B

Kigoriak Ice Strength Influence on Shaft Ice Torque

R.P. Browne Marine Consultants Limited
223 - 23rd Avenue N.E.
Calgary, Alberta
Canada
T2E 1V8
Tel/Fax (403) 276-3832

14 May 1997

DESIGN LOAD MODEL PROJECT
ICE STRENGTH INFLUENCE

INTRODUCTION

It has not been possible as yet, either from full-scale or model scale data analysis, to determine the influence of ice strength on propeller and ice interaction loads, with any certainty. However, previously confidential information in CANMAR reports has recently become available, and is used below to provide a further indication of this influence.

CANMAR KIGORIAK FULL-SCALE DATA

In 1980, the gearbox of Canmar Kigoriak was fitted with a Renk Checker, in order to measure the gear tooth contact pressures over periods of ship operation (Reference 5) . Very detailed measurements of ice conditions were made. The most important data for our purposes are summarized below. They cover two trials in the Canadian Beaufort Sea in 1980, both in level ice conditions - mid-Winter, March 7/10 (81 hours) and Spring, June 13 (11.7 hours).

1980 Date	Duration hours	Level Ice Thickness m	Ice Strength Comp. MPa	Surface Temp. ^{o}C
March 7/10	81	1.5 to 1.6	24	-15
June 13	11.7	1.95	12	-0.5

Ice strength, through-ice measurements were taken by borehole jack. The exact meaning of the ice crushing strength levels with respect to propeller loads is not known. However, it is clear that the Winter ice strength was twice that of the Spring ice strength.

Amplitude - Frequency of occurrence histograms of gear tooth maximum contact pressures are given in Figures 1 and 2, for the Winter and Spring trials.

ANALYSIS

The maximum out- to-out range of gear tooth pressures, corresponding to a measure of the shaft torque due to propeller and ice interaction, are 221+196 = 417 for Winter, and 234+ 208 = 442 for Spring. The ratio of maximum shaft torques for the two trial periods is therefore, Winter/Spring = 0.94.

The number of shaft torsional cycles is 1,818,249 in Winter and 292,769 in Spring. An estimate of the influence of this difference in exposure on the maximum expected values is made from Figure 3, the probability of occurrence of maximum port propeller torque for the Oden 1991 Arctic trials. The Oden propeller is ducted, as is Kigoriak's, and diameter is 4.5m, versus 5.3m for Kigoriak.

From Figure 3, the ratio of maximum torque at probability of 0.000003, to probability of 0.00000055 is 0.94. The same factor is obtained for the Oden starboard shaft, and from Robert Lemeur and Ikaluk probability plots.

The ratio of maximum shaft torques for the two trial periods, both at the same exposure of 11.7 hours, is therefore 0.94* 0.94 = **Winter/Spring = 0.88**

UNIFIED LOAD MODEL COMPARISON

The Unified Load Model influence of ice strength and thickness upon maximum ice torque is proportional to $\sigma^{0.195} * (Hice/D)^{1.07}$

The predicted ratio of maximum ice torque for the Winter versus Spring conditions is therefore:

Winter/Spring = $2^{0.195} * (1.55/1.95)^{1.07}$ = **0.89**

CONCLUSION

The level of agreement between the Kigoriak full-scale data and the Unified Load Model is almost exact. The two parameters influencing this comparison are ice thickness and strength, of which the ice thickness influence is considered in little doubt. The comparison therefore supports the relatively modest influence of ice strength upon propeller and ice interaction loads, incorporated in the Unified Load Model.

Previous failure to isolate the ice strength influence is probably due in part to its relatively modest influence.

AML-X4 Full-scale Tests
DataMite 400 Recorded Data

Amplitude-Frequency Histogram for Renk Checker Data Collection Begun at 10:00 on 10:00 80/03/07
Elapsed time During Data Collection:81 Hours
Calibration 24.525 MPa/BIN
Ultimate Strength of Gear Teeth 1500MPa
Hysteresis:1 DIAS:0

Bin	Count	Bin Range (MPa)	
7	1	-245.25	-220.725
8	18	-220.725	-192.2
9	333	-192.2	-171.675
10	5062	-171.675	-147.15
11	130451	-147.15	-122.625
12	389405	-122.625	-98.1
13	210484	-98.1	-73.575
14	249039	-73.575	-49.05
15	833456	-49.05	-24.525
17	460664	0	24.525
18	533152	24.525	49.05
19	188770	49.05	73.575
20	264341	73.575	98.1
21	328156	98.1	122.625
22	41685	122.625	147.15
23	1397	147.15	171.675
24	63	171.675	196.2
25	1	196.2	220.725

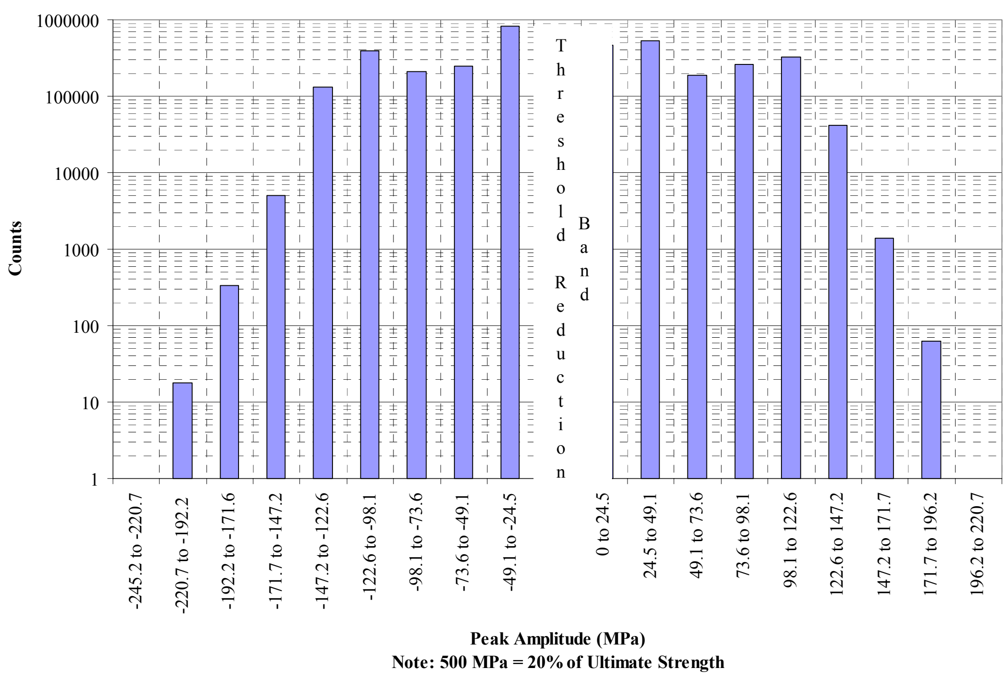

AML-X4 Full-scale Tests
DataMite 400 Recorded Data

Amplitude-Frequency Histogram for Renk Checker Data Collection Begun at 16:13 on 80/06/13
Elapsed time During Data Collection: 11.7 Hours
Calibration 26 MPa/BIN
Ultimate Strength of Gear Teeth 1500 KG/mm^2
Hysteresis:3 DIAS:-1

Bin	Count	Bin Range (MPa)	
8	2	-234	-208
9	124	-208	-182
10	2982	-182	-156
11	55811	-156	-130
12	91269	-130	-104
13	76303	-104	-78
14	65927	-78	-52
15	351	-52	-26
16	1	-26	0
17	88	0	26
18	47861	26	52
19	69906	52	78
20	117332	78	104
21	55245	104	130
22	2209	130	156
23	125	156	182
24	5	182	208

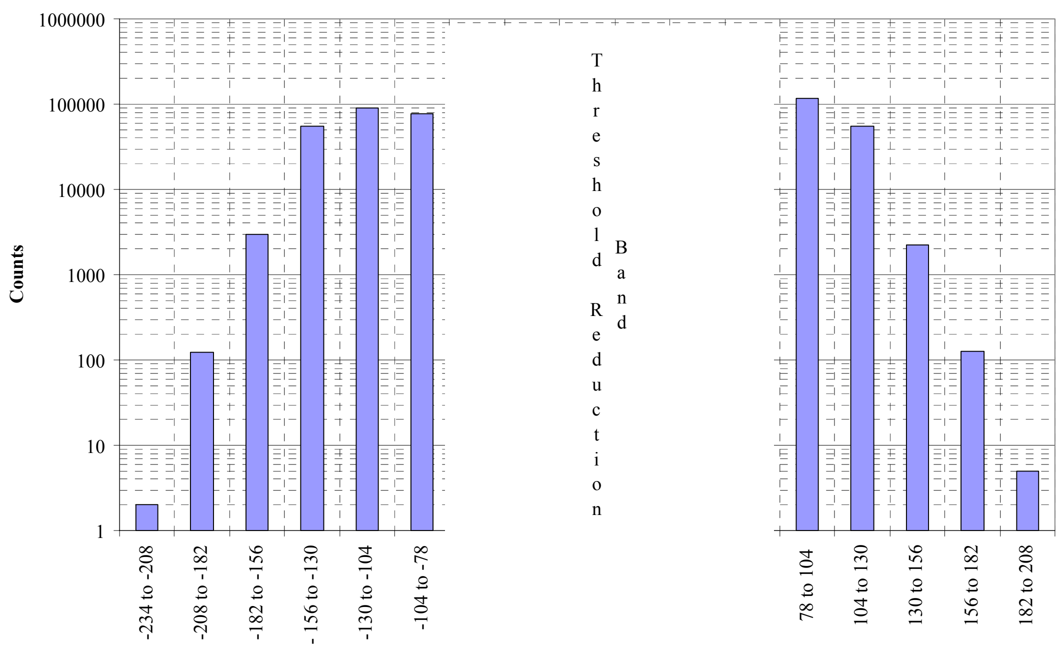

Peak Amplitude (MPa)
Note: 300 MPa = 20% of Ultimate Strength